

**“ROLE OF MULTIPARAMETRIC MAGNETIC RESONANCE
IMAGING OF BRAIN IN DIFFERENTIATING
NEUROCYSTICERCOSIS FROM TUBERCULOMA”**

By

Dr. LYNN JOY



**DISSERTATION SUBMITTED TO SRI DEVARAJ URS ACADEMY OF
HIGHER EDUCATION AND RESEARCH, KOLAR, KARNATAKA**

In partial fulfilment of the requirements for the degree of

**DOCTOR OF MEDICINE
IN
RADIODIAGNOSIS**

Under the Guidance of

**Dr. ANIL KUMAR SAKALECHA, MBBS, M.D
PROFESSOR & HOD
DEPARTMENT OF RADIODIAGNOSIS**



**DEPARTMENT OF RADIODIAGNOSIS,
SRI DEVARAJ URS MEDICAL COLLEGE,
TAMAKA, KOLAR-563101**

2023

**SRI DEVARAJ URS ACADEMY OF HIGHER EDUCATION AND
RESEARCH, TAMAKA, KOLAR, KARNATAKA**

DECLARATION BY THE CANDIDATE

I hereby declare that this dissertation entitled **“ROLE OF MULTIPARAMETRIC MAGNETIC RESONANCE IMAGING OF BRAIN IN DIFFERENTIATING NEUROCYSTICERCOSIS FROM TUBERCULOMA”** is a bonafide and genuine research work carried out by me under the guidance of **Dr. ANIL KUMAR SAKALECHA**, Professor & HOD, Department of Radiodiagnosis, Sri Devaraj Urs Medical College, Kolar, in partial fulfilment of University regulation for the award **“M. D. DEGREE IN RADIODIAGNOSIS”**, the examination to be held in 2023 by SDUAHER. This has not been submitted by me previously for the award of any degree from the university or any other university.

Date:

Dr. LYNN JOY

Postgraduate in Radiodiagnosis

Sri Devaraj Urs Medical College

Tamaka, Kolar.

**SRI DEVARAJ URS ACADEMY OF HIGHER EDUCATION AND
RESEARCH, TAMAKA, KOLAR, KARNATAKA**

CERTIFICATE BY THE GUIDE

This is to certify that the dissertation entitled **“ROLE OF MULTIPARAMETRIC MAGNETIC RESONANCE IMAGING OF BRAIN IN DIFFERENTIATING NEUROCYSTICERCOSIS FROM TUBERCULOMA”** is a bonafide research work done by **Dr. LYNN JOY**, under my direct guidance and supervision at Sri Devaraj Urs Medical College, Kolar, in partial fulfilment of the requirement for the degree of **“M.D. RADIODIAGNOSIS”**.

Date:
Place: Kolar

Dr. ANIL KUMAR SAKALECHA, MBBS, MD
Professor and HOD,
Department of Radiodiagnosis
Sri Devaraj Urs Medical College
Tamaka, Kolar

**SRI DEVARAJ URS ACADEMY OF HIGHER EDUCATION AND
RESEARCH, TAMAKA, KOLAR, KARNATAKA**

CERTIFICATE BY THE HEAD OF DEPARTMENT

This is to certify that the dissertation entitled **“ROLE OF
MULTIPARAMETRIC MAGNETIC RESONANCE IMAGING OF BRAIN IN
DIFFERENTIATING NEUROCYSTICERCOSIS FROM TUBERCULOMA”** is a
bonafide research work done by **Dr. LYNN JOY**, under my supervision at Sri Devaraj
Urs Medical College, Kolar, in partial fulfilment of the requirement for the degree of
“M.D. RADIODIAGNOSIS”.

Date:
Place: Kolar

Dr. ANIL KUMAR SAKALECHA, MBBS, MD
Professor & HOD
Department Of Radiodiagnosis
Sri Devaraj Urs medical college & hospital
Tamaka, Kolar.

**SRI DEVARAJ URS ACADEMY OF HIGHER EDUCATION AND
RESEARCH, TAMAKA, KOLAR, KARNATAKA**

**ENDORSEMENT BY THE HEAD OF THE DEPARTMENT AND
PRINCIPAL**

This is to certify that the dissertation entitled, **“ROLE OF MULTIPARAMETRIC MAGNETIC RESONANCE IMAGING OF BRAIN IN DIFFERENTIATING NEUROCYSTICERCOSIS FROM TUBERCULOMA”** is a bonafide research work done by **Dr. LYNN JOY**, under the direct guidance and supervision of **Dr. ANIL KUMAR SAKALECHA**, Professor & HOD, Department of Radiodiagnosis, Sri Devaraj Urs Medical College, Kolar, in partial fulfilment of University regulation for the award **“M.D. DEGREE IN RADIODIAGNOSIS”**.

Dr. ANIL KUMAR SAKALECHA
Professor & HOD
Department Of Radiodiagnosis,
Sri Devaraj Urs Medical College,
Tamaka, Kolar.

Date:
Place: Kolar

DR. P.N.SREERAMULU
Principal,
Sri Devaraj Urs medical college,
Tamaka,
Kolar.

Date:
Place: Kolar

SRI DEVARAJ URS ACADEMY OF HIGHER EDUCATION AND RESEARCH

TAMAKA, KOLAR, KARNATAKA

ETHICAL COMMITTEE CERTIFICATE

This is to certify that the Ethical committee of Sri Devaraj Urs Medical College,
Tamaka, Kolar has unanimously approved

Dr. LYNN JOY

Post-Graduate student in the subject of

RADIODIAGNOSIS at Sri Devaraj Urs Medical College, Kolar

to take up the Dissertation work entitled

**“ROLE OF MULTIPARAMETRIC MAGNETIC RESONANCE
IMAGING OF BRAIN IN DIFFERENTIATING NEUROCYSTICERCOSIS
FROM TUBERCULOMA”**

to be submitted to the

SRI DEVARAJ URS ACADEMY OF HIGHER EDUCATION AND

RESEARCH, TAMAKA, KOLAR, KARNATAKA.

Date:

Place: Kolar

**Signature of Member Secretary
Ethical Committee**

**SRI DEVARAJ URS ACADEMY OF HIGHER EDUCATION AND
RESEARCH TAMAKA, KOLAR, KARNATAKA**

COPY RIGHT DECLARATION BY THE CANDIDATE

I hereby declare that Sri Devaraj Urs Academy of Higher Education and Research, Kolar, Karnataka shall have the rights to preserve, use and disseminate this dissertation/thesis in print or electronic format for academic/research purpose.

Date:

Place: Kolar

DR. LYNN JOY

Postgraduate

Department of Radio-diagnosis

Sri Devaraj Urs Medical College

Tamaka, Kolar

ACKNOWLEDGEMENT

*I owe debt and gratitude to my parents **P. A. JOY** and **LISSY JOY** and my sister **ANNE MARY JOY** for their moral support and constant encouragement during the study.*

*With humble gratitude and great respect, I would like to thank my teacher, mentor and guide, **Dr. ANIL KUMAR SAKALECHA**, Professor & Head of Department of Radiodiagnosis, Sri Devaraj Urs Medical College, Kolar, for his able guidance, constant encouragement, immense help and valuable advices which went a long way in moulding and enabling me to complete this work successfully. Without his initiative and constant encouragement this study would not have been possible. His vast experience, knowledge, able supervision and valuable advices have served as a constant source of inspiration during the entire course of my study.*

*I would like to express my sincere thanks to **Dr. DEEPTI NAIK**, Professor, Department of Radio-diagnosis, Sri Devaraj Urs Medical College for, valuable support, guidance and encouragement throughout the study. I would also like to thank **Dr. RAJESWARI**, Asso. Prof, Department of Radio-diagnosis, and **Dr. HARINI BOPAIAH**, Asso. Prof, Department of Radio-diagnosis, Sri Devaraj Urs Medical College for their wholehearted support and guidance.*

*I would also like to thank, **Dr. ANEES**, Assistant. Prof, Department of Radio-diagnosis and **Dr. RAHUL DEEP**, Assistant. Prof, Department of Radio-diagnosis for their support, guidance and encouragement throughout the study.*

*I would like to thank **Dr. VINEELA, Dr. MONISHA V, Dr. CHAITHANYA, Dr. AASHISH, Dr. YASHAS ULLAS L, Dr. SURAJ, Dr. VARSHITHA G.R.** and all my teachers of Department of Radio diagnosis, Sri Devaraj Urs Medical College and Research Institute, Kolar, for their constant guidance and encouragement during the study period.*

I am extremely grateful to the patients who volunteered for this study, without them this study would just be a dream.

*I am thankful to my postgraduates **Dr. MADAN, Dr. PRAVEEN, Dr. ARUN, Dr. R MAHIMA, Dr. UHASAI, , Dr. NIKHIL, Dr. SANDEEP, Dr. REVANTH, Dr. KRISHNA, Dr. GAURAV , Dr. POOJITHA, Dr. SHANTALA, Dr. SURYA, Dr. GURU YOGENDRA, Dr. SIVA, Dr. MANNAN and Dr. RISHI** for having rendered all their co-operation and help to me during my study.*

*I am also thankful to **Mr. RAVI, and Mr. SUBRAMANI** with other technicians of Department of Radiodiagnosis, R.L Jalappa Hospital & Research Centre, Tamaka, Kolar for their help.*

*My sincere thanks to **Mr. SUNIL, Mrs. NASEEBA, Mrs. HAMSA** and rest of the computer operators.*

Dr. LYNN JOY

Postgraduate,

Department of Radio-diagnosis

2/2/23, 10:42 AM

Turnitin - Originality Report - Role of Multiparametric Magnetic Resonance Im...

Turnitin Originality Report

Document Viewer

Processed on: 02-Feb-2023 10:37 IST
 ID: 2004596126
 Word Count: 10928
 Submitted: 1

Role of Multiparametric Magnetic Resonance
 Im... By Lynn Joy

Similarity Index
8%

Similarity by Source
 Internet Sources: 5%
 Publications: 6%
 Student Papers: 1%

☐ include quoted ☐ include bibliography ☐ excluding matches < 14 words mode:

-
- 1% match (Internet from 21-Oct-2022)
<http://jcdri.in> ☐
 - 1% match (Internet from 09-Mar-2016)
<http://louisdl.louislibraries.org> ☐
 - 1% match (Internet from 19-Jan-2023)
<https://core.ac.uk/download/pdf/235669068.pdf> ☐
 - 1% match (student papers from 02-Jan-2023)
 Submitted to Sharda University on 2023-01-02 ☐
 - 1% match (Internet from 12-Aug-2021)
https://biomedscidirect.com/download/UJMR-20162137/13/case_study_of_100_patients_with_intracranial_lesions_and_evaluation_of_int ☐
 - <1% match (Vasanthakumar Venugopal, Alex Daniel Prabhu, Ishrat Afshan, Mehvash Haider, Ekram Ullah, "Initial Experiences With a New MRI Scoring System for Differentiating Advanced Femoral Osteonecrosis From Tubercular Arthritis", Orthopedics, 2014)
 Vasanthakumar Venugopal, Alex Daniel Prabhu, Ishrat Afshan, Mehvash Haider, Ekram Ullah, "Initial Experiences With a New MRI Scoring System for Differentiating Advanced Femoral Osteonecrosis From Tubercular Arthritis", Orthopedics, 2014 ☐
 - <1% match ("ECR 2016 Book of Abstracts - B - Scientific Sessions and Clinical Trials in Radiology", Insights into Imaging, 2016.)
 "ECR 2016 Book of Abstracts - B - Scientific Sessions and Clinical Trials in Radiology", Insights into Imaging, 2016. ☐
 - <1% match (Pediatric Oncology, 2004.)
 Pediatric Oncology, 2004. ☐
 - <1% match (Jae Hoon Lee, Duke Whan Chung, Chung Soo Han, "Outcomes of anterolateral thigh-free flaps and conversion from external to internal fixation with bone grafting in gustilo type IIIB open tibial fractures", Microsurgery, 2012)
 Jae Hoon Lee, Duke Whan Chung, Chung Soo Han, "Outcomes of anterolateral thigh-free flaps and conversion from external to internal fixation with bone grafting in gustilo type IIIB open tibial fractures", Microsurgery, 2012 ☐
 - <1% match (A.A.K. A. Razek, "Role of Diffusion-Weighted Echo-Planar MR Imaging in Differentiation of Residual or Recurrent Head and Neck Tumors and Posttreatment Changes", American Journal of Neuroradiology, 06/01/2007)
 A.A.K. A. Razek, "Role of Diffusion-Weighted Echo-Planar MR Imaging in Differentiation of Residual or Recurrent Head and Neck Tumors and Posttreatment Changes", American Journal of Neuroradiology, 06/01/2007 ☐
 - <1% match (Internet from 14-Aug-2020)
https://maliadoc.com/imaging-spectrum-of-neurocysticercosis-core_5ba08939097c47ba7b8b4568.html ☐
 - <1% match (Diffusion-Weighted MR Imaging of the Brain, 2009.)
 Diffusion-Weighted MR Imaging of the Brain, 2009. ☐
 - <1% match (Internet from 13-Oct-2019)
<https://www.ncbi.nlm.nih.gov/pubmed/25977902> ☐
 - <1% match (G. Luthra, "Comparative Evaluation of Fungal, Tubercular, and Pyogenic Brain Abscesses with Conventional and Diffusion MR Imaging and Proton MR Spectroscopy", American Journal of Neuroradiology, 08/01/2007)
 G. Luthra, "Comparative Evaluation of Fungal, Tubercular, and Pyogenic Brain Abscesses with Conventional and Diffusion MR Imaging and Proton MR Spectroscopy", American Journal of Neuroradiology, 08/01/2007 ☐
 - <1% match (Internet from 29-Jan-2023)
https://www.researchgate.net/publication/339521275_Management_of_intracranial_tuberculous_mass_lesions_How_long_should_we_trea ☐
 - <1% match ("Neuroimaging", Springer Science and Business Media LLC, 2000)
 "Neuroimaging", Springer Science and Business Media LLC, 2000 ☐
 - <1% match (Internet from 07-May-2021)
https://mts.intechopen.com/storage/books/1348/authors_book/authors_book.pdf ☐
 - <1% match ("Imaging of CNS Infections and Neuroimmunology", Springer Science and Business Media LLC, 2019)
 "Imaging of CNS Infections and Neuroimmunology", Springer Science and Business Media LLC, 2019 ☐
 - <1% match (Pratibha Singh, ARUSHI GAHLOT, "Pediatric neurocysticercosis: current challenges and future prospects", Pediatric Health, Medicine and Therapeutics, 2016)
 Pratibha Singh, ARUSHI GAHLOT, "Pediatric neurocysticercosis: current challenges and future prospects", Pediatric Health, Medicine and Therapeutics, 2016 ☐
 - <1% match ("Functional Imaging in Oncology", Springer Science and Business Media LLC, 2014)
 "Functional Imaging in Oncology", Springer Science and Business Media LLC, 2014 ☐

https://www.turnitin.com/newreport_classic.asp?lang=en_us&oid=2004596126&ft=1&bypass_cv=1

University Library
 Learning Resource Centre
 SDUAHER, Tamaka
 KOLAR-563103

Prof. & HOD
 Dept. of Radiodiagnosis
 Sri Devaraj Urs Medical College
 Tamaka, Kolar-563101.



Digital Receipt

This receipt acknowledges that Turnitin received your paper. Below you will find the receipt information regarding your submission.

The first page of your submissions is displayed below.

Submission author: Lynn Joy
Assignment title: Role of Multiparametric Magnetic Resonance Imaging of Bra...
Submission title: Role of Multiparametric Magnetic Resonance Imaging of bra...
File name: thesis_ncc_tub.docx
File size: 10.2M
Page count: 121
Word count: 10,928
Character count: 60,181
Submission date: 02-Feb-2023 10:36AM (UTC+0530)
Submission ID: 2004596126

ABSTRACT

Introduction: The two most common infectious causes of ring enhancing lesions are neurocysticercosis (NCC) & tuberculoma. It is a challenge to differentiate NCC and tuberculoma radiologically since they show the same imaging findings on computed tomography (CT). Hence, this study was performed to assess the role of Magnetic Resonance Imaging (MRI) as an additional advanced modality to apply characterize the lesions. Conventional MRI with additional advanced imaging sequences like Diffusion Weighted Imaging (DWI), Apparent Diffusion Coefficient (ADC), Magnetic Resonance Spectroscopy (MRS) and Post Contrast T1 weighted imaging aids in characterizing the lesions and help in differentiating NCC and tuberculoma.

Material and methods: Individuals who matched the inclusion criterion underwent Magnetic Resonance Imaging (MRI) of Brain (Plain & Contrast) in 1.5 Tesla, 18 channel, MR Scanner (Siemens Magnetom Avanto). Following imaging sequences were included: T1WI (Axial & Sagittal), T2WI (Axial & Coronal), FLAIR, DWI at 0, 100 and 1000 mm/s² b values with corresponding ADC values & Multivoxel MRS. Based on MRI features such as number, size, shape, location, wall thickness, enhance nodule, surrounding edema, diffusion weighted imaging features with corresponding ADC values, enhancement pattern of lesions and spectroscopy findings, we evaluated and differentiated the lesions as neurocysticercosis or Tuberculoma. Radiological diagnosis were correlated in terms of response to treatment.

Results: In our study, 42 subjects were included of which total number of neurocysticercosis cases were 25 (59.52 %) and tuberculoma were 17 (40.47 %). The mean

[Signature] 2/2/23
University Library
Learning Resource Centre
SDUAHER, Tamaka
KOLAR-563103

[Signature]
Prof. & HOD
Dept. of Radiodiagnosis
Sri Devaraj Urs Medical College
Tamaka, Kolar-563101.

Copyright 2023 Turnitin. All rights reserved.




SRI DEVARAJ URS ACADEMY OF HIGHER EDUCATION & RESEARCH
Tamaka, Kolar 563103

Certificate of Plagiarism Check


Title of the Thesis/Dissertation	ROLE OF MULTIPARAMETRIC MAGNETIC RESONANCE IMAGING OF BRAIN IN DIFFERENTIATING NEUROCYSTICERCOSIS FROM TUBERCULOMA
Name of the Student	Dr. LYNN JOY
Registration Number	20RD1027
Name of the Supervisor / Guide	Dr. ANIL KUMAR SAKALECHA
Department	RADIO-DIAGNOSIS
Acceptable Maximum Limit (%) of Similarity (PG Dissertation /Ph.D. Thesis)	10%
Similarity	8%
Software used	Turnitin
Paper ID	2004596126
Submission Date	02/02/2023


Signature of Student


Signature of Guide/Supervisor
Prof. & HOD


HOD Signature
Dept. of Radiodiagnosis
Sri Devaraj Urs Medical College
Tamaka, Kolar-563101.


University Librarian
University Library
Learning Resource Centre
SDUAHER, Tamaka
KOLAR-563103


Coordinator UG and PG Program
Co-Ordinator,
UG&PG Program, Faculty of Medicine,
Sri Devaraj Urs Medical College,
Tamaka, Kolar- 563103

LIST OF ABBREVIATIONS:

Glossary	Expansion
ADC	Apparent Diffusion Coefficient
BBB	Blood Brain Barrier
CECT	Contrast Enhanced CT
CISS	Constructive Interference in Steady State
CMI	Cell Mediated Immunity
CNS	Central Nervous System
CSF	Cerebro Spinal Fluid
CSI	Chemical Shifting Imaging
CT	Computed Tomography
DCE	Dynamic Contrast Enhanced
DOT	Directly Observed Treatment
DWI	Diffusion Weighted Imaging
ELISA	Enzyme Linked Immunosorbent Assay
FLAIR	Fluid-Attenuated Inversion Recovery
HIV	Human Immuno Deficiency Virus
ICT	Intra Cranial Tension
MRI	Magnetic Resonance Imaging
MRS	Magnetic Resonance Spectroscopy
NAA	N-Acetylaspartate
NCC	Neurocysticercosis
rCBV	Relative Cerebral Blood Volume
SAN	Subarachnoid Neurocysticercosis
SI	Signal Intensity
SRS	Stereotactic Radiosurgery

SWI	Susceptibility-weighted Imaging
TB	Tuberculosis
TBM	Tubercular Meningitis
TNF	Tumor Necrosis Factor
VOI	Volume of Interest
WHO	World Health Organisation

ABSTRACT

Introduction: The two most common infectious causes of ring enhancing lesions are neurocysticercosis (NCC) & tuberculoma. It is a challenge to differentiate NCC and tuberculomas radiologically since they show the same imaging findings on computed tomography (CT). Hence, this study was performed to assess the role of Magnetic Resonance Imaging (MRI) as an additional advanced modality to aptly characterize the lesion. Conventional MRI with additional advanced imaging sequences like Diffusion Weighted Imaging (DWI), Apparent Diffusion Coefficient (ADC), Magnetic Resonance Spectroscopy (MRS) and Post Contrast T1 weighted imaging aids in characterizing the lesion and help in differentiating NCC and tuberculomas.

Objectives: To compare the findings of diffusion weighted imaging, apparent diffusion coefficient cut off values, spectroscopy and contrast enhanced MRI in differentiating neurocysticercosis from tuberculoma.

Material and Methods: Individuals who matched the inclusion criterion underwent Magnetic Resonance Imaging (MRI) of Brain (Plain & Contrast) in 1.5 Tesla, 18 channel, MR Scanner (Siemens® Magnetom Avanto®). Following Imaging sequences were included -T1WI (Axial & Sagittal), T2WI (Axial & Coronal), FLAIR, DWI at 0, 500 and 1000 mm²/s 'b' values with corresponding ADC values & Single Voxel MRS . Based on MRI features such as number, size, location, margins of lesions, scolex, surrounding edema, diffusion weighted imaging features with corresponding ADC values, enhancement pattern of lesions and spectroscopy findings, we evaluated and differentiated the lesions as neurocysticercosis or Tuberculoma. Radiological diagnosis were correlated in terms of clinical symptoms and response to treatment.

Results: In our study, 42 subjects were included of which total number of neurocysticercosis cases were 25 (59.52 %) and tuberculoma were 17 (40.47 %). The mean age of patients included was 42.85 ± 14.76 years (21 to 78 years). On post contrast imaging, all 25 cases of Neurocysticercosis (100 %) showed thin ring enhancement whereas majority of Tuberculomas (64.7%) showed thick irregular ring enhancement. On MR Spectroscopy, all 25 cases (100 %) of Neurocysticercosis showed amino acid peak and all 17 cases (100 %) of Tuberculoma showed lipid lactate peak. On DWI, out of 25 Neurocysticercosis cases, restriction of diffusion was absent in majority of cases (88 %) and out of 17 cases of Tuberculoma, restriction of diffusion was present in 12 cases (70.5 %) (T2 hyperintense tuberculoma, indicative of caseating tuberculoma with central liquefaction) and was absent in the rest. In our study, mean ADC value of NCC lesions ($1.30 \pm 0.137 \times 10^{-3} \text{ mm}^2/\text{s}$) was found to be greater than that of Tuberculoma ($0.74 \pm 0.090 \times 10^{-3} \text{ mm}^2/\text{s}$). ADC value of 1.2×10^{-3} was obtained as cut-off to differentiate Neurocysticercosis and Tuberculoma. The ADC cut off value of $1.2 \times 10^{-3} \text{ mm}^2/\text{s}$ showed sensitivity of 92 % and specificity of 94.1 % in differentiating Neurocysticercosis from Tuberculoma.

Conclusions: Conventional MRI with additional advanced imaging sequence likes DWI, ADC, MRS and post contrast T1WI aids in characterizing the lesion and thereby helps in differentiating NCC and tuberculomas. Hence, Multiparametric MRI assessment is useful in making a prompt diagnosis and eliminating the need for biopsy.

Key words: NCC, Tuberculoma, Diffusion weighted Imaging, ADC values, MR Spectroscopy.



TABLE OF CONTENTS

S. NO	TOPIC	PAGE NO
1.	INTRODUCTION	1
2.	AIMS & OBJECTIVES	4
3.	REVIEW OF LITERATURE	5
4.	MATERIALS & METHODS	53
5.	RESULTS	58
6.	IMAGES	77
7.	DISCUSSION	89
8.	LIMITATIONS	95
9.	CONCLUSION	96
10.	SUMMARY	97
11.	BIBLIOGRAPHY	99
12.	ANNEXURE	111

LIST OF TABLES

S. NO	DESCRIPTION	PAGE NO
1	Most common MR sequences and their TE and TR durations	8
2	Meningeal and parenchymal patterns of involvement of intracranial tuberculosis	16
3	MR imaging features of different stages of Tuberculoma	25
4	Role of MRI in differentiating NCC and Tuberculoma	50
5	Descriptive analysis of age in study population (n=42)	58
6	Descriptive analysis of gender distribution in the study population (n=42)	59
7	Descriptive analysis of number of lesions in study population (n=42)	61
8	Descriptive analysis of number of lesions in NCC and Tuberculoma (n=42)	62
9	Descriptive analysis of location of lesion in the study population (n=42)	63
10	Descriptive analysis of size of lesions in the study population (n=42)	64
11	Descriptive analysis showing margin of lesions (n=42)	65
12	Descriptive analysis showing degree of peri-lesional edema in the study population (n=42)	66
13	Descriptive analysis of presence of scolex within the lesion in the study population (n=42)	67
14	Descriptive analysis of features of meningitis in the study population (n=42)	68

15	Descriptive analysis of post contrast features of lesions in the study population (n=42)	69
16	Descriptive analysis of diffusion-weighted imaging findings of lesions in the study population (n=42)	70
17	Comparative analysis of ADC value of Neurocysticercosis and Tuberculoma in study population(n= 42)	71
18	Comparative analysis of ADC value of T2 hyperintense and T2 hypointense Tuberculomas in study population (n= 17)	71
19	Descriptive analysis of ADC cut off value in study population (n= 42)	73
20	Predictive validity of ADC cut off value of 1.2×10^{-3} in differentiating NCC from Tuberculoma (n=42)	74
21	Descriptive analysis of MR Spectroscopy imaging findings of lesions in the study population (n=42)	75
22	Descriptive analysis of final MRI diagnosis and final clinical diagnosis (n=42)	76

LIST OF FIGURES

SL.NO	DESCRIPTION	PAGE NO
1	Schematic representation of DWI.	9
2	Schematic representation of Signal intensity of DWI and ADC in diffusion restriction, increased diffusion	10
3	Normal brain proton MR spectroscopy in a healthy volunteer.	11
4	Mycobacterium Tuberculosis	12
5	Schematic representation of Bacilli reaching the lungs provoking a host immune response.	14
6	Pathogenesis of CNS tuberculosis	15
7	Meningeal tuberculosis	17
8	Tubercular abscess	19
9	Illustration of Tuberculoma with caseous necrotic center	22
10	Target sign in Tuberculoma.	24
11	Axial contrast enhanced T1 Weighted MR images showing multiple tuberculomas with accompanying meningitis	26
12	Axial contrast enhanced T1 Weighted MR images showing multiple conglomerate tuberculomas with accompanying meningitis	26
13	Magnetic resonance imaging appearance of tuberculoma based on different stages of maturation	27
14	MRI DWI and ADC images of non-caseating and caseating granuloma in Tuberculoma	29
15	MR Spectroscopy Image showing lipid lactate peak in left frontal parafalcine tuberculoma	31

16	Image of Adult Taenia Solium	33
17	Development cycle of T.Solium	35
18	MRI Brain images demonstrating subarachnoid Neurocytsicercosis	40
19	MRI Spine images demonstrating Spinal Neurocysticercosis	41
20	Vesicular stage of NCC	42
21	Colloid Vesicular stage of NCC	43
22	Multiple ring enhancing lesions in Colloid Vesicular Stage of NCC	44
23	Nodular-granular stage of Neurocysticercosis	44
24	MR images demonstrating restricted diffusion in scolex in a case of NCC	46
25	MRS in NCC	47
26	1.5 Tesla, 18 channel, MR Scanner (Siemens® Magnetom Avanto)	56
27	Bar chart showing age distribution in our study cases (n=42)	58
28	Pie chart showing gender distribution in the study population (n=42)	59
29	Doughnut chart showing total number of cases included(n=42)	60
30	Pie chart showing number of lesions in study population (n=42)	61
31	Bar chart showing number of lesions in NCC and Tuberculoma (n=42)	62
32	Bar chart showing location of lesions in the study population (n=42)	63

33	Bar chart showing size of lesions in NCC and Tuberculoma (n=42)	64
34	Bar chart showing margin of lesions (n=42)	65
35	Bar chart showing peri-lesional edema (n=42)	66
36	Bar chart showing presence of scolex within the lesion in the study population (n =42)	67
37	Bar diagram showing pattern of ring enhancement of lesions in the study population (n=42)	69
38	Bar diagram showing diffusion weighted imaging features of lesions in the study population (n=42)	70
39	ROC analysis of Predictive validity of ADC value of lesions in differentiating Neurocysticercosis from Tuberculoma (n=42)	72
40	MRI images demonstrating number of lesions in our study cases	77
41	MR FLAIR images showing Degrees of edema surrounding lesions	77
42	MRI images demonstrating size of lesions in our study cases	78
43	MRI T1W Axial and Saggital images showing Scolex in a case of Neurocysticercosis	78
44	MR Post Contrast images in Neurocysticercosis and Tuberculoma	79
45	MR spectroscopy peaks in NCC and Tuberculoma	79
46	Diffusion weighted imaging features in a case of Neurocysticercosis	80
47	Diffusion weighted imaging features in a case of Tuberculoma	80
48	Vesicular Stage of NCC	81
49	Colloidal vesicular stage of Neurocysticercosis	82

50	Granular Nodular stage of NCC	83
51	Calcified stage of Neurocysticercosis	83
52	Intraventricular NCC	84
53	Tuberculoma- Caseating granulomas with central liquefaction	85
54	Tuberculoma- Caseating granulomas without central liquefaction	86
55	Follow up of a case of Neurocysticercosis	87
56	Follow up of a case of Tuberculoma	88

INTRODUCTION



INTRODUCTION

The two most common granulomatous lesions encountered in India are tuberculomas and NCC which are also the two most common causes of ring-enhancing lesions on CT and MRI.¹

Tuberculosis is caused by *Mycobacterium tuberculosis*. The most common form of central nervous system (CNS) tuberculosis is tuberculoma.^{2,3} CNS tuberculomas are difficult to diagnose and because of their vague symptoms, early radiological diagnosis is essential.³ Biopsy with histopathological analysis provides a definitive diagnosis but it is only used when non-invasive methods are not conclusive.⁴

Neurocysticercosis is endemic in many underdeveloped countries.^{5,6} The larval stage of the pig tapeworm, *Taenia Solium* causes cysticercosis.^{7,8} Symptoms such as seizures and/or headaches are seen in cysticercosis.⁹

Patients with suspected CNS tuberculoma and NCC should be evaluated with CT and MRI scan of the brain.¹⁰ It is a challenge to differentiate NCC and tuberculomas on computed tomography (CT) since they show similar imaging findings. Hence, this study was performed to assess the role of Magnetic Resonance Imaging (MRI) as an additional advanced modality to aptly characterize the lesion. The morphological and anatomical details of these lesions can be revealed by conventional MRI. In conventional MRI, the number, size, shape, location, wall thickness of lesions, presence of scolex, extent of surrounding edema can be assessed which would help in characterizing both these granulomatous lesions.¹¹

In addition to the conventional MRI sequences, MRI sequences such as T1 W post contrast sequence, Diffusion Weighted Imaging (DWI), Apparent Diffusion Coefficient (ADC) and Magnetic Resonance Spectroscopy (MRS) alone or in combination help in

further characterization and differentiation of these granulomatous ring enhancing lesions.

Diffusion-weighted imaging (DWI) is a form of MR imaging based upon measuring the random Brownian motion of water molecules within a voxel of tissue. DWI would increase the possibility of accurate diagnosis and differentiation of NCC and Tuberculoma as it is based on restriction of water molecules by lesion. ADC is a quantitative measurement of diffusion derived from DWI. In lesions with hampered diffusion, ADC value will be low and in lesions where is free movement of water molecules without restriction, ADC value will be high.

MR Spectroscopy is a non-invasive MR sequence that has been used to study metabolic changes in neuroinfection, seizure disorders, brain tumors, strokes, Alzheimer's disease, depression and other diseases affecting the brain. It provides additional biochemical information of the lesion. MRS can help in differentiating granulomatous ring enhancing conditions like Tuberculoma and NCC as specific peaks are found on MRS in Tuberculoma and NCC.

This study was performed to assess the role of Multiparametric Magnetic Resonance Imaging (MRI) in aptly differentiating Neurocysticercosis and Tuberculomas.

NEED FOR THE STUDY

In developing countries, Neurocysticercosis (NCC) and Tuberculoma are the two most common infectious causes of ring enhancing lesions. The differentials of ring enhancing lesions include both neoplastic and non-neoplastic causes and differentiating these lesions are a diagnostic problem in neuroimaging.¹² Tuberculoma and Neurocysticercosis are common causes of acquired seizures in the developing countries especially in pediatric population.¹³

NCC is caused by the larval stage of *Taenia solium* (pork tapeworm). NCC has four different stages- the vesicular, colloidal vesicular, granular nodular and nodular calcified which are recognized on imaging.

Tuberculosis is caused by *Mycobacterium tuberculosis*. The most common form of central nervous system (CNS) tuberculosis is tuberculoma.¹⁴

It is a challenge to differentiate NCC and tuberculomas radiologically since they show the same imaging findings on computed tomography (CT). Hence, an additional modality is required to aptly characterize the lesions. Conventional MRI with additional imaging sequences like diffusion weighted imaging (DWI), apparent diffusion coefficient (ADC), magnetic resonance spectroscopy (MRS) and post contrast T1 weighted imaging aids in characterizing the lesion and thereby helps in differentiating NCC and tuberculomas for appropriate treatment.¹⁵ MRS can provide additional biochemical information of the lesion and DWI would increase the possibility of accurate diagnosis as it is based on restriction of water molecules by lesion.¹⁶

AIMS AND OBJECTIVES



AIMS AND OBJECTIVES

- To compare the findings of diffusion weighted imaging, Apparent Diffusion Coefficient cut off values, Spectroscopy and contrast enhanced MRI in differentiating Neurocysticercosis from Tuberculoma.

REVIEW OF LITERATURE



Ring Enhancing Lesions in CNS:

One of the most common abnormalities in neuroimaging is multiple ring-enhancing lesions. These lesions are found on CT and MRI, two imaging methods that are widely available. Multiple ring-enhancing lesions in the brain may be caused by a variety of different etiologies.^{17,18} These lesions appear as iso- to hypodense or hypointense lesions on plain CT or MRI. Following injection of contrast, the area of hypodensity or hypointensity shows a ring- or homogenous disc-like enhancement. The enhancing lesions typically have different sizes and varying degrees of perilesional edema around them and are generally seen adjacent to the grey-white matter junction.¹⁹

Multiple ring-enhancing lesions in the brain can be caused by viral, neoplastic, inflammatory or vascular diseases. It can be caused by a variety of brain tumours, including low-grade gliomas, glioblastomas, brain metastases and lymphomas. Other conditions include pyogenic abscess, tuberculosis, cysticercosis, toxoplasmosis, radiation encephalopathy, demyelinating illnesses, neurosyphilis, and a number of other vasculitic conditions.^{20, 21}

The two most common causes of ring-enhancing lesions on CT and MRI are tuberculomas and NCC which are also the two most common granulomatous lesions encountered in India.¹

Imaging techniques in cerebral ring enhancing lesions:

Role of computed tomography (CT)

Computed tomography (CT) is a diagnostic imaging test used to create detailed images of internal organs. The cross-sectional images generated during a CT scan can be reformatted in multiple planes, and can even generate three-dimensional images

which can be viewed on a computer monitor, printed on film or transferred to electronic media.²²

On Plain CT, granulomatous infectious diseases like NCC and tuberculoma can be identified as iso-hypodense parenchymal lesions. Calcifications can also be identified on plain CT. On contrast enhanced computed tomography, these appears as iso-hypodense ring enhancing lesions with varying degrees of peri-lesional edema. However, the use of CT in differentiating neurocysticercosis from tuberculoma is limited and MRI is considered superior for the same.²²

Role of magnetic resonance imaging (MRI):

MRI is a non-invasive method of mapping the internal structure and certain aspects of function within the body . It uses non-ionizing electromagnetic radiation with no risk of exposure related hazard. It uses radio frequency (RF) radiation in the presence of precisely controlled magnetic fields to generate high-quality cross-sectional figures of the body in any plane. The MR image is created by placing the patient inside a large magnet that generates a relatively strong external magnetic field. This causes the nuclei of many atoms in the body, including hydrogen, to align with the magnetic field, and the RF signal to be applied later. The body emits energy, which is detected and used by the computer to create the MR image.²³

Multiparametric MRI Protocol

The morphological and anatomical details of these lesions can be revealed by conventional MRI. Conventional MRI sequences include T1WI, T2WI and FLAIR sequences. In addition to these conventional MRI sequences, Multiparametric MRI protocol includes sequences like Post contrast T1W, and Diffusion-Weighted Imaging

(DWI), Apparent diffusion co-efficient (ADC) sequence and Magnetic Resonance Spectroscopy (MRS).²³

Multiparametric MRI protocol includes :

- T1W axial and sagittal
- T2W axial and coronal
- FLAIR axial and sagittal
- Axial Diffusion-weighted Imaging (DWI) at 0, 500 and 1000 mm²/s b values with corresponding ADC values.
- Post contrast T1W 3D axial MPRAGE. Contrast used will be gadolinium in the dose of 1.5ml/Kg.
- Single Voxel Spectroscopy- Performed using chemical shift imaging.

T1 Weighted Imaging :

It is the most frequently employed MR sequence. Images are produced using Short TE and TR timings. T1 weighted images are used mostly to evaluate the normal anatomy.²³ Ring enhancing granulomatous lesions like Tuberculoma and NCC appear as iso-hypointense parenchymal lesions in this sequence.

T2 Weighted Imaging :

T2W imaging is included in standard MRI protocol. In order to obtain T2-weighted images, longer TE and TR durations are used. T2W images with FS will enable easy visualization of cystic lesion in the brain. T2W images without FS allows better depiction of the lesion morphology.²³ For example, while evaluating granulomatous lesions like tuberculoma, the signal intensity of core of the lesion is important. Caseating granulomas with central liquefaction appear hyperintense on T2 Weighted

images and caseating granulomas without central liquefaction appear hypointense on T2 Weighted images.

Flair sequence :

Another widely used sequence is fluid attenuated inversion recovery (FLAIR). When compared to a T2-weighted images, the TE and TR timings of the Flair sequence are much longer.

Brain tissue on FLAIR images appears similar to T2 weighted images with grey matter brighter than white matter but CSF is dark instead of bright. As a result, any abnormalities or lesions remain visible. This sequence helps in easy distinction between CSF and an abnormality and is highly sensitive to disease or lesion detection.²³ This sequence is also helpful in the detection of peri-lesional edema.

Table 1: Most common MR sequences and their TE and TR durations

	TR (msec)	TE (msec)
T1-Weighted (short TR and TE)	500	14
T2-Weighted (long TR and TE)	4000	90
Flair (very long TR and TE)	9000	114

Contrast-Enhanced MR Imaging:

Prior to the delivery of contrast material, a native T1W sequence should be obtained. Contrast should be given at a max dose of 0.1 mmol/kg body weight. These post-contrast images are mostly used for lesion detection. For MR imaging of the CNS, gadolinium-based contrast agents are injected. These agents have the capacity to momentarily aggregate in regions with a compromised blood-brain barrier (BBB), which causes visible contrast enhancement.²⁴

Smooth and thin ring enhancements are seen in organising abscesses and granulomatous lesions like Neurocysticercosis whereas thick, uneven and nodular ring enhancement points to a necrotic tumour or another granulomatous ring enhancing lesion like Tuberculoma. Other patterns of enhancement include incomplete ring enhancement which is seen in demyelinating conditions.²⁴

Diffusion Weighted MR Imaging, Apparent diffusion co-efficient (ADC) sequence & its corresponding values.

The use of spin diffusion measurements in MRI by Le Bihan and Breton in 1985 resulted in a new technique known as 'diffusion-weighted' imaging. The random water molecular movement within tissue is quantified by DWI which is influenced by microstructure of tissue and its cellular density. Normal tissue without restriction of diffusion appears darker in diffusion images and damaged tissue with restricted diffusion appears brighter in diffusion images.

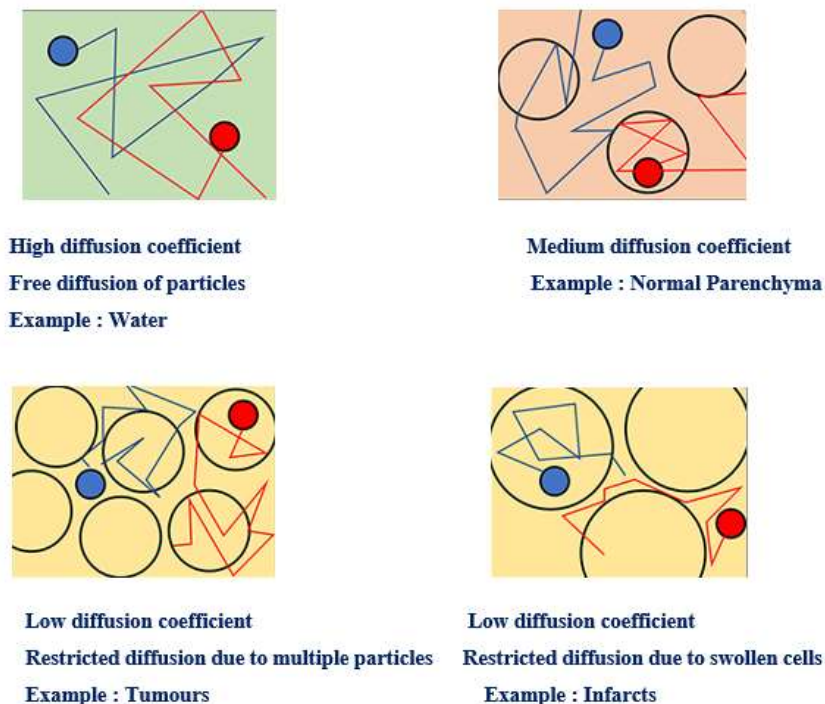


Figure 1: Schematic representation of DWI.

The apparent diffusion coefficient (ADC), which is the net displacement of molecules, is used in diffusion weighted MRI to study the diffusion of water in tissues. Each tissue voxel's ADC is determined, and the signal intensity is assigned based on this ADC value, to produce ADC maps. In ADC maps, restricted tissue (i.e. with pathology) has a low ADC and appears darker (low signal) whereas normal tissue with no restriction has high ADC.²⁵

ADC is a quantitative measurement of diffusion derived from DWI. Values are expressed in $10^{-3} \text{ mm}^2/\text{s}$. Because of the hampered diffusion in carcinomas and lesions with liquefactive necrosis like Tuberculomas, mean ADC is generally low (range: $0.7\text{--}1.2 \times 10^{-3} \text{ mm}^2/\text{s}$) compared with to that of benign lesions and other granulomatous lesions like NCC (range: $1.2\text{--}1.8 \times 10^{-3} \text{ mm}^2/\text{s}$).²⁵

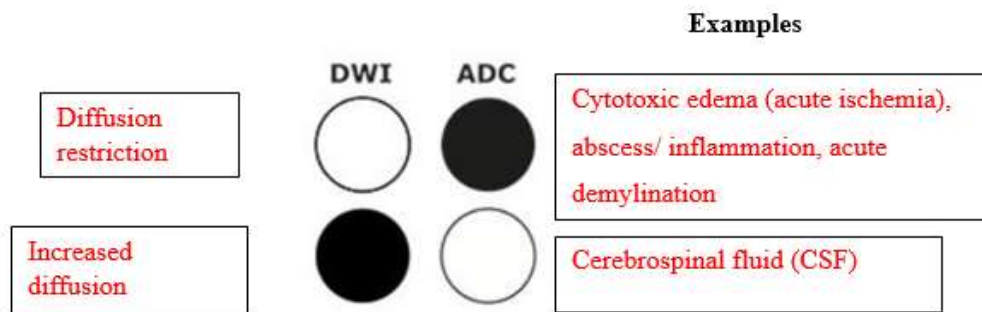


Figure 2: Schematic representation of Signal intensity of DWI and ADC in diffusion restriction, increased diffusion

Magnetic Resonance Spectroscopy (MRS)

Magnetic resonance (MR) spectroscopy is an MRI sequence that can measure metabolic changes in the brain. MRS data is presented as line spectra, with the area beneath each peak denoting the relative concentration of nuclei seen for a particular chemical species. The frequency shift localising the metabolite is indicated on the x-axis in parts per million. A volume of interest (VOI; voxel) is chosen for MRS using

the acquired picture, and the field therein is further refined using a technique called shimming. Then, by suppressing their specific frequency band, the H₂O protons within the VOI are rendered silent (termed water suppression). The identical switching magnetic field arrangement from an MRI scan is then used to acquire a frequency profile or spectrum. The spectrum is a typical outcome of the metabolite composition of the sample because frequency is a measure of chemical structure.²⁴

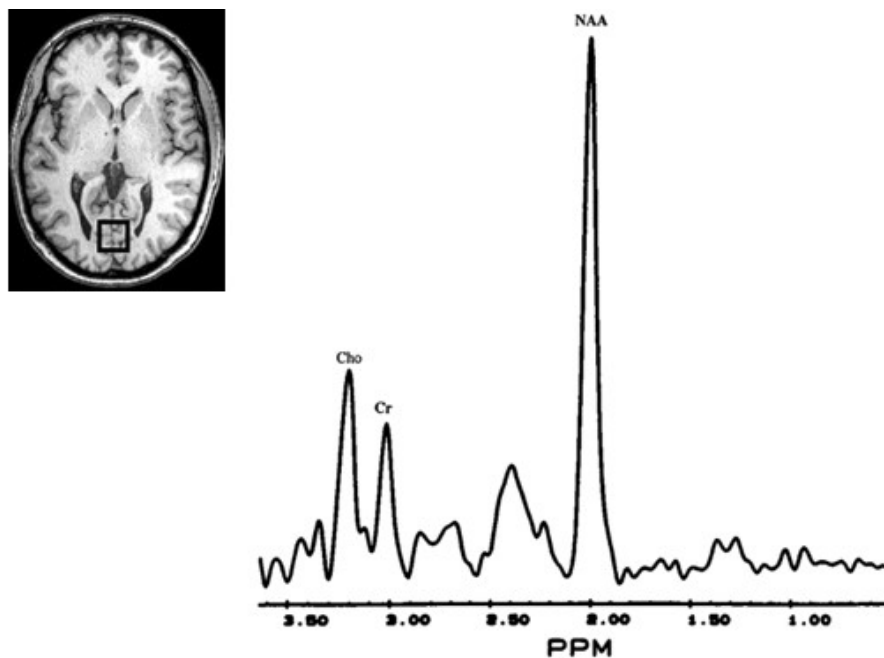


Figure 3: Normal brain proton MR spectroscopy obtained in a healthy volunteer.

Different lesions show different MR Spectroscopy peaks. Based on the peak, we can differentiate different cerebral lesions. For example, the presence of choline peak points towards a tumour, amino acid peaks such as acetate or succinate point towards NCC and lipid lactate peak points towards tuberculoma.

Tuberculosis:

The most common infectious cause of death globally is *Mycobacterium tuberculosis*, which causes tuberculosis (TB). *M. tuberculosis*' natural reservoir is the human host. Inhalation of *M. tuberculosis*-containing aerosol droplets, followed by deposition in the lungs, results in one of two outcomes:

- Primary disease: the first instance of an active illness
- Reactivation disease: Appearance of active disease several years after a period of dormant infection.²⁶ Reactivation is more likely in patients with HIV and other medical problems.²⁷

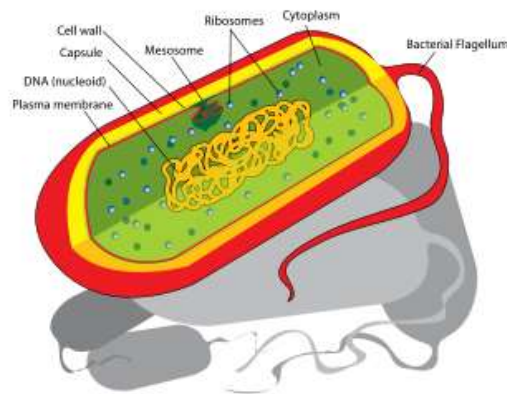


Figure 4: Mycobacterium Tuberculosis³⁰

Epidemiology of tuberculosis:

M. tuberculosis is thought to infect more than 1.7 billion individuals and approximately 22% of the world's population. The prevalence of TB peaked worldwide in 2003 and has since been progressively declining.²⁸ The self-reported incidence of TB in India is 305/100,000, as per data from the National Family Health Survey (NFHS-4). Compared to the current figures, the true prevalence of tuberculosis in India is probably higher. This may be due to underreporting of cases or due to undiagnosed cases.²⁹

Etiopathogenesis:

When the tubercle bacteria are transported in droplets small enough to enter the alveolar space, they cause infection in the lungs (5 to 10 microns). When in the lungs, macrophages secrete cytokines and chemokines that draw in neutrophils, monocytes, and other alveolar macrophages. These phagocytic cells eventually join together to create a tubercle, which is a nodular granulomatous structure. If the bacterial growth is not controlled, the tubercle will grow and eventually the bacteria will enter the adjacent draining lymph nodes. As a result, lymphadenopathy, a classic indication of primary TB, appears. The lesion (called Ghon focus) produced by the extension of the tubercle into the lung parenchyma along with lymph node enlargement and calcification together comprise the Ranke complex.³⁰

In majority (90%) of the exposed and infected people, the bacilli continues to multiply until an efficient cell-mediated immune (CMI) response develops, often 3 to 11 weeks after first infection. The host's inability to develop a potent CMI response may result in progressive lung deterioration. Reactive oxygen and nitrogen intermediates, Tumor necrosis factor (TNF)-alpha, as well as cytotoxic cell components (granzymes, perforin), which are responsible for killing *M. tuberculosis*, may also result in collateral host cell damage and the formation of caseating necrosis.³⁰

Undiagnosed or untreated bacterial growth can cause bacilli to spread hematogenously and cause disseminated TB. Miliary TB is the word used to describe a widespread illness with lesions that resemble millet seeds. In up to 80% of cases, death results from lack of care.³¹ The other patients either develop a chronic illness or recover. Rarely do the bacilli completely disappear spontaneously.

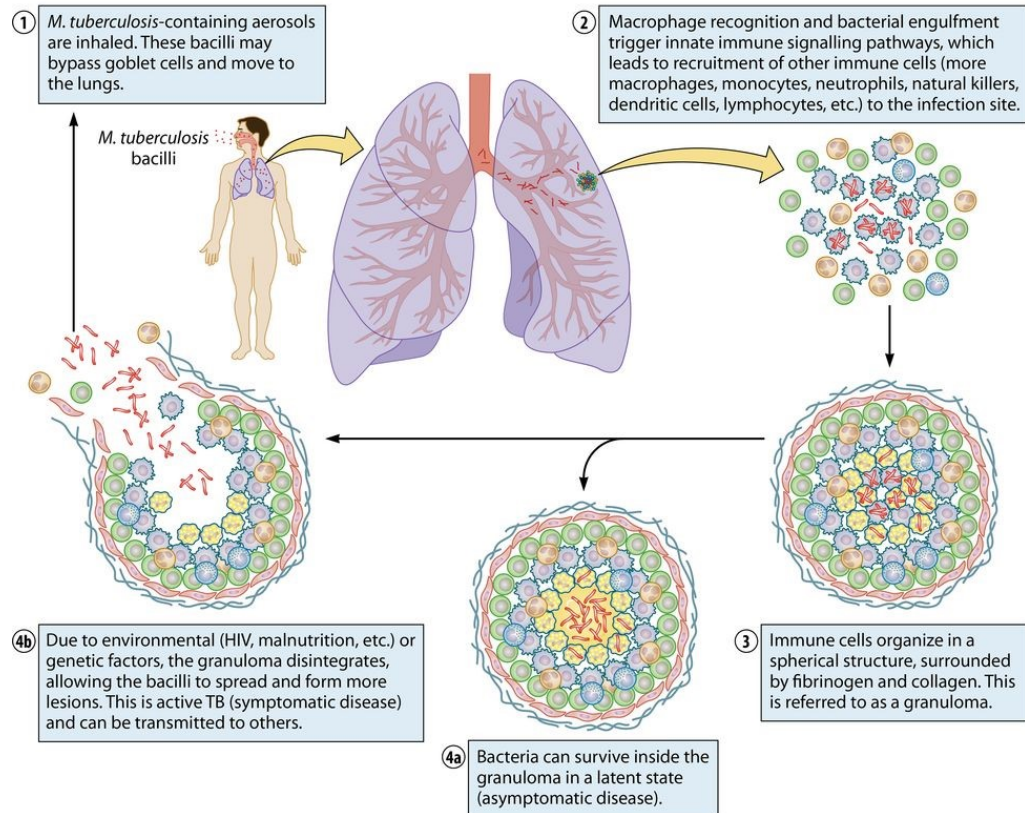


Figure 5 : Schematic representation of Bacilli reaching the lungs provoking a host immune response³²

Step 1- Bacilli reaching the lungs; step 2- provoking a host immune response

Step 3 - Granuloma formation ; step 4a- Suppression of infection in latent stage

Step 4b- Reactivation resulting in an active disease state in which the disease can spread to other individuals.

CNS Tuberculosis:

Approximately 1 to 5 percent of patients with tuberculosis develop CNS TB.³² This is seen in regions where there is high rate of post-primary spread of Tuberculosis among children and young people. A major risk factor for CNS TB is HIV.³³ The presence of HIV infection raises the probability of CNS involvement in patients by five times compared to those patients without HIV infection; this risk is significantly higher in those patients with low CD4 counts.^{34, 35}

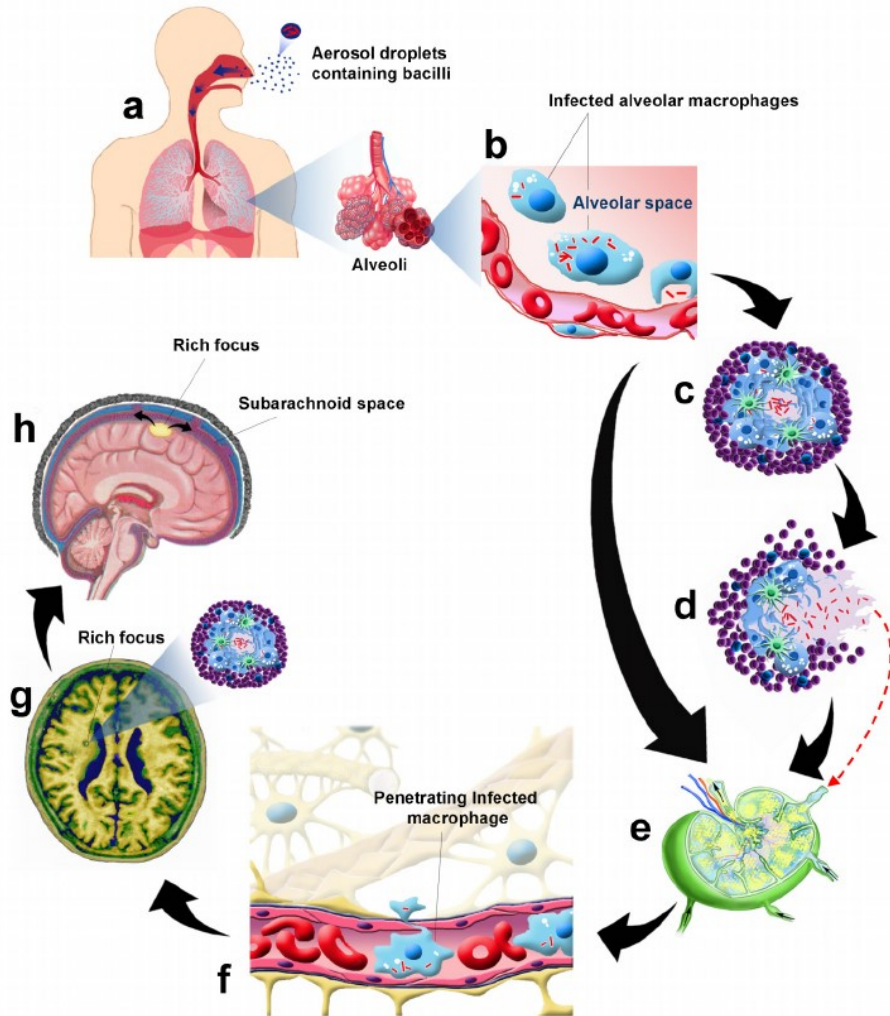


Figure 6: Pathogenesis of CNS tuberculosis³⁷

TBM pathogenesis and the theory behind Rich foci development.

(a) The MTB aerosol transmission chain, (a) Alveolar macrophages in alveoli phagocytose MTB. (c) The development of granulomas in the lungs, which are then brought on by cellular and cytokine network responses; 90% of hosts who develop granulomas do so during the course of their lives. (d) In 10% of people with latent TB, MTB escapes from the granuloma. (e) MTB may escalate from the lung or undergo a secondary reactivation from a "leaked granuloma," which is then filtered into a local lymph node, to develop TBM. (f) MTB can enter the CNS across the BBB after spreading through the bloodstream (g) Bacilli attach to the brain parenchyma or meninges and produce subpial or sub-ependymal primary complexes.

Spectrum of intracranial tuberculosis:

Intracranial tuberculosis can be broadly divided into meningeal and parenchymal patterns of involvement as under ³⁶

I) Meningeal tuberculosis	II) Parenchymal Tuberculosis
a) Leptomeninges	a) Cerebritis
b) Pachymeningitis	b) Abscess
	c) Rhombencephalitis
	d) Encephalopathy
	e) Tuberculoma

Table 2: Meningeal and parenchymal patterns of involvement of intracranial tuberculosis

I) Meningeal tuberculosis

a) Tubercular leptomeningitis

Tubercular leptomeninges is the most typical pattern of complication of CNS TB. The "Rich focus," a subpial (rarely subependymal) focus of infection bursts into the subarachnoid space causing an inflammatory reaction.

The most frequent finding on MRI is diffuse leptomeningeal enhancement involving the affected areas. The leptomeningeal enhancement shows a distinctive predilection to involve the basal cisterns in TB, particularly the peri-mesencephalic, interpeduncular, prepontine, and suprasellar cisterns. It frequently extends over the floor of the third ventricle, the anteromedial surface of the temporal lobes and along the sylvian fissures.

b) Tubercular pachymeningitis

Compared to tubercular leptomeningitis, tubercular pachymeningitis is not common. It is distinguished on MRI by focal or widespread dural thickening visualized on FLAIR sequence with intense post-contrast dural enhancement. The diagnosis is simple in situations where there are other tuberculosis related pathologies like CNS tuberculoma. However, it could be challenging to distinguish the condition from other causes of pachymeningitis such as neurosarcoidosis, autoimmune diseases (example Wegener's granulomatosis) and neurosyphilis.³⁶

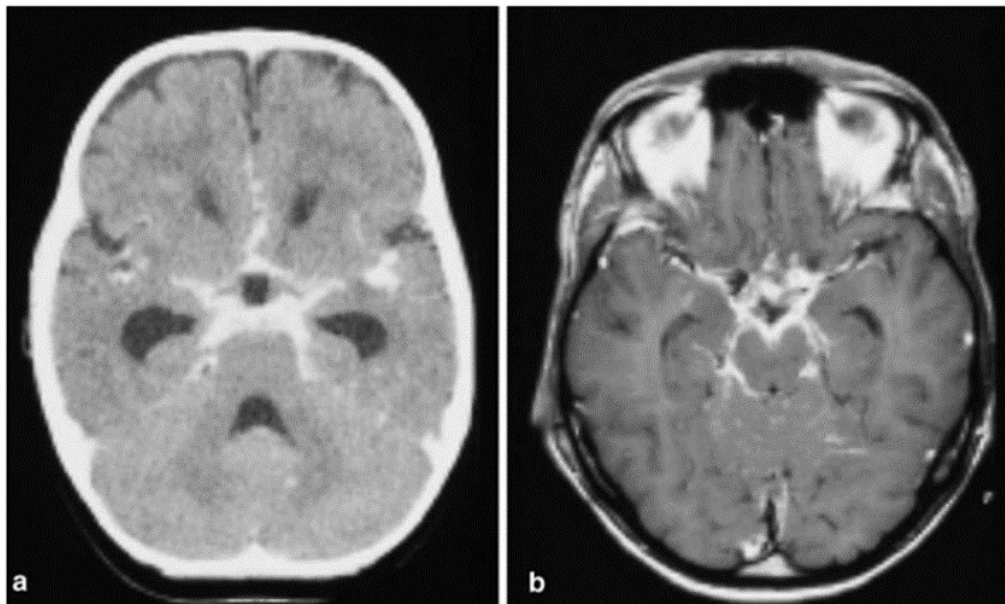


Figure 7: Meningeal tuberculosis³⁶

a, b Basal exudative tuberculous meningitis.

a) Contrast-enhanced CT scan demonstrates an intense enhancement of the basal meninges. Note the widening of the temporal horns, due to communicating hydrocephalus. b) Axial gadolinium-enhanced T1-weighted MR image demonstrates marked enhancement in the basal subarachnoid cisterns

II) Parenchymal tuberculosis

a) Tubercular cerebritis

“Cerebritis refers to involvement of a focal area of brain parenchyma in the infective process. It is recognised on MRI as a focal area of gyral swelling and enhancement. In contrast to normal parenchyma, on T1W images, gyri appear hypointense, while on T2W images, they appear hyperintense and exhibit patchy post-contrast enhancement.³⁶

b) Tubercular abscess

A tubercular abscess occurs in less than 10% of cases. It is more commonly seen in older patients as well as patients with compromised immune systems. There are two theories regarding the formation of tubercular abscesses. In the first, tubercular cerebritis is hypothesised to occur, whereas in the second, tuberculomas are thought to liquefy.³⁶

On imaging, they appear as a large, well-defined, localised lesions that usually measures more than 3 cm with mass effect. Peri-lesional edema will be present. The wall of abscess is typically thin and smooth. Frequently, the abscess's contents exhibit hypointensity on T1W, heterogenous hyperintensity on T2W, and different degrees of suppression on FLAIR. DWI often exhibits restricted diffusion with low apparent diffusion coefficient (ADC) values. Sometimes it can be difficult to distinguish between a tubercular abscess and a caseating tuberculoma with liquefaction.³⁶

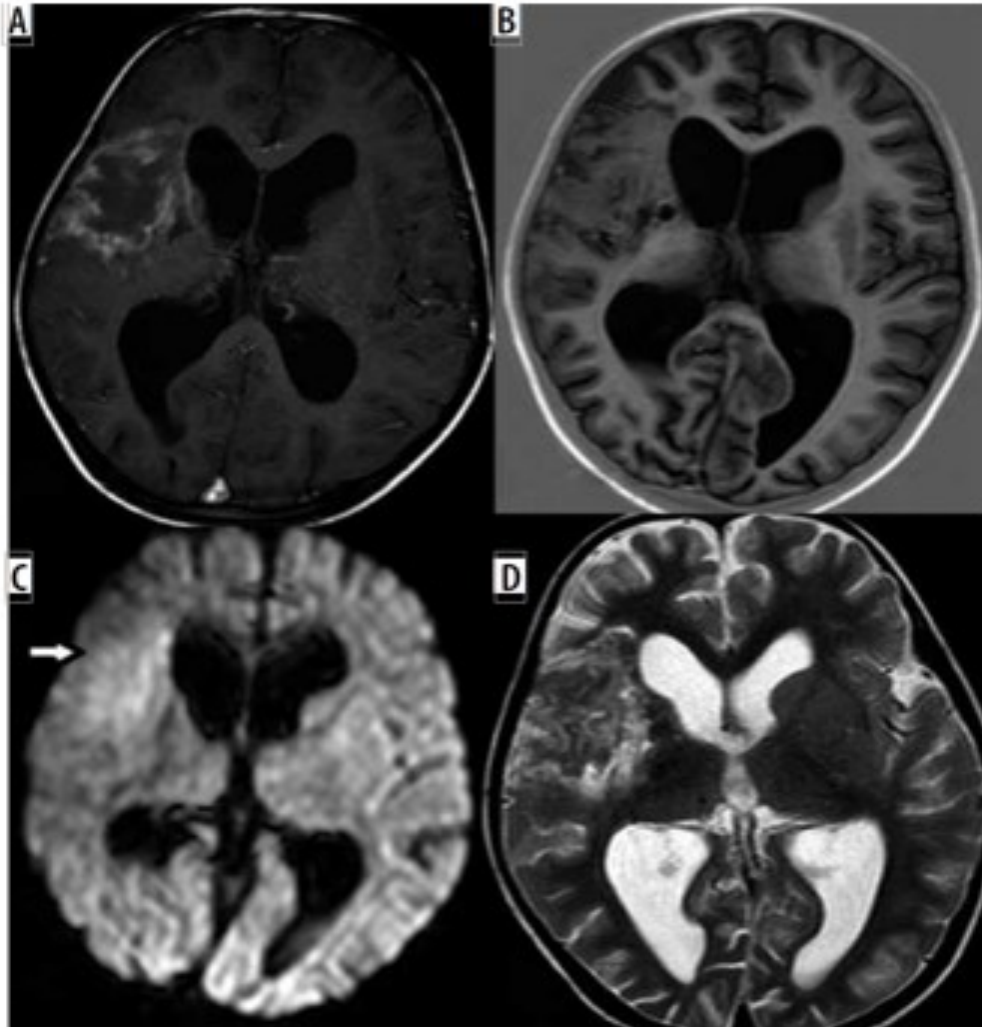


Figure 8: Tubercular abscess³⁶

- A) T1W Post contrast axial MR images- Irregular hypointense lesion with a thin rim of peripheral enhancement in right temporal lobe and insular cortex.**
- B) T1W axial MR images– Lesion appears hypointense.**
- C) DWI axial MR images - The lesion shows diffusion restriction**
- d) T2W axial MR images- Lesion is heterogeneous in signal intensity in this sequence. These findings were suggestive of tubercular abscess in right temporal lobe and insular cortex.**

c) Tuberculous rhombencephalitis

Tuberculous rhombencephalitis is a rare pattern of neurotuberculosis encompassing < 5% of the cases, although it is more frequent in patients with AIDS (~25%). Patients usually present with cerebellar symptoms or focal neurological deficits of cranial nerve palsies pointing to brainstem involvement. There is primary involvement of the cerebellum and brainstem (hindbrain). It is generally in the form of tuberculomas involving the parenchyma of the hindbrain and is frequently associated with leptomeningitis involving the basal cisterns. Associated inflammatory edema can be visualised as T2W/FLAIR hyperintensity with swelling of the brainstem structures. The hallmark of this condition is the high incidence of associated complications such as cranial nerve palsies (leading to focal neurological deficits) and hydrocephalus.³⁶

d) Tubercular encephalitis

This typically occurs in young children with onset of seizures, altered sensorium, stupor, and coma without signs of meningitis. Pathologically, extensive white matter injury and perivascular de-myelination is present in the brain parenchyma. On MRI, extensive cerebral edema is found, with unilateral or bilateral extensive T2W/FLAIR hyperintensity. Diffuse post-contrast enhancement of the involved white matter may be seen. It has a poor prognosis, with death usually occurring within one to two months of onset.³⁶

e) Tuberculoma:

Conglomerate caseous foci called tuberculomas form inside the brain parenchyma from tubercles that were acquired during an episode of bacilleemia. These are the outcome of an extensive inflammatory process. Although they can develop in the cord, tuberculomas usually develop in the brain. In underdeveloped nations, tuberculomas are more prevalent, especially in children.³⁷

Clinical manifestations:

The most typical features include seizures and/ or headaches in adults. More serious symptoms include drowsiness, hydrocephalus and altered mental status.^{38,39} In children, common symptoms are fever, headache, seizures, nausea and vomiting. If there is accompanying meningitis, there will be clinical symptoms of meningitis.⁴⁰ Sometimes, in the absence of meningitis, tuberculoma may be asymptomatic.^{41,42}

Pathogenesis:

The lesions are often granulomatous, have a necrotic centre surrounded by lymphocytes, astrocytes, and epithelioid cells (which combine to create Langhans giant cells).^{43, 44} On contrast enhanced computed tomography, the tubercles become organised throughout with a rim of connective tissue made of reticulin fibres surrounding them.⁴⁵

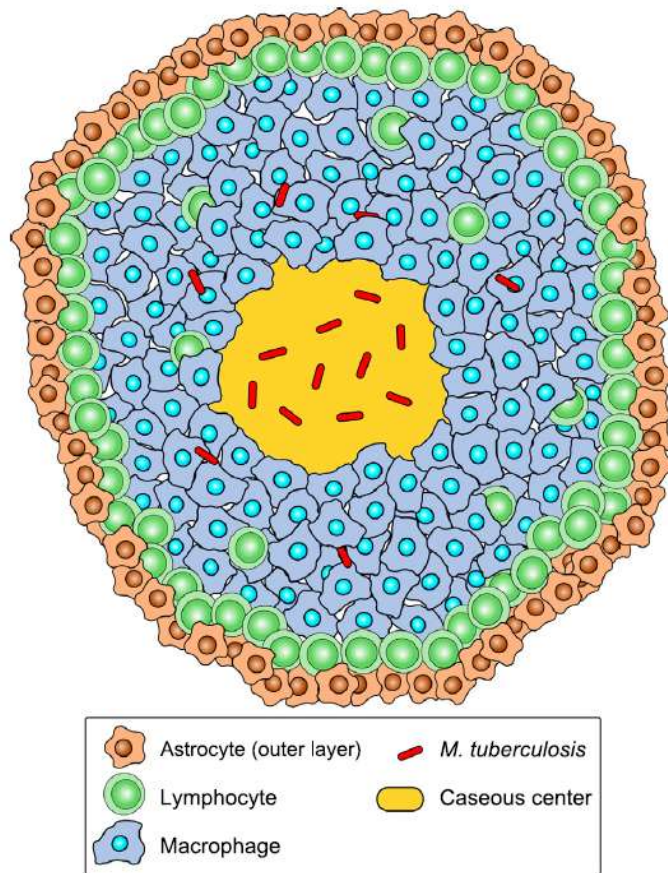


Figure 9 : Illustration of Tuberculoma with caseous necrotic center⁴

There are four stages of Tuberculoma³⁷

- A. Non caseating granuloma,
- B. Caseating granuloma,
- C. Caseating granuloma with central liquefaction,
- D. Calcified granuloma.

IMAGING IN TUBERCULOMA

Tuberculomas are round to oval lesions that range in diameter from 2 - 10 cm. They are usually well-defined with varying degrees of peri-lesional edema. In some instances, authors have noted racemose patterns that are comparable to NCC.^{46,47} Other observations may include peri-lesional edema (33%), mass effect (18%), enhancement of the meninges (12%), calcification (10%), and cortical and subcortical infarcts (12%).^{48,49}

In a study done by Wasay M. et al⁵⁰, it was noted that around 30 % of patients had a single lesion, and approximately 70 % had numerous lesions. Lesions ranged in number from one to more than hundred (mean = four lesions per patient). Tuberculomas had a width that varied from 2 mm to approximately 6 cm. The lesions larger than 1.5 cm may show irregular, nodular rim enhancement on post contrast study.⁵⁰

CT Appearance of Tuberculoma:

Some writers believe that tuberculoma can be distinguished by the presence of a ring of enhancement surrounding a nidus of calcification known as the “target sign”.⁵¹

Early-stage tuberculomas can be detected on contrast computed tomography imaging as isodense or low density lesions, frequently with edema that is not proportional to the mass effect.⁵² In the later stages, tuberculomas are well defined, iso- hyperdense lesion with peripheral ring enhancement. The enhancement can be irregular nodular ring enhancement.⁵³

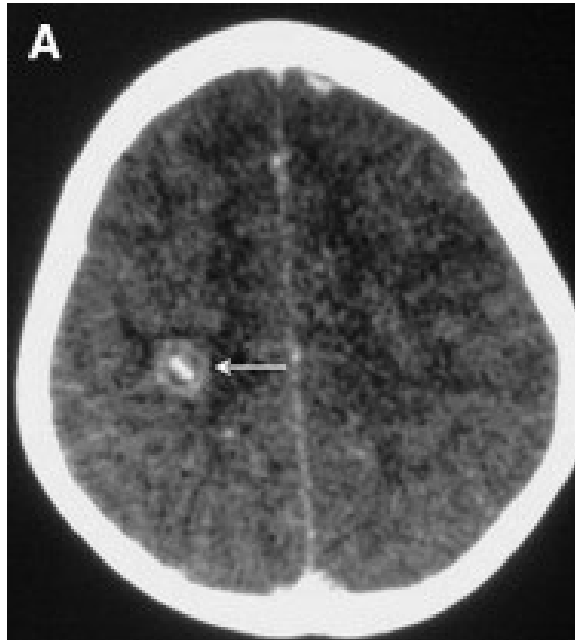


Figure 10: Target sign in Tuberculoma

Axial CECT Brain image showing a central calcific nidus with surrounding rim enhancement (arrow) giving the “target sign” ⁵²

MRI appearance of Tuberculoma

Depending on whether a tuberculoma is non-caseating, caseating with a solid centre, or caseating with a liquefied centre, the lesion's features change .⁴⁸

Caseating tuberculoma are generally composed of three zones- an inner T1W iso-intense and T2WI hypo-intense layer image due to caseous necrosis.⁴⁹ The middle layer appears as hypo-intense on T1WI and hyperintense on T2WI due to the presence of Langhans giant cells and epithelioid cells and an external layer which shows T1W iso-intense and T2W hypo-intense signals due to the collagenous capsule.^{49, 50}

Non-caseating tuberculomas, images usually show slight hypo-intensity on T1-WI and hyperintensity on T2-WI.⁵¹

Table 3: MRI imaging features of different stages of Tuberculoma. ³⁶

Lesion	T1W	T2W	FLAIR	DWI	T1WCE
Non caseating granuloma	Iso- to hypointense	Hyperintense	No suppression	No restriction	Homogeneous enhancement
Caseating granuloma	Iso- to hypointense with hyperintense rim	Hypointense	No suppression	No restriction	Homogeneous or ring enhancement
Caseating granuloma with central liquefaction	Isointense to hypointense with hyperintense rim	Hypointense rim with central hyperintensity	Partial suppression	May or may not show restriction	Ring enhancement
Calcified granuloma	Iso- to hypointense	Hypointense	No suppression	No restriction	No enhancement

Role of Post contrast T1W sequence:

Post contrast MRI helps in visualising the degree of edema as well as soft tissue involvement of lesions.³⁸ After contrast, both caseating as well as non-caseating tuberculomas show ring enhancement and range in size from approximately 3 mm to 6 cm. Larger lesions (>1-1.5 cm) show irregular, nodular ring enhancement.⁵²

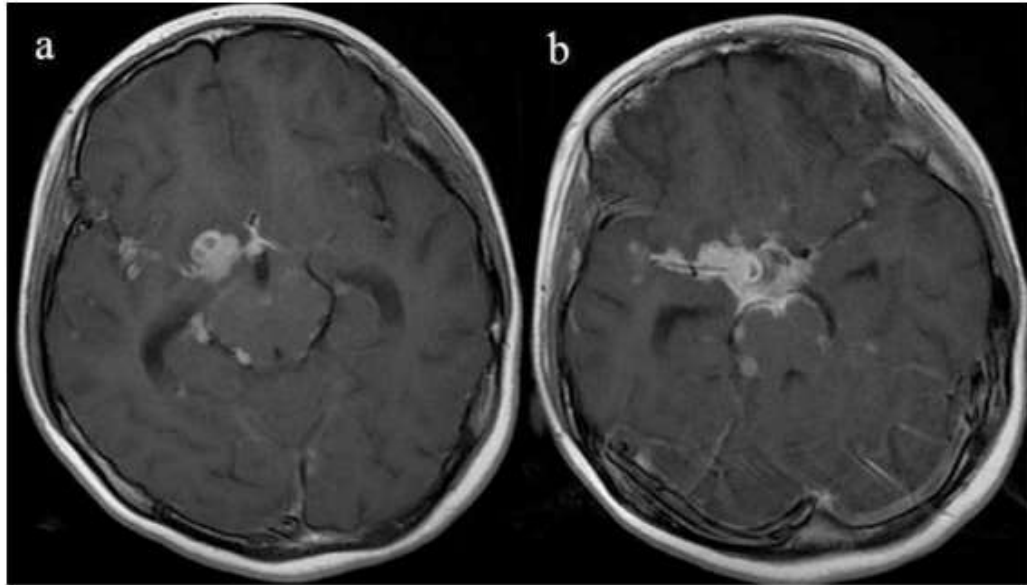


Figure 11: Axial contrast enhanced T1 Weighted MR images showing multiple tuberculomas with accompanying meningitis⁵⁸

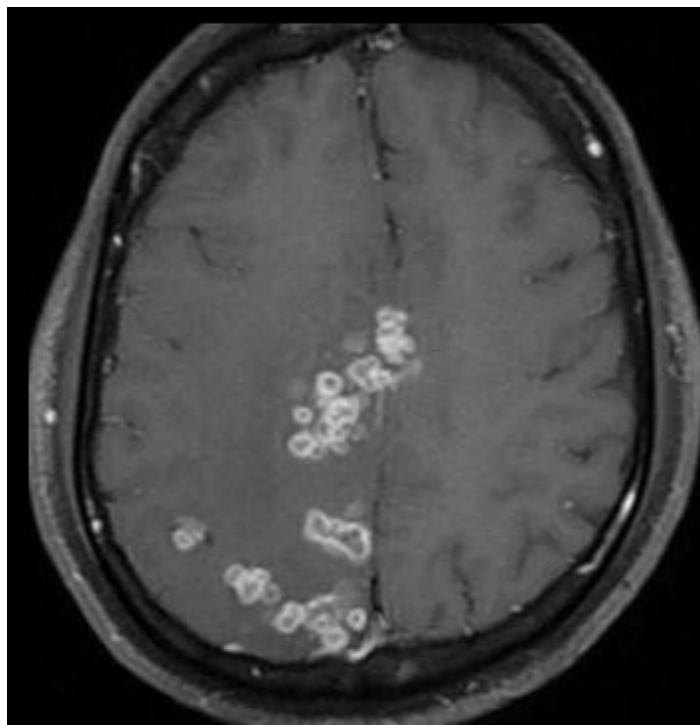


Figure 12: Axial contrast enhanced T1 Weighted MR images showing multiple tuberculomas with accompanying meningitis⁵⁸

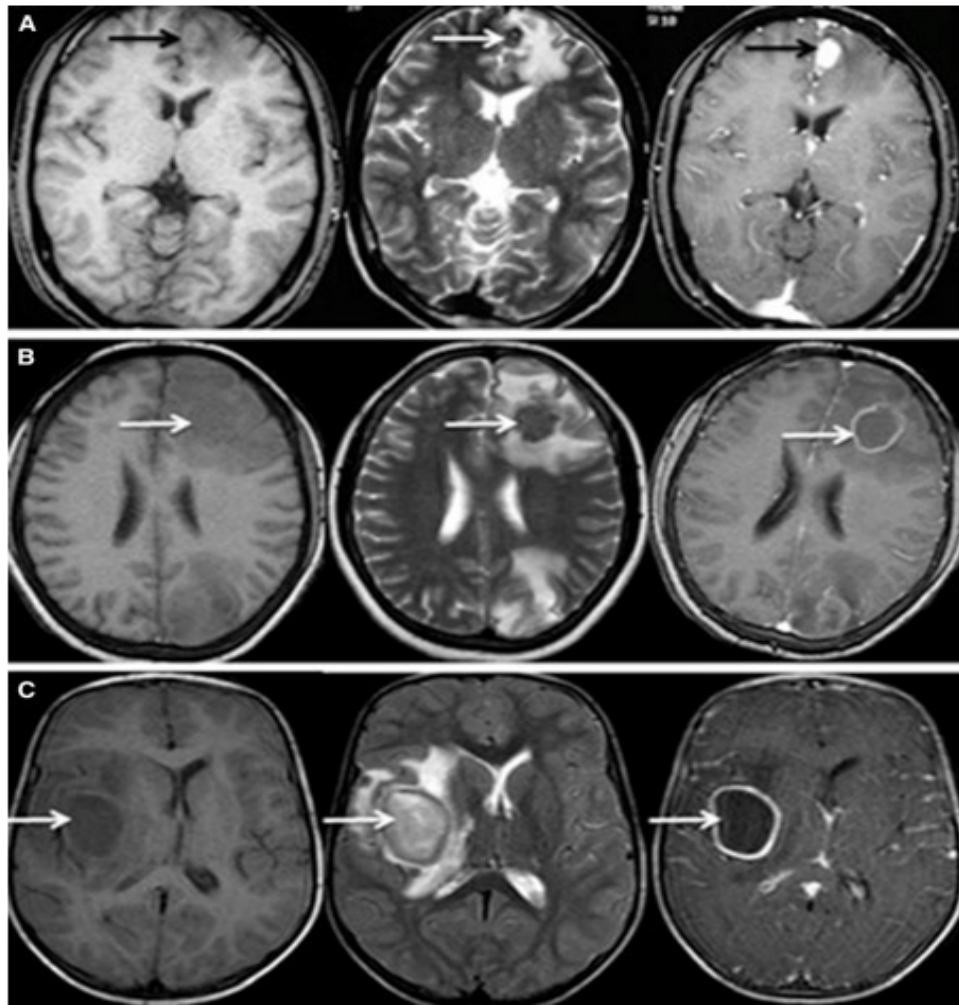


Figure 13 : Magnetic resonance imaging appearance of tuberculoma based on different stage of maturation⁵²

(A) A non-caseating granuloma (arrow), isointense on T1-weighted and hyperintense on T2-weighted images, with nodular homogenous post contrast enhancement. (B) A caseating solid granuloma (arrow), isointense on T1-weighted and strikingly hypointense on T2-weighted images with rim enhancement on post contrast image. (C) A caseating granuloma (arrow) with central liquefaction, hypointense on T1-weighted and hyperintense on T2-weighted images with peripheral hypointense rim of collagenous capsule. The lesion shows rim enhancement after contrast. A variable degree of vasogenic oedema is present in all the 3 stages

Diffusion Weighted Imaging:

DWI is an MRI sequence for identifying infectious processes, although it is limited in tuberculomas with liquid necrosis as opposed to those with solid necrosis. Tuberculomas can be divided into two groups on the basis of their T2W morphology.

T2 hyperintense lesions, suggestive of central liquefaction necrosis show hyperintensity on DWI with reduced ADC values. Caseating granulomas without central liquefaction which appear hypointense on T2WI showed no restriction of diffusion on DWI with high ADC values.⁵²

There are only a few papers that describe the DWI appearance of tuberculomas in brain. In two individuals with multiple tuberculomas, Kaminogo et al.⁵⁴ reported hyperintense DWI signal intensity in the core of the lesions. The lesions had low ADC values, which varied from 0.58 to $1.086 \times 10^{-23} \text{ mm}^2/\text{s}$. However, in a different case report, Basoglu et al.⁵⁵ discovered that lesions were isointense and had normal ADC values.

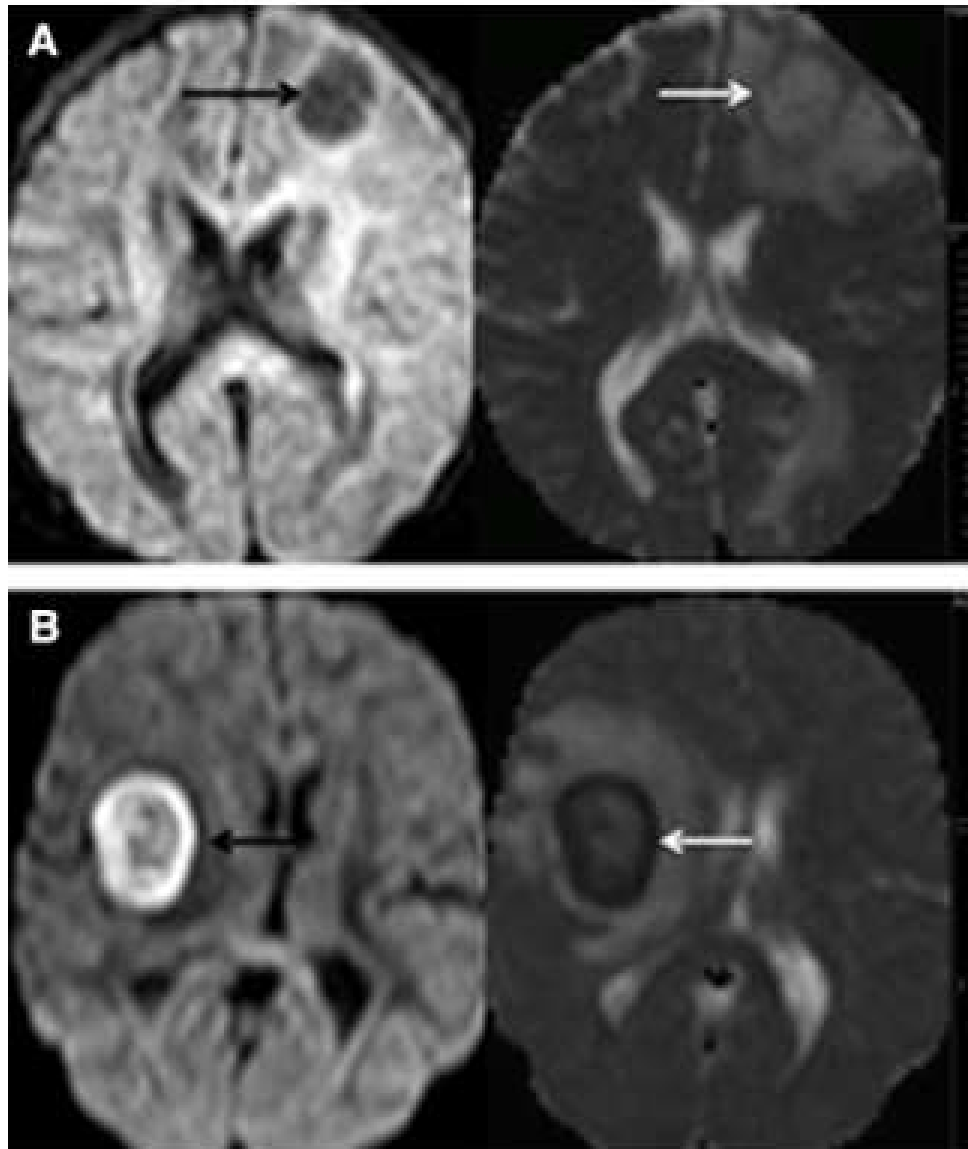


Figure 14: MRI DWI and ADC images of non-caseating and caseating granuloma in Tuberculoma⁵²

A) T2 hypointense , non caseating granuloma with solid centre shows no restriction of diffusion on DWI with high ADC values. B) T2 hyperintense, caseating granuloma revealed increased signal intensity cores on DWI with low ADC values

MR Spectroscopy:

MRS can provide information on the biochemical processes occurring in the central nervous system. The chemical makeup of the brain is revealed by proton MRS. Gupta et al. have identified distinct lipid peaks that correlate to methylene, terminal methyl & fatty acyl chain components.⁵⁶

The MR spectral pattern of intracranial tuberculomas is characterised by a predominance of lipid peaks. The lipid peaks are seen at 0.9, 1.3, 2.0 and 2.8 ppm.^{56,57}

The presence of lipids in the cell wall of the tubercle bacillus is what causes the lipid peak in tuberculoma. However, an associated rise in choline has also been noted.⁵⁸

Choline levels are related to the amount of cell membrane turnover and due to increased cellularity of lesions.⁵⁹ T2-hypointense tuberculomas, suggestive of caseating granulomas without central liquefaction have an isolated lipid peak at 0.9 & 1.3 ppm. In addition to a large lipid peak, T2-hyperintense tuberculomas, suggestive of caseating granulomas with central liquefaction may sometimes show choline peak at 3.22 ppm. A phosphoserine peak at 3.7 ppm is may also be frequently observed.⁵⁶

MR spectroscopy is also useful in differentiating tubercular from pyogenic abscesses. While pyogenic abscesses show amino acids at 0.9 ppm with varying combinations of succinate, acetate, alanine, and glycine, tubercular abscesses mostly show lipid peak

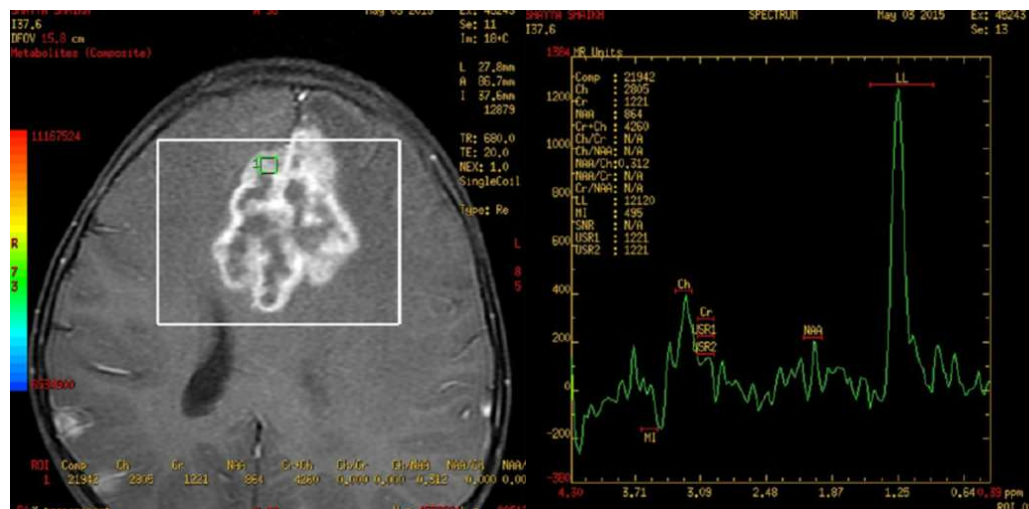


Figure 15 : MRI brain spectroscopy demonstrating lipid lactate peak in left frontal parafalcine tuberculoma⁵⁸

Biopsy for Diagnosis:

When a tuberculoma cannot be diagnosed radiologically, stereotactic biopsy should be performed which minimises damage to tissue.^{51, 60} Additionally, a biopsy is necessary when imaging examinations reveal that brain lesions are progressing, such as when a patient has treatment-resistant TB, exhibits a paradoxical reaction to antituberculosis drug therapy, or is uncooperative.^{61, 62}

According to Assefa et al., 58 (26.1%) out of 223 cases with tuberculosis-related lesions in the brain, after biopsy as per histological investigation, it was noted that there was one tuberculous abscess (0.4%), 28 tuberculomas with caseous necrosis, and 29 non-caseating tuberculomas (12.6%).^{63, 64}

Complications:

Complications of tuberculous meningitis include:

- Up to 70% of individuals with tuberculous meningitis develop hydrocephalus. Head CT may demonstrate hydrocephalus, but MRI is the modality of choice for identification of tuberculous meningitis.⁶⁵
- At any stage during the entire duration of tuberculous meningitis, hyponatremia can occur. With vague symptoms (such as nausea, disorientation, delirium, and seizures) it may be misdiagnosed.⁶⁶
- A disruptive side effect of tuberculous meningitis that affects about 25% of patients is vision loss due to high intracranial pressure and direct M. tuberculosis invasion of the optic nerves.
- Vascular complications:
 - a. Arterial complications – Infarcts and vasculitis
 - b. Venous complications like venous infarcts and dural venous sinus thrombosis.

Treatment:

Directly observed therapy (DOT) should be used to treat every patient with TB. Antituberculous therapy and glucocorticoids are used to treat tuberculoma.⁶⁷ Treatment for CNS TB typically lasts between 9 and 12 months and consists of a two-month initial intensive phase (four drugs) and a long continuing phase (often two treatments administered for an additional 7 to 10 months).⁶⁷ The antitubercular drugs are isoniazid, rifampicin, and pyrazinamide. Isoniazid has good CNS penetration and is more effective against organisms that are actively dividing as opposed to those that are dormant. Despite having relatively weak CNS penetration, rifampin is effective against both organisms that divide quickly and ones that are quiescent.⁶⁷ There is a need for surgical consultation for people with hydrocephalus.

Cysticercosis:

Cysticercosis is caused by the larval stage of the tapeworm, *Taenia solium*. It is further divided into Neurocysticercosis when it affects the Central Nervous System and extraneural cysticercosis when it affects other tissues like muscles. In endemic locations, neurocysticercosis is a major contributor to adult-onset seizures.⁶⁸

Epidemiology:

Cysticercosis is endemic in many rural & periurban regions of India.⁶⁹ Data on the global prevalence of neurocysticercosis is limited. There are a few population-based studies on prevalence which are neuroimaging studies.⁷⁰ On computed tomography scans, 15 to 25% of people in endemic areas have evidence of neurocysticercosis, primarily in the form of calcified lesions.⁷¹

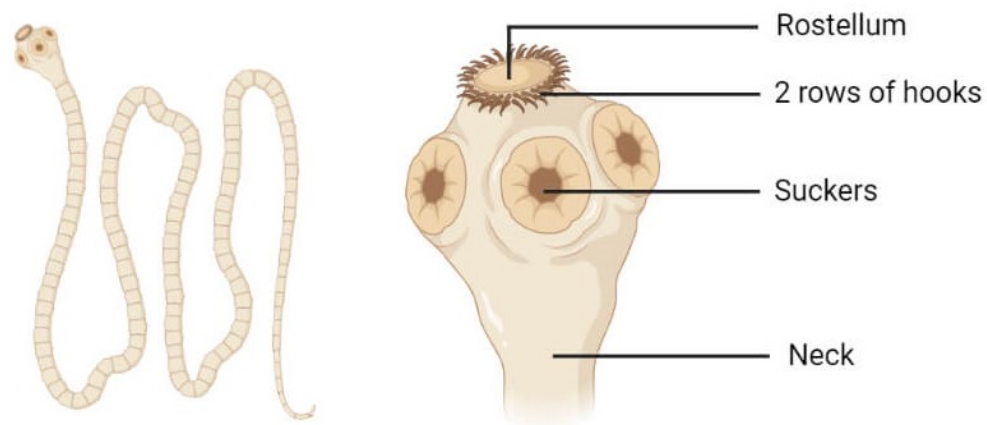


Figure 16: Image of Adult *Taenia Solium*⁷⁷

Life Cycle and Transmission:

Humans, the definite hosts develop cysticercosis after consuming undercooked pork which contains cysticerci in muscle tissue. Pigs, the intermediate hosts get affected when they consume proglotids, infected human excrement, or food that has been polluted. Oncospheres (embryos) that have been ingested develop in the intestine, invade the gut wall & spread hematogenously to the brain, striated muscles, liver, and/or other organs.⁷²

The scolex enters the body after being consumed and uses its suckers and hooks to cling to the human small intestine. Over a period of two to four months, proglottids develop. Pigs can get sick from the proglottids or eggs. The eggs hatch after ingestion, and the larvae are then transported to various tissues by the bloodstream. Neurocysticercosis is caused by cysts in the brain; people who already have cysticercosis are unintentional dead-end hosts. The incubation period for cysticercosis is approximately 3.5 years.⁷³

A household tapeworm carrier who is asymptomatic is the most typical source of infectious eggs.⁷⁴ Therefore, it is best to think of cysticercosis as a condition that is mostly spread from person to person, with diseased pigs serving as carriers of the virus.

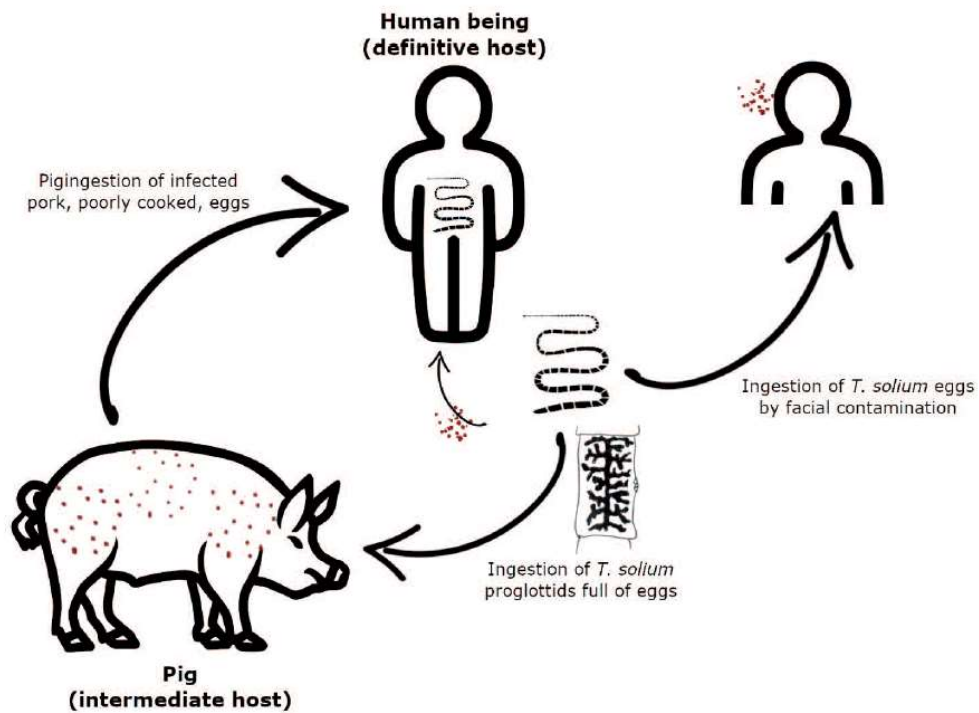


Figure 17 : Development cycle of *T. Solium*⁸¹

Neurocysticercosis:

Cysticercosis frequently infects the CNS causing neurocysticercosis. In endemic areas, the disease has a seroprevalence of around 4% of the population. 50 million people are estimated to be affected worldwide. *T. Solium* is indigenous to Asia, South America, China, India, Africa, and Nepal, where it causes NCC.⁷⁵ In adults, NCC is the main cause of seizures as well as hydrocephalus.

Pathogenesis:

Neurocysticercosis is caused by the ingestion of larval cysts of the pork tapeworm (*Taenia solium*). The infection is brought on by consuming food or water that has been tainted with human faeces that contain the parasite eggs. Cysticerci, small tissue larvae, are generated from the embryos (oncospheres), which penetrate the small intestinal mucosa, enter the circulation, and then reach various tissues and organs. Cysticerci have specific affinity for the central nervous system, eyes and striated muscles what is accounted for high concentration of glucose or glycogen in these organs.⁷⁶

Clinical Manifestations of NCC:

The location, number, size, and stage of development of cysticerci, as well as the host immune response to the parasite, all have a significant role in the clinical symptoms of NCC. NCC may be asymptomatic. The most prevalent symptom, occurring in 80–90% of patients is seizures. In endemic areas, NCC is considered to be the primary cause of late-onset epilepsy. The other symptoms include focal deficit, intracranial hypertension, and cognitive impairment are the most common clinical symptoms. The most frequent clinical and imaging symptoms of neurocysticercosis in children are partial seizures.⁷⁷

Intraventricular neurocysticercosis can lead to the restriction of the CSF flow resulting in hydrocephalus and acute intracranial hypertension. They are most frequently detected in the fourth ventricle.⁷⁸ The presence of a mobile intraventricular cyst may even cause acute intermittent hydrocephalus, severe positional vertigo, headaches and loss of consciousness.⁷⁹ As a result, intraventricular neurocysticercosis is regarded as dangerous.

The term "racemose" cysticercosis refers to the initial appearance of the developing membranes, which initially resemble a bunch of grapes. Intense inflammation and fibrosis of the leptomeninges of the brain are associated with it.

The CSF circulation is obstructed in roughly 50–60% of cases, which leads to hydrocephalus, progressive intracranial pressure, and death in over 22% of cases.⁷⁹ Cerebellopontine-angle syndrome, cranial nerve palsy and cerebral infarcts brought on by occlusive endarteritis may all manifest.⁸⁰

Mortality is high in cases of hydrocephalus owing to cysticercotic meningitis (55 %) and most patients pass away within three years of CSF shunting.⁸¹

Classification:

Neurocysticercosis is classified into four types based on its location into-

- Parenchymal,
- Subarachnoid,
- Intraventricular,
- Spinal and ocular forms.⁸²

Parenchymal NCC is further classified into 4stages by Escobar⁸³

- Vesicular,
- Colloidal vesicular,
- Granular nodular and
- Calcified nodular.⁸³

1) Intraparenchymal neurocysticercosis:

The most prevalent form of cysticercosis, affecting more than 65% of patients, is intraparenchymal NCC.^{84,85} The onset of symptomatic parenchymal NCC often happens two to four years after infection, but it can happen up to 20 years later. Nonviable (calcified) lesions are frequently found in patients who arrive later.⁸⁵

The clinical features depend on the number, location of cysticercus as well as degree of inflammation.^{86, 87} Usually parenchymal NCC are asymptomatic and discovered by chance during imaging done for other purposes. Seizures followed by headache are the most common symptom of NCC.^{84, 85} Usually, a fever is not present. Patients with a single lesion have a more favourable prognosis than those patients with multiple cysticerci.

A) Vesicular-stage:

A cystic lesion filled with fluid with no debris is noted in the vesicular stage. It has a thin wall and an eccentric, opaque, 4-5 mm marginal nodule called scolex. In this stage, the parasites are alive and they cause little to no inflammation in the tissue around them. Since the cystic lesions are subcentimetric and have minimal mass effect, there are typically no symptoms at vesicular stage.⁸³

B) Colloidal - vesicular stage:

The larva gradually gets smaller as it starts to degenerate from the scolex. Due to the surrounding inflammatory reaction in the brain parenchyma, the cyst fluid turns turbid and the cyst wall thickens. In this stage, peri-lesional edema is predominant.

C) Granular nodular stage:

In this stage, the cystic lesion further reduces in diameter & changes into a small nodule. The cyst may appear as a thick, tiny, nodular ring-enhancing lesion. The most typical pathologic feature is pericystic gliosis, which can range in severity. The surrounding edema eventually lessens and is not as severe as it was in the colloidal vesicular stage.⁸⁸

D) Nodular - calcified stage

When a lesion reaches this stage, it has almost entirely calcified, fully shrunken in size, and is free of any surrounding edema.

2) Subarachnoid neurocysticercosis (SAN):

SAN in the basilar cisterns is the worst type of NCC.⁸⁸ CT is not useful in demonstrating these lesions, similar to the intraventricular type of neurocysticercosis. Hence, MRI may be better in visualizing these lesions.

SAN may be associated with chronic arachnoiditis.⁸⁹ The presence of arachnoiditis is shown by the enhancement of the leptomeninges following administration of contrast. Chronic arachnoiditis may also be associated with communicating hydrocephalus due to secondary obstruction of the foramina of Magendie and Luschka.⁸⁸ If cysts grow to 10 cm or greater within the subarachnoid space, patient can suffer mass effect and focal neurologic abnormalities.⁸⁷

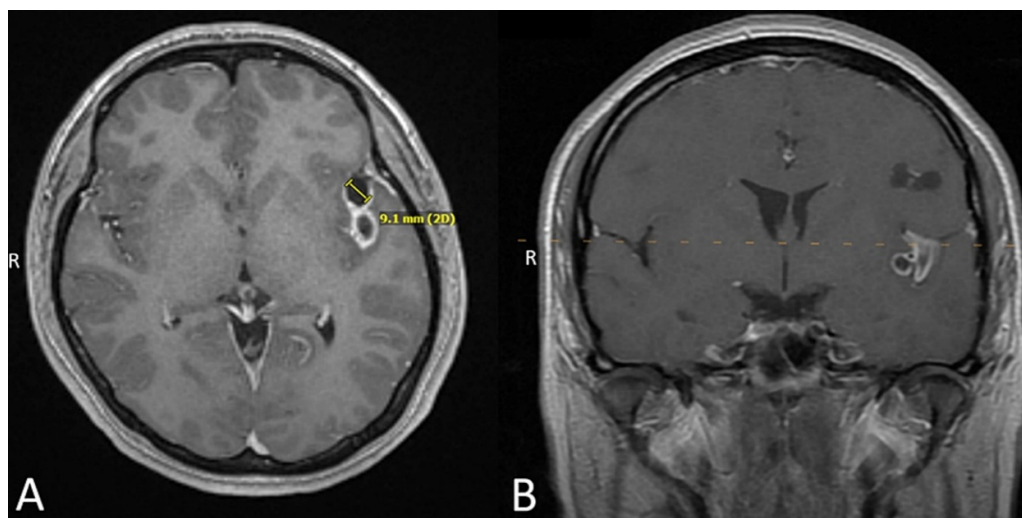


Figure 18 : MRI Brain image demonstrating subarachnoid Neurocysticercosis⁹⁸ (A – axial; B – coronal Post Contrast images) Complex Cysticerci cysts in the subarachnoid space of the left Sylvian fissure between the temporal and parietal lobes.

3) Spinal NCC:

Roughly 1% of cases result in spinal cord involvement. Spinal cysticerci are typically found in the subarachnoid area, where they can affect peripheral nerve roots by inducing inflammation and demyelination. Radicular discomfort and paraesthesias are frequently seen in patients. The lesion's location affects the neurologic deficits, which can often be clinically indistinguishable from those caused by other spinal cord lesions. Basal subarachnoid involvement and spinal subarachnoid cysticerci are strongly correlated.¹¹ Less commonly, intramedullary cysticercosis can occur and may be associated with transverse myelitis.

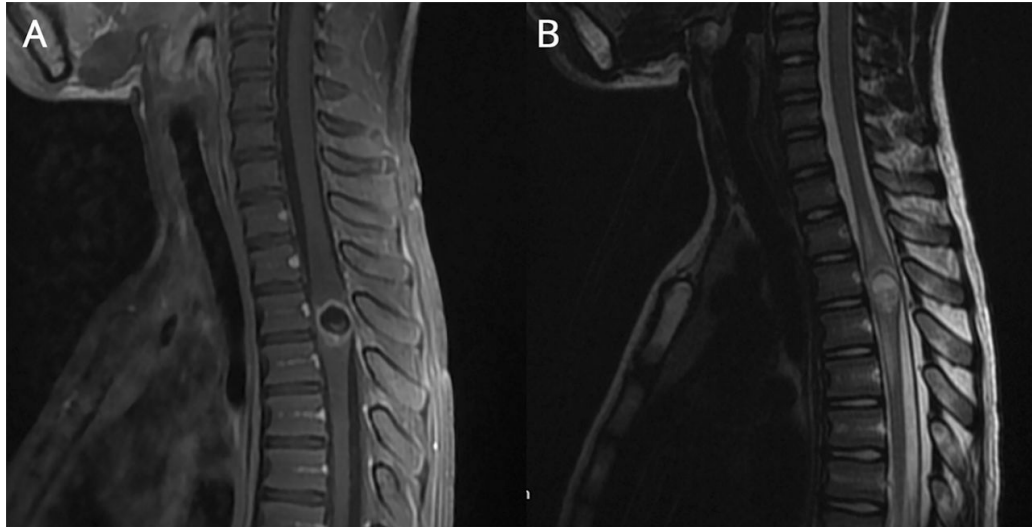


Figure 19 : MRI Spine images demonstrating spinal Neurocysticercosis⁹⁹
(A) Gadolinium-enhanced sagittal T1, (B) Sagittal T2 Magnetic resonance imaging showing intramedullary cystic lesion located at T3-T4 level

4) Intra Ventricular NCC:

Intraventricular NCC is most frequently seen in the fourth ventricle, followed by the third and lateral ventricles. On computed tomography and magnetic resonance imaging, the cysts have the density and signal intensity as CSF. MRI, especially FLAIR sequence is useful in characterizing the lesion. It is crucial to determine the cyst's location before surgery because it may be affixed to the ventricle wall or move inside or outside of the ventricular system.⁸⁹

Neuroimaging in NCC:

CT is useful for identifying parenchymal cysticerci as well as calcifications. CT is also useful for diagnosis of ocular cysticercosis. However, MRI is the investigation of choice for diagnosing NCC and its many sequelae. It can also help in diagnosis of disseminated cysticercosis. The imaging appearance depends on the stage of the NCC.⁹⁰

Vesicular stage:

On both CT and MRI, a well-defined cystic lesion with a thin wall (2-4 mm) and no post-contrast enhancement is noted. The cyst fluid's density or signal intensity is similar to that of the cerebrospinal fluid (CSF). No peri-lesional edema or mass effect noted.

In this stage, a distinct, eccentric scolex within the cystic lesion serves as the main imaging finding. The scolex exhibits iso- to hyper-intensity on T1-weighted and T2-weighted MR sequence. On Post contrast study, scolex appears as a round enhancing structure within the cyst. The scolex may demonstrate restricted diffusion on DWI.

In this stage, the parasites can occasionally be so abundant that the brain has a "swiss cheese" appearance. The cyst might persist in this stage for years.⁹⁰

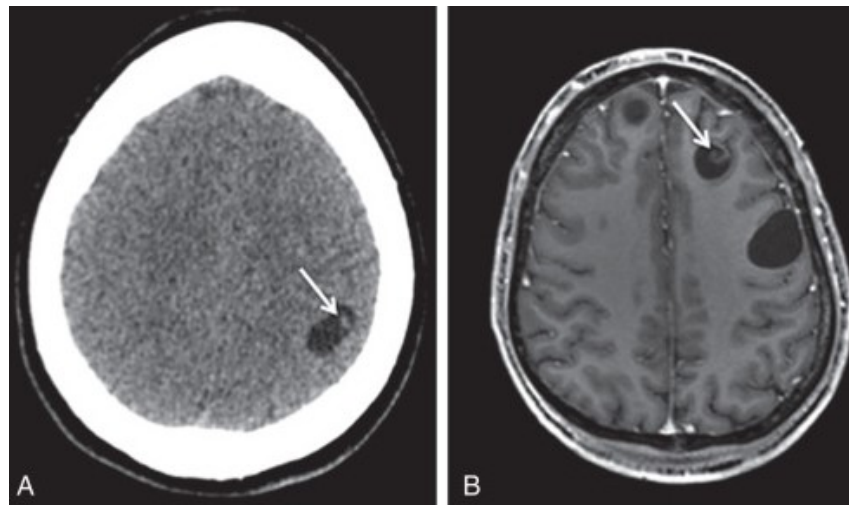


Figure 20 : Vesicular stage of neurocysticercosis (NCC)¹⁰⁰

(A) Axial contrast-enhanced computed tomography, (B) Postcontrast T1 magnetic resonance imaging (MRI) demonstrates fluid-filled cysts without wall enhancement or surrounding parenchymal edema. Eccentric intracystic nodules (arrow) represent the scolices.

Colloidal vesicular stage:

In this stage, cystic fluid becomes turbid and is hyperintense as compared to the CSF and appears hyperattenuating on CT and hyperintense on T1-weighted images. The cyst wall becomes thick and brightly enhances on administration of contrast giving ring enhancement. The scolex shrinks and eventually vanishes as a result of degeneration. Extensive perilesional edema is seen in this stage.⁹⁰ Multiple lesions at this stage may result in diffuse brain edema and ventricular system collapse without midline shift due to the host immunological response to the degraded cysts.^{91,92}

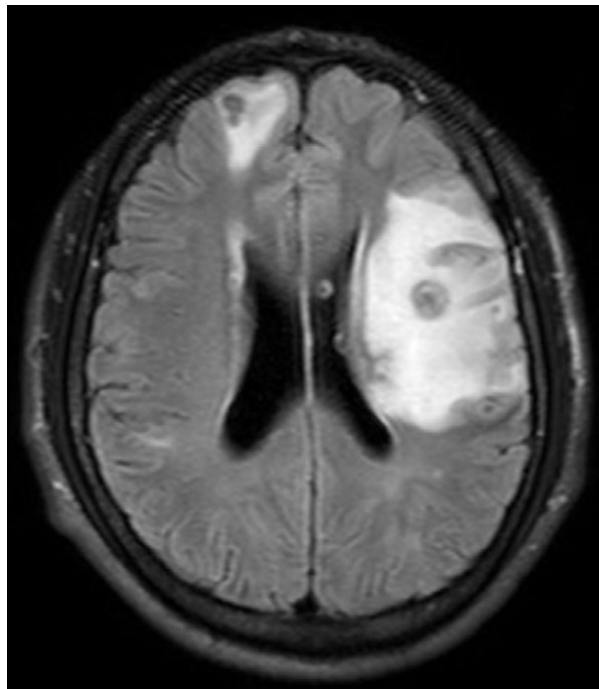


Figure 21: Colloid Vesicular stage of NCC ¹⁰⁰

MRI Brain Axial FLAIR image shows two heterogeneously hypointense lesions with moderate perilesional edema in left parietal and right frontal lobes- Colloid Vesicular stage of NCC

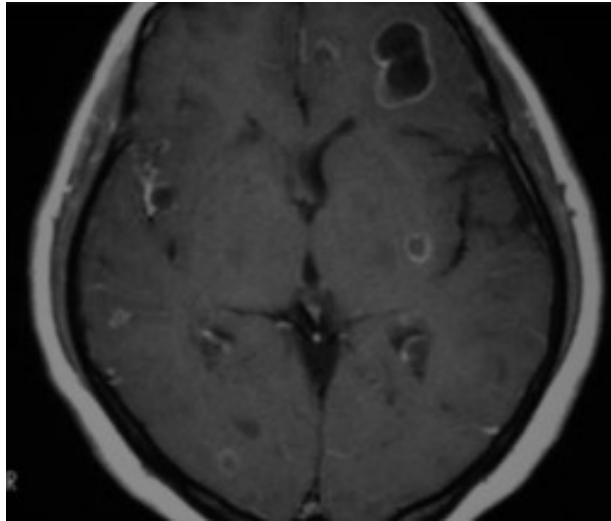


Figure 22: Multiple ring enhancing lesions in Colloid Vesicular Stage of NCC¹⁰⁰
MRI Brain T1W Post Contrast Image shows multiple ring enhancing lesions in Colloid Vesicular Stage of NCC

Granular Nodular Stage:

In this stage, the cysts appear as small, ring enhancing nodules. The amount of perilesional edema gradually lessens and is not as severe as colloidal vesicular stage.^{93,94}

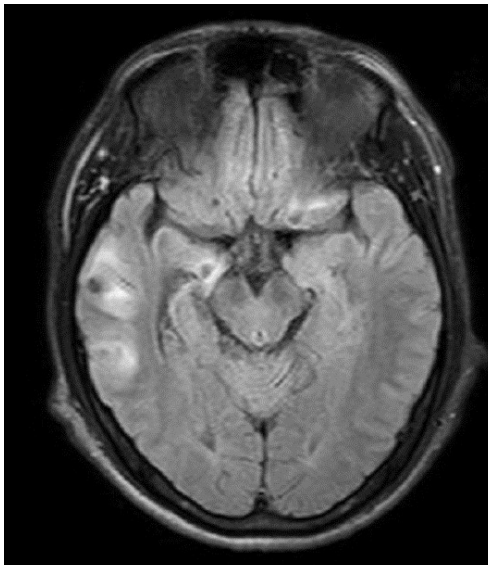


Figure 23: Nodular-granular stage neurocysticercosis¹⁰⁰
MRI Brain Axial FLAIR-Lesions have retracted appearing as low signal intensity with minimal perilesional edema

Nodular calcified stage:

The calcified lesion can be seen clearly on CT. Small, high-density calcified nodules without edema or enhancement can be seen on CT scan.⁹⁵ In MRI, due to calcification, the nodules look hypointense on all sequences with the absence of perilesional edema or significant enhancement.⁹⁵

Role of DWI and corresponding ADC values in NCC:

The discovery of the scolex is pathognomonic for NCC. On DWI, the vesicular stage of NCC shows eccentric hyperintense signal. This eccentric DWI hyperintensity that represents the scolex has significant diagnostic implications as restriction of diffusion is present in scolex. Hence, DWI helps in the identification of the scolex.⁹⁶ The other stages of Neurocysticercosis usually show no restriction of diffusion on DWI.⁹⁶

In a study done, ADC values from the core of cysticercus showed a value of $1.66 \pm 0.29 \times 10^{-3} \text{ mm}^2/\text{s}$, which was significantly higher than the core of all groups of tuberculomas and tuberculous abscess.⁹⁶

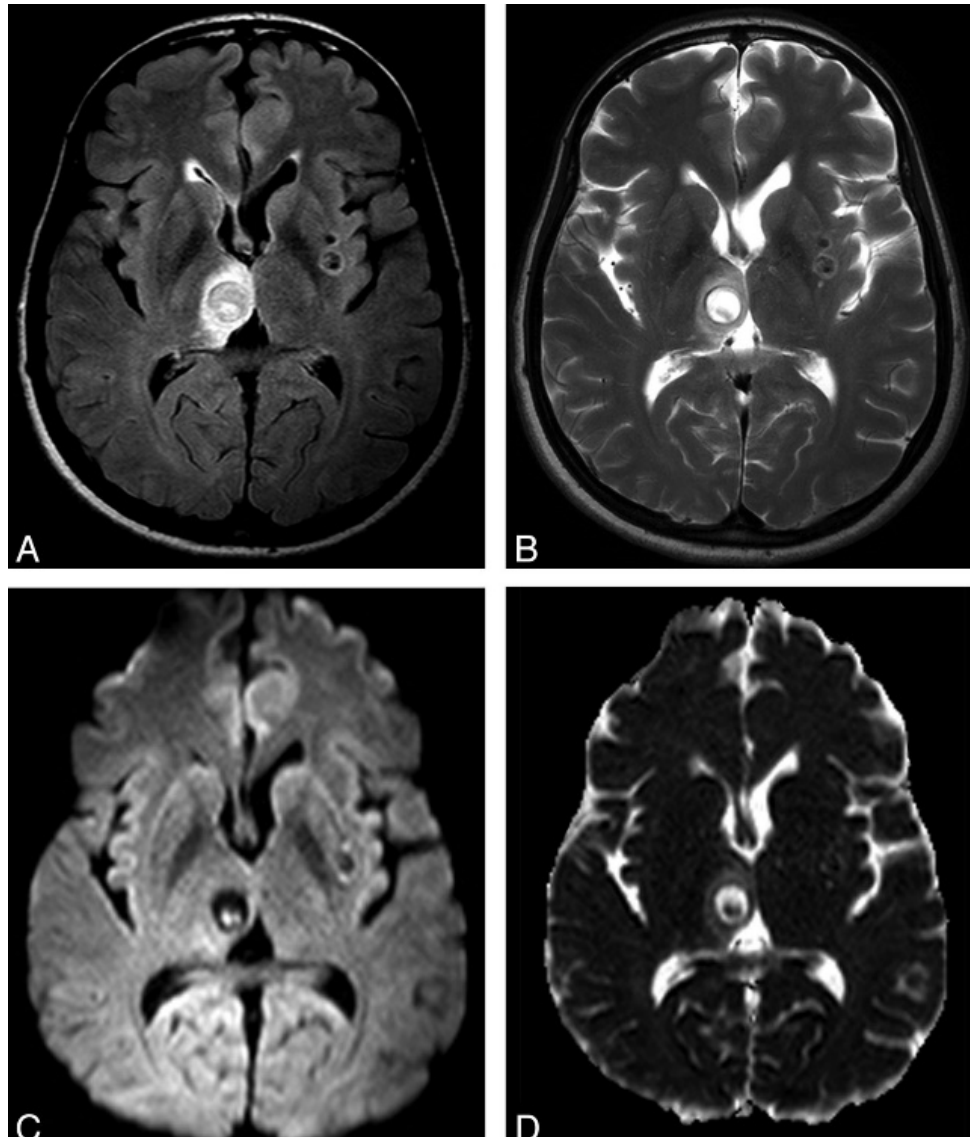


Figure 24: MR images demonstrating restricted diffusion in scolex in a case of NCC⁹⁷

(A-D) MRI images (A) Axial FLAIR B) Axial T2 Fast spine Echo C) Axial DWI D) Axial ADC images :(A) &(B) These images show lesions in the right thalamus and the left lentiform nucleus; the thalamic lesion is compatible with NCC in the colloidal stage. On DWI (C), In this lesion, the curvilinear scolex is clearly seen in a transverse section, as 2 hyperintense contiguous dots. ADC map (D) discloses the scolex as iso-/hypointense dots.

MR spectroscopy in NCC:

When conventional MR sequences cannot reliably diagnose NCC, MRS provides specificity and aids in these circumstances. Amino acid peaks like alanine, threonine, succinate, pyruvate, acetate and choline are seen in NCC with low levels of N-acetylaspartate (NAA) and creatine.

Alanine peaks at 1.3 and 1.4 ppm and inverts at 144 ms. Threonine peaks at 1.33 ppm, and another peak is seen at 3.6 ppm which inverts at 135 ms. Pyruvate and succinate resonate close to each other at 2.4 ppm with a narrow difference in chemical shift that is difficult to distinguish.⁹⁷

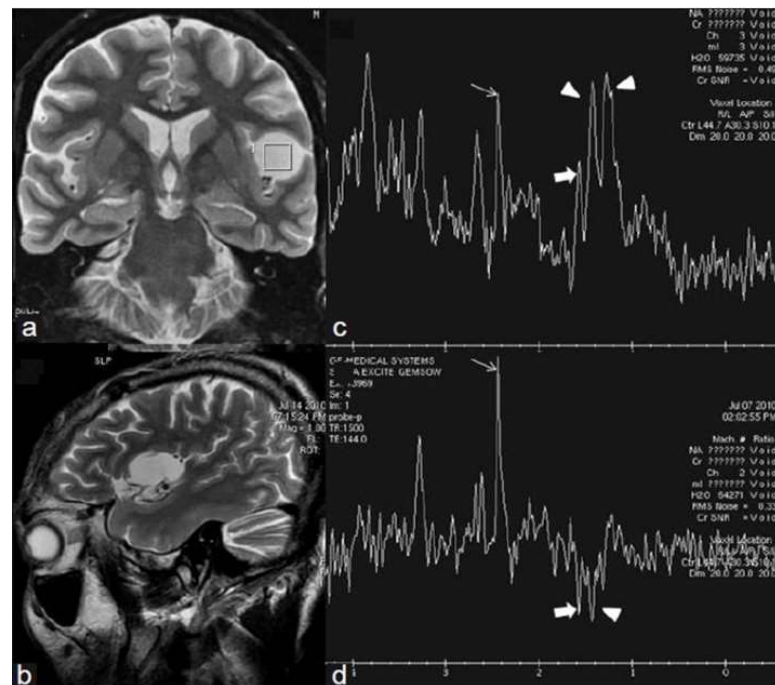


Figure 25: MRS in NCC.⁹⁷

(a-d) MRI images (a) Coronal T2WI (b) Sagittal T2WI (c) & (d) MRS

(a & b): Well-defined cystic lesion with mass effect is seen in the left sylvian fissure.

(c & d): MRS shows lactate (arrowhead in c and d), alanine (thick arrow in c and d) and succinate (thin arrow in c and d) peaks characteristic of neurocysticercosis'

Differential Diagnosis:

Other many ring or nodular enhancing lesions like pyogenic brain abscess, tuberculoma, mycotic granuloma, toxoplasmosis, nocardiosis, primary or metastatic tumours, and septic emboli.

Other diagnostic methods:

A blood sample from the patient is taken, immunoblots utilising pure glycoproteins and recombinant chimeric antigens are confirmed serologically, and the presence or absence of a particular reaction to any of the antigens is then determined. Serological testing is another technique employed.⁹⁸ Only if the patient has several cysts is a serological examination performed; it is ineffective for single lesions. Electroimmuno-transfer blot assays are common procedures in the field of molecular biology. For individuals with at least two cysts, these tests are 100% specific and have a sensitivity of 94–98%.

Enzyme-linked immunosorbent assays such as Ag-ELISAs with a sensitivity of 86% and a specificity of 96% are also used.⁹⁹ It is advised that it be used in conjunction with clinical information and radiological examinations. Due to its limited specificity and sensitivity, the use of the ELISA approach in the diagnoses of NCC has not been successful.¹⁰⁰

Treatment:

The first step in treating individuals with NCC include managing immediate symptoms like seizures (by antiseizure drugs). Antiparasitic treatment shouldn't be started right away and shouldn't even be thought about until after initial symptomatic treatment.

Albendazole and combination therapy with albendazole and praziquantel are antiparasitic regimens for the treatment of patients with viable and/or degenerating cysts on neuroimaging.

The choice of antiparasitic regimen depends on the burden of disease.¹⁰¹

- For patients with one to two cysts, treatment consists of albendazole (15 mg/kg per day in two daily doses up to 1200 mg per day, with food).
- For patients with more than two cysts, treatment consists of albendazole (15 mg/kg per day in two daily doses up to 1200 mg per day, with food) and praziquantel (50 mg/kg per day in three daily doses).

The combination of albendazole and praziquantel has been associated with a higher rate of radiographic resolution than albendazole alone.¹⁰²

Adjunctive corticosteroids should be administered prior to and during antiparasitic therapy. Corticosteroid treatment (dexamethasone 0.2 to 0.4 mg/kg per day) is used to treat diffuse cerebral edema in order to minimise inflammation. Surgery is typically used to treat obstructive hydrocephalus (by placement of an external ventricular drain or shunt).

Table 4: Role of MRI in differentiating NCC and Tuberculoma

Features	Neurocysticercosis	Tuberculoma of the brain
Lesion size	Smaller (<15 mm)	Larger (>15 mm),
Number	Single or multiple	Often multiple, conglomerated
Location	Junction of grey-white matter	Common in posterior fossa
Perilesional edema	Mild or moderate	Mostly moderate to severe
Wall thickness	Usually thin walled	Thick irregular walls
Associated meningitis	Absent	Present
Post contrast features	Thin regular ring enhancement	Thick irregular ring enhancement
MR spectroscopy	Multiple amino acid peaks	Lipid peaks
Focal neurological deficits	Absent	Present
Raised ICP	Transient	Present
Constitutional symptoms	Absent	Present

CLINICAL STUDIES:

Sachin L et al¹⁰³ studied the characteristic imaging findings in various ring enhancing lesions and the role of MR spectroscopy. Out of the 50 patients evaluated, 22 cases were tuberculomas, 16 were NCC, 5 abscesses, 5 metastasis, 1 case of pilocytic astrocytoma and 1 case of tumefactive demyelination. It was concluded that MRI is the most sensitive modality in the characterization of intracranial ring enhancing lesions. On MRI, each lesion had its own characteristic imaging findings which helps in differentiating different various ring enhancing lesions.

Sharma BB et al¹⁰⁴ studied 10 patients between 5 - 15 years (mean age 10.4 years) with complaints of headache and/or seizures who had undergone MRI with or without CT scan. Out of the ten patients, four patients were diagnosed as NCC and six were diagnosed as CNS tuberculomas. All 10 cases showed ring enhancement on post contrast study. MRS further helped to differentiate NCC and tuberculoma. NCC cases

showed amino acid peak in MR spectroscopy and tuberculoma cases showed lipid lactate peak. The reasonable achievable target to differentiate between NCC and tuberculomas in the brain was achieved by analysing the post contrast and MRS findings.

In their retrospective study to assess the value of MRS and DWI as an adjuvant in differentiating tuberculoma and NCC among 30 patients, **Maheshwarappa RP et al**¹⁶ found that on DWI, Out of the 17 cases, in 14 cases, the lesions had diffusion restriction. These lesions were hyperintense on T2 weighted images indicative of caseating granulomas with central liquefaction. However, the 3 lesions which did not show restriction of diffusion on DWI were hypointense on T2 weighted images suggestive of caseating tuberculomas without central liquefaction. All cases of NCC examined were hypointense on DWI, that is there was no restriction of diffusion. On MRS, NCC cases did not exhibit a lipid peak while all tuberculoma lesions, with the exception of one, exhibited predominant lipid peaks. Reduced N-acetylaspartate (NAA) levels were seen in both lesions. Acetate/succinate or both peaks were present in NCC lesions, however they were not in tuberculoma lesions. All NCC patients had normal Cho/creatinine ratios. Out of 17 tuberculoma lesions, seven showed increased Cho/creatinine ratio (greater than 1).

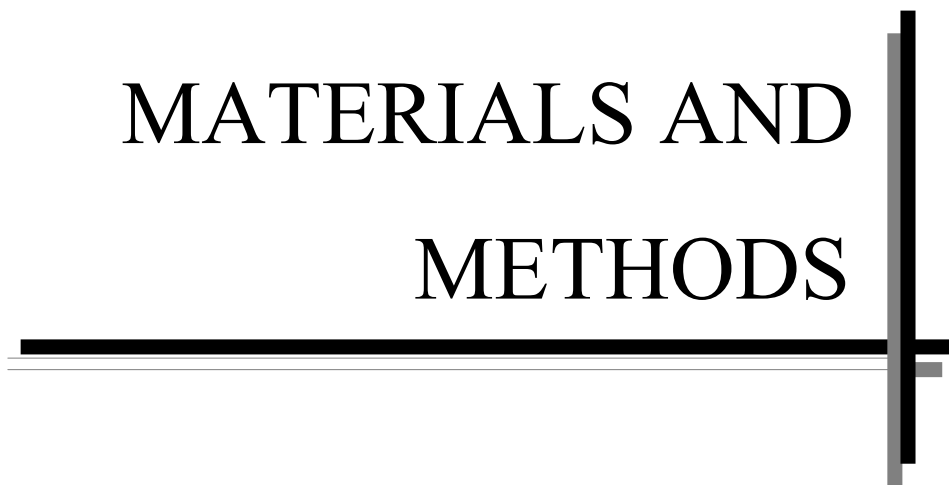
Gupta RK et al¹⁰⁵ in their research work involving 70 tuberculomas divided tuberculomas into three groups based on the intensity in the core of the lesion on T2 weighted images. 12 patients with 12 distinct neurocysticercosis lesions at various stages of development were also included for comparison. This was to demonstrate spectrum of diffusion weighted imaging (DWI) abnormalities in tuberculomas and to distinguish these from degenerating neurocysticercosis. The mean ADC value from the core of T2 hyperintense Tuberculoma lesions, indicative of caseating granulomas with

central liquefaction was $0.80 \pm 0.08 \times 10^{-3}$. This was significantly higher than the mean ADC value from the core of T2 hypointense lesions, suggestive of caseating granulomas without central liquefaction- 1.24 ± 0.32 . Mean ADC value from core of Neurocysticercosis lesions was $1.66 \pm 0.29 \times 10^{-3}$ which was found to be significantly higher than the core of all groups of tuberculomas. Hence, it was concluded that the mean ADC value from the core of NCC was the highest, followed by caseating tuberculoma without central liquefaction followed by caseating tuberculomas with central liquefaction.

Singh et al.¹⁰⁶ in their study to differentiate ring enhancing Neurocysticercosis and Tuberculoma, noted that the maximum numbers of cases were seen in the second and third decade of life with majority of patients being male. MR Spectroscopy in tuberculomas showed a lipid peak whereas in NCC showed amino acid peaks, predominantly acetate and succinate peaks. They concluded that MR Spectroscopy greatly helps to differentiate NCC from Tuberculomas and should be done to differentiate various ring enhancing lesions.

A study done by **E Javier Pretell et al**⁹⁶ showed that cerebral ring enhancing brain lesions (SELs), mostly as a result of neurocysticercosis or tuberculosis, are a common cause of seizures. Ten patients with ring enhancing lesions caused by neurocysticercosis (n=6) or tuberculosis (n=4) were examined by proton magnetic resonance spectroscopy. Tuberculomas had lipid lactate peaks and reduced N-acetylaspartate (NAA). The choline/creatine ratio was greater than 1 in all tuberculomas. On other hand, NCC showed specific amino acid peaks with reduced NAA level. It was concluded that Magnetic resonance spectroscopy differentiates ring enhancing lesions caused by cysticercosis or tuberculosis and may avoid brain biopsies or unnecessary antituberculosis treatments.

MATERIALS AND METHODS



MATERIALS AND METHODS:

Study site: This study was performed in the Department of Radio-diagnosis at R.L Jalappa Hospital and Research center attached to SDUMC, Kolar.

Study population: All the eligible patients who would fulfilled the inclusion criteria underwent MRI Brain (Plain & Contrast) at the Department of Radio-diagnosis at R.L Jalappa Hospital and Research center were considered as the study population.

Study design: The present study was a hospital-based cross sectional study.

Sample Size: 42 patients

Jitendra Singh et al 6 . had reported the sensitivity and specificity of lesion size to differentiate Tuberculoma and NCC to be 79.5% and 73.8% respectively. Assuming alpha error of 5% (95% confidence limit) and an absolute precision (d) of 3%, the minimum required sample size to estimate the sensitivity of MRS in differentiating neurocysticercosis from tuberculoma in brain imaging was estimated to be 42 patients.

The sample size was derived from the following formula:

$$\text{Sample size} = \frac{Z_{1-\alpha/2}^2 p(1-p)}{d^2}$$

$Z_{1-\alpha/2} = 1.96$ at 5 % error alpha. As in majority of studies p values are considered significant below 0.05 hence 1.96 is used in formula.

D is the absolute precision

P is sensitivity and $q=1-p$

Sampling method: Until the sample size was met, all eligible subjects were sequentially recruited into the study using easy sampling.

Study duration: The data collection for the study was done between January 2021 to June 2022

Sampling technique and methodology:

Sampling technique:

Estimating 4 cases per month, accounting for 72 cases for one and a half years and sample size being 42, considering sampling interval of 2, 42 cases will be recruited by systematic random sampling.

Minimum of 42 patients with neurocysticercosis and tuberculoma were included in the study. Baseline data was collected from the patients along with pertinent clinical history and relevant lab investigations. Patients who met the inclusion criteria underwent MRI Brain in 1.5 Tesla, 18 channel, MR Scanner (Siemens[®] Magnetom Avanto[®]). Patient was informed and consent was taken prior to administration of contrast. Patients were in supine position with proper positioning and immobilization of the body. Standard head coil was used in MR.

➤ Following Imaging sequences will be included –

- T1WI (axial and sagittal).
- T2WI (axial and coronal).
- FLAIR.
- Post contrast T1W fat suppressed images. Contrast used will be gadolinium in the dose of 1.5ml/Kg.
- DWI at 0, 500 and 1000 mm²/s b values with corresponding ADC values.
- Single Voxel Spectroscopy- will be performed using chemical shift imaging.

Field of view (FOV)- 220 mm; Slice thickness- 4 mm.

-
- Initially, T1 (axial and sagittal), T2 (axial and coronal) & FLAIR (axial & sagittal) sequences were acquired. Next DWI sequences at 0, 500 and 1000 s/mm² b values are taken followed by its ADC sequence is acquired. Both the sequences; i.e. DWI at 1000 s/mm² b value and ADC sequence are compared to assess the presence or absence of restricted diffusion within the lesions. For derived ADC values, single or few oval shaped region of interest (ROI) are drawn over the core of the lesion. Value of each ROI is measured and mean of all the ROIs is taken as the final ADC. Following this, post contrast images are acquired by injection of 1.5 ml/kg of Gadolinium. Finally, Single Voxel Spectroscopy will be performed using chemical shift imaging.
 - Based on the MRI features such as size, shape, location, wall thickness, intrinsic nodule, surrounding edema, diffusion weighted imaging features with corresponding ADC values, enhancement pattern of lesions and spectroscopy findings, we will evaluate and differentiate the lesion as Neurocysticercosis or Tuberculoma.
 - Radiological diagnosis were correlated in terms of clinical symptoms and response to treatment.



Figure 26 : 1.5 Tesla, 18 channel, MR Scanner (Siemens® Magnetom Avanto)

Inclusion criteria:

- Patients referred for MRI brain with clinical suspicion of neuroinfection.
- Patients with granulomatous lesion on Computed Tomography and referred for Magnetic Resonance Imaging of brain.

Exclusion criteria:

- Patients having cardiac pacemakers, metallic foreign body or implants in situ.
- Altered renal function test and allergy to contrast.

Ethical considerations: The study was approved by the institutional human ethics committee. Informed written consent was obtained from all the study participants ,and only those participants willing to sign the informed consent were included in the study. The risks and benefits involved in the study and the voluntary nature of participation were explained to the participants before obtaining consent. The confidentiality of the study participants was maintained.

Data collection tools: Patients who fulfilled the inclusion/exclusion criteria were included in the study. Written Informed Consent was taken for their willingness to participate in the study. Baseline data were collected from the patients along with pertinent clinical history and relevant lab data. Data was entered into Microsoft excel data sheet and analyzed using SPSS 22 version software. Categorical data was represented in frequencies and proportions. Chi- square was used as test of significance. Continuous data was represented as mean and standard deviation. P value of 0.05 will be considered statistically significant.

ROC analysis : The utility of ADC value of the lesions in differentiating NCC and tuberculoma was assessed by Receiver Operator Curve (ROC) analysis. The area under the curve, along with its 95 % CI and p-value, are presented. The sensitivity and specificity, diagnostic accuracy and predictive values of screening tests with the decided cut-off along with 95 % CI are presented.

RESULTS



OBSERVATIONS & RESULTS

A total of 42 subjects were included in the final analysis.

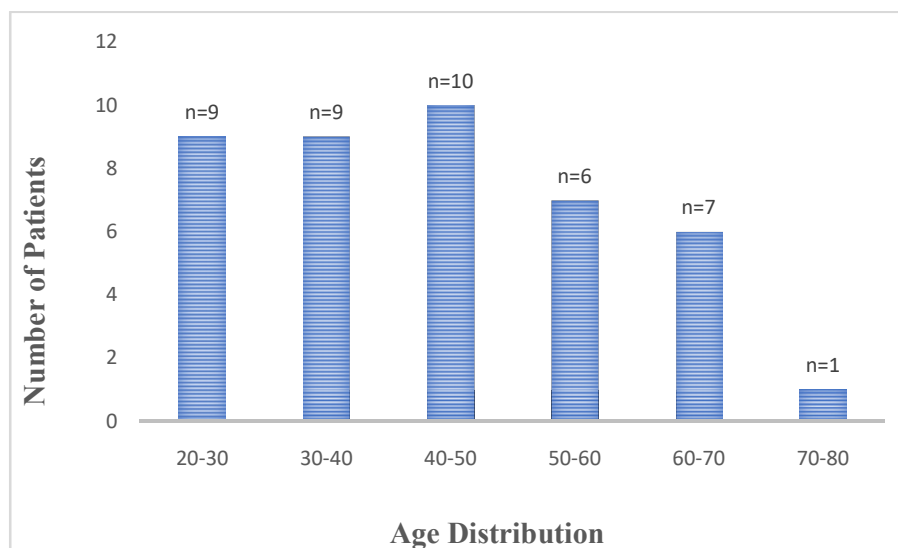


Figure 27: Bar chart showing age distribution in our study cases (n=42)

Table5: Descriptive analysis of age in study population(n=42)

Parameter	Mean ±SD	Median	Minimum	Maximum
Age	42.85 ± 14.76	42	21	78

The mean age was 42.85 ± 14.76 years, ranged between 21 to 78 years in the study population.(Table 5)

Table6: Descriptive analysis of gender distribution in the study population(n=42)

Gender	Frequency	Percentages
Male	25	59.52 %
Female	17	40.47 %

Among the study population, 25 (59.52 %) participants were male, and 17 (40.47 %) were female (Table 6 & Figure 28)

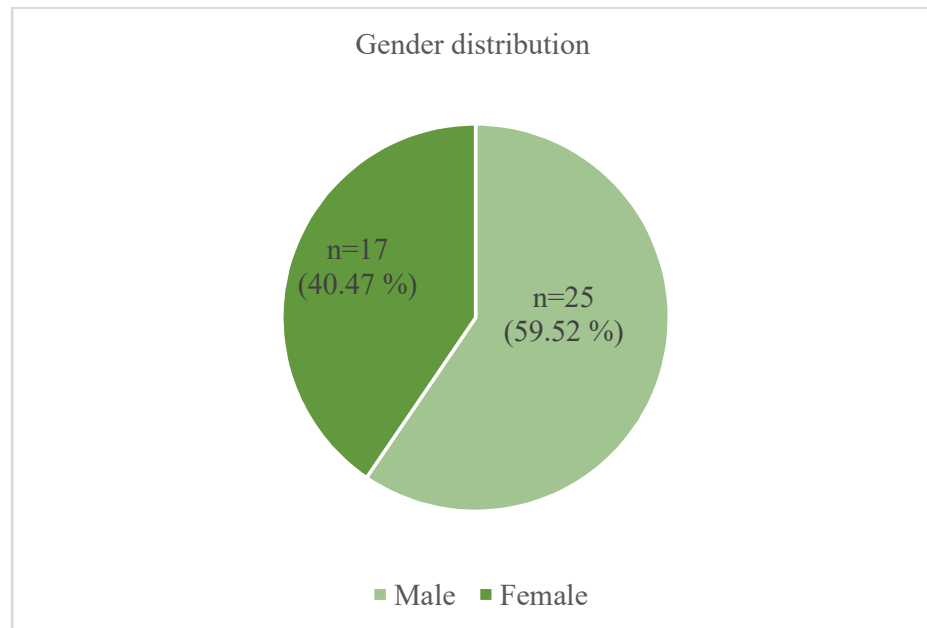


Figure 28: Pie chart showing gender distribution in the study population (n=42)

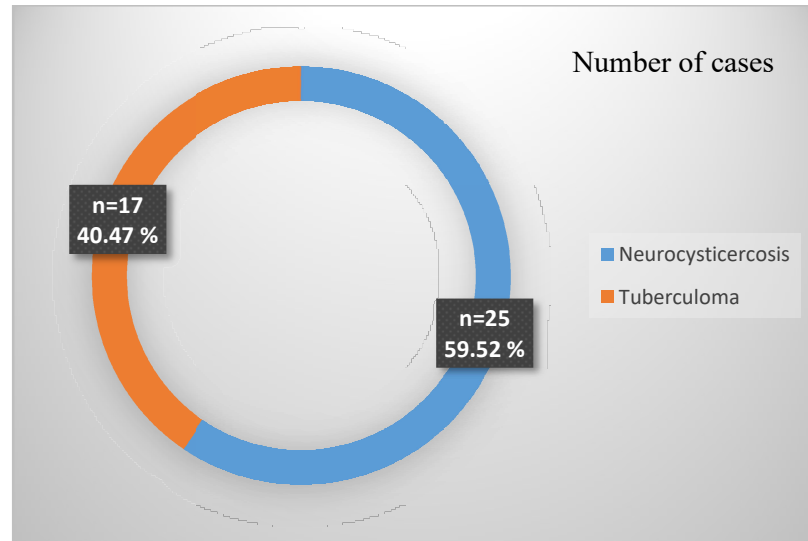


Figure 29: Doughnut chart showing total number of cases included (n=42)

Total number of Neurocysticercosis cases included in the study– 25 (59.25 %)

Total number of Tuberculoma cases included in the study – 17 (40.47 %)

(Figure 29)

Table 7 : Descriptive analysis of number of lesions in the study population (n=42)

NUMBER OF LESIONS	
Single lesion	28 (66.66 %)
Multiple lesion	12 (28.57 %)
Conglomerate lesions	2 (4.76 %)
Total	42

Overall, Out of 42 cases, Single lesion was seen in 28 cases (66.66 %), multiple lesions were seen in 12 cases 28.57 % cases and 2 cases (4.76 %) had conglomerate lesions (Table 7& Figure 30)

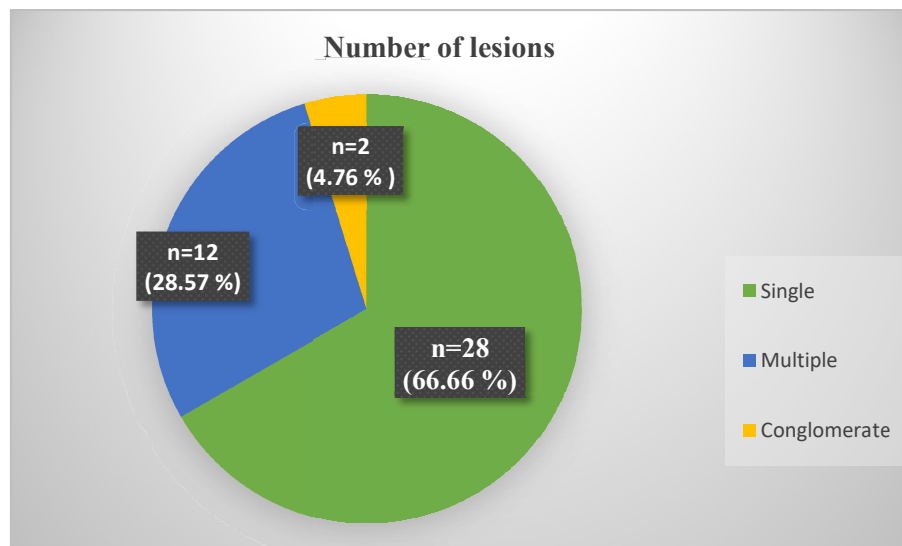


Figure 30: Pie chart showing number of lesions in study population (n=42)

Table 8: Descriptive analysis of number of lesions in NCC and Tuberculoma (n=42)

NUMBER OF LESIONS			
	Single	Multiple	Conglomerate
Neurocysticercosis	18 (72 %)	7 (28 %)	0
Tuberculoma	10 (58.82 %)	5 (29.41 %)	2 (2.2 %)
Total	28	12	2

Out of 25 cases of Neurocysticercosis, 18 cases (72 %) had a single lesion and 7 cases (28 %) had multiple lesions.

Out of 17 cases of Tuberculoma, Single lesion was seen in 10 cases (58.82 %), Multiple lesions were seen in (29.41 %) cases and conglomerate lesion were seen in 2 cases (2.2 %). (Table 8 and Figure 31)

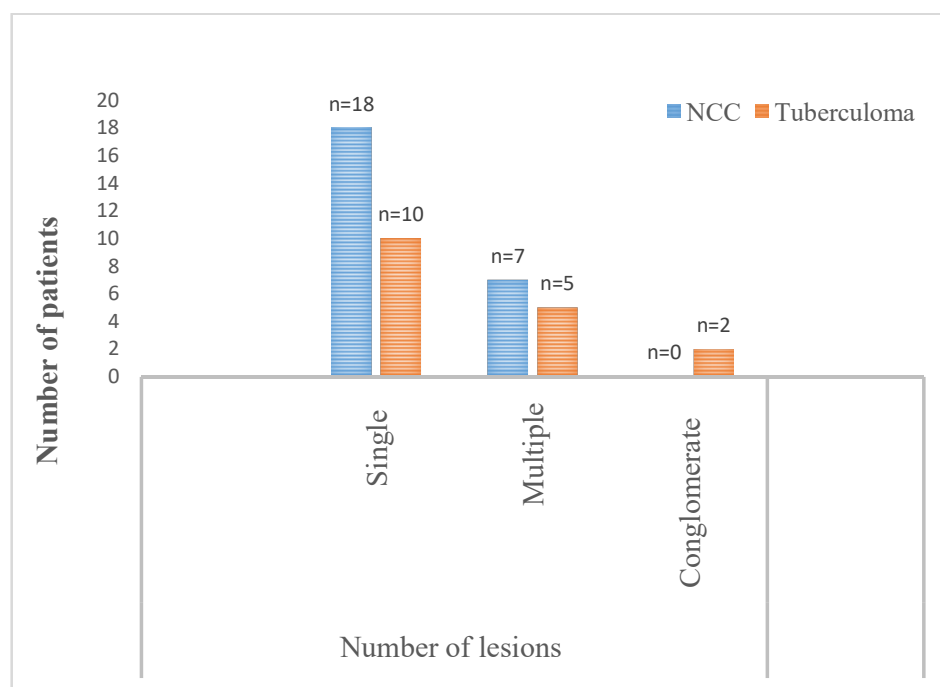


Figure 31: Bar chart showing number of lesions in NCC and tuberculoma (n=42)

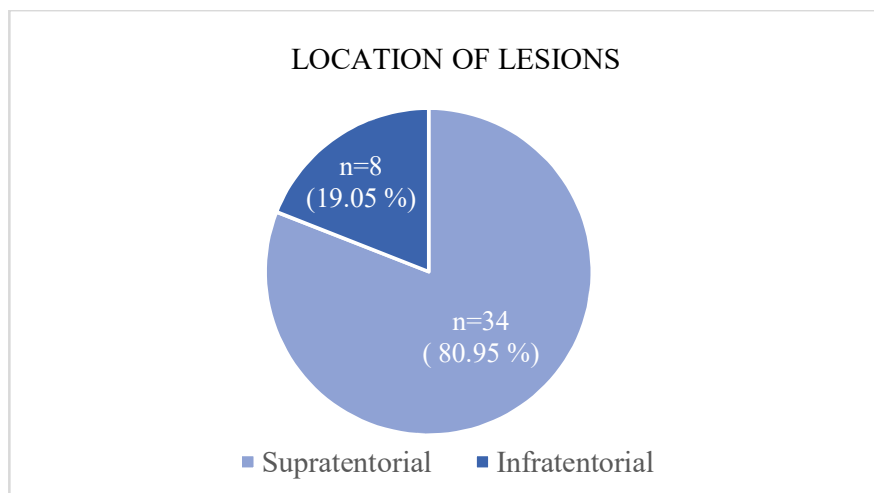


Figure 32: Bar chart showing location of lesions in the study population (n=42)

Out of 42 cases, supratentorial lesions were seen in 34 cases (80.95 %) and infratentorial lesions were in 8 (19.05 %) cases (Figure 32). Hence, Supratentorial lesions were significantly greater than infratentorial. The most frequent location in the supratentorium was the parietal lobe, closely followed by the frontal lobe. In a few cases patients, lesions were scattered all over the brain parenchyma.

Table 9: Descriptive analysis of location of lesion in the study population (n=42)

LOCATION OF LESIONS		
	Supratentorial	Infratentorial
Neurocysticercosis (n=25)	20 (80.0 %)	5 (20.0 %)
Tuberculoma (n=17)	14 (82.35 %)	3 (17.64 %)
Total (n=42)	34	8

Out of 25

cases of neurocysticercosis, supratentorial lesions were seen in 20 cases (80 %) and infratentorial lesions were in 5 (20 %) cases.

Out of 17 cases of tuberculoma, supratentorial lesions were seen in 14 cases (82.35 %) and infratentorial lesions were seen in 3 cases (17.64 %) (Table 9)

Table10: Descriptive analysis of size of lesions in the study population (n=42)

SIZE OF LESIONS		
	Size < 1.5 cm	Size > 1.5 cm
Neurocysticercosis (n=25)	25 (100 %)	0
Tuberculoma (n=17)	15 (88.23 %)	2 (11.76 %)
Total (n=42)	40	2

Overall, Out of 42 cases, size of lesion < 1.5 cm was seen in 40 cases (95.23 %) and > 1.5 cm was seen in 2 cases (4.76 %) (Table 10 and Figure 33)

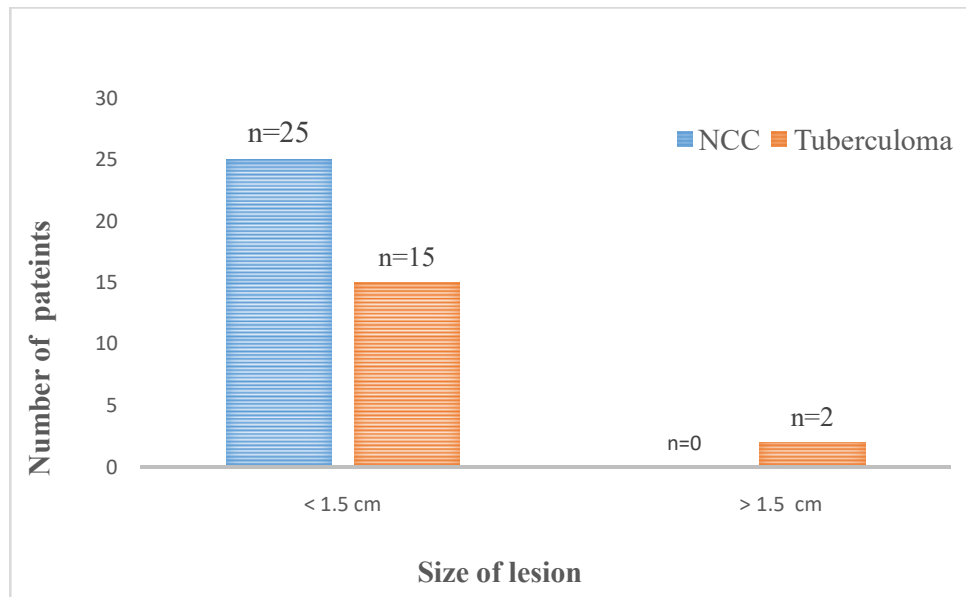


Figure 33: Bar chart showing size of lesions in NCC and Tuberculoma (n=42)

Out of 25 cases of Neurocysticercosis, size of lesion < 1.5 cm was seen in all 25 cases (100 %).

Out of 17 cases of Tuberculoma, size of lesion < 1.5 cm was seen in all 15 cases (88.23 %) and > 1.5 cm was seen in 2 cases (11.76 %) (Figure 33)

Table 11: Descriptive analysis showing margin of lesions (n=42)

MARGINS OF LESIONS		
	Smooth	Irregular
Neurocysticercosis (n=25)	25 (100 %)	0
Tuberculoma (n=17)	6 (88.23 %)	11 (11.76 %)
Total (n=42)	31	11

Overall, Out of 42 cases, smooth margin was seen in 31 cases (73.80 %) and irregular margin was seen in 11 cases (26.19 %).

Out of 25 cases of Neurocysticercosis, smooth margin of lesion was seen in all 25 cases (100 %) and none of the lesions showed irregular margins.

Out of 17 cases of Tuberculoma, smooth margin of lesion was seen in 6 cases (35.29 %), and irregular margin was seen in 11 cases (64.70 %). (Table11 and Figure 34)

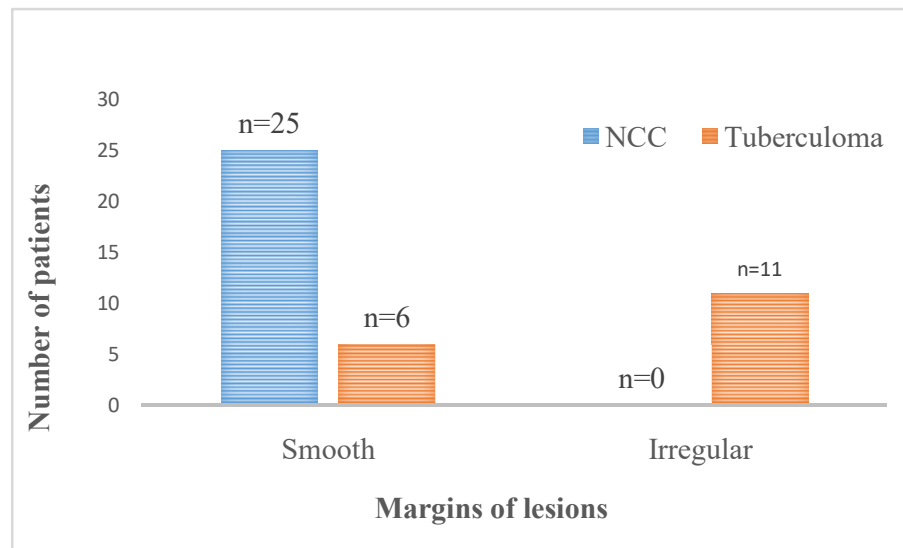


Figure 34: Bar chart showing margin of lesions (n=42)

Table 12: Descriptive analysis showing degree of peri-lesional edema (n=42)

DEGREE OF PERI-LESIONAL EDEMA			
	Mild	Moderate	Severe
NCC (n=25)	18 (72 %)	7 (28.0 %)	0
Tuberculoma (n=17)	1 (5.88 %)	7 (41.17 %)	6 (35.29 %)
Total (n=42)	19	14	6

Overall, Out of 42 cases, mild perilesional was seen in 19 cases (45.23 %), moderate in 17 cases (40.47 %) and severe perilesional edema in 6 cases (14.28 %).

Out of 25 cases of Neurocysticercosis, mild perilesional was seen in 18 cases (72.0 %), moderate in 7 cases (28.0 %). Severe perilesional edema was not seen in any case. Out of 17 cases of Tuberculoma, mild perilesional was seen in 1 case (5.88 %), moderate in 7 cases (41.17 %) and severe perilesional edema in 6 cases (35.29 %) (Table 12 and Figure 35)

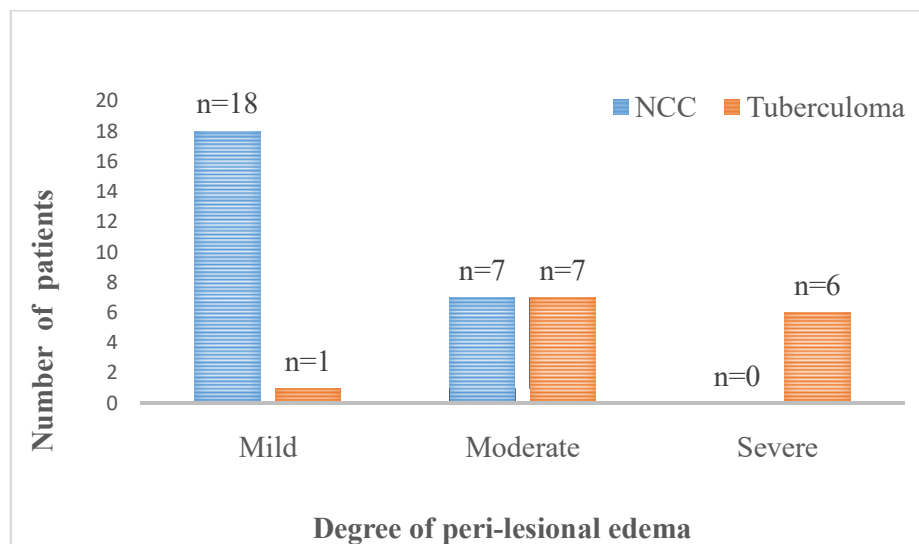


Figure 35 : Bar chart showing peri-lesional edema (n=42)

Table 13: Descriptive analysis of presence of scolex within the lesion in the study population (n=42)

SCOLEX WITHIN THE LESION			
	Present	Absent	TOTAL
Neurocysticercosis (N=25)	10 (40.0 %)	15 (60.0 %)	25
Tuberculoma (N=17)	0 (0 %)	17 (100 %)	17
Total	10	32	42

Out of 25 cases of Neurocysticercosis, Scolex was present in 10 cases (40.0 %) and was absent in 15 cases (60.0 %).

Scolex was absent in all cases of Tuberculoma (100 %).

Hence, among the study population (N= 42) scolex was present in 10 cases (23.80 %) and was absent in 32 cases (76.19 %).(Table 13 and Figure 36)

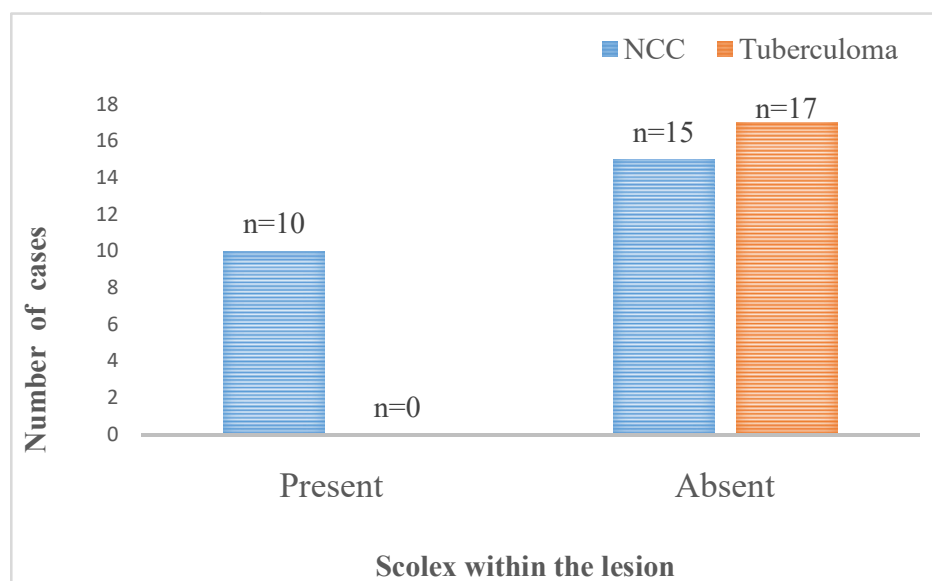


Figure 36: Bar chart showing presence of scolex within the lesion in the study population (n =42)

Table 14: Descriptive analysis of features of meningitis in the study population (n=42)

FEATURES OF MENINGITIS		
	Present	Absent
Neurocysticercosis (n=25)	0	25 (100 %)
Tuberculoma (n=17)	3 (17.67 %)	14 (82.35 %)
Total (n=42)	3	39

Features of meningitis were absent in all 25 cases of Neurocysticercosis (100 %).

Out of the 17 cases of Tuberculoma, features of meningitis were present in 3 cases (17.64 %) and absent in 14 cases (82.35 %). (Table 14)

Table 15: Descriptive analysis of post contrast features of lesions in the study population (n=42)

POST CONTRAST FEATURES		
	Thin walled ring enhancement	Thick irregular ring enhancement
Neurocysticercosis (n =25)	25 (100 %)	0
Tuberculoma (n =17)	6 (35.29 %)	11 (64.70%)
Total (n=42)	31	11

Among the study population (n= 42) thin walled ring enhancement was present in 31 cases (73.80 %) and thick irregular ring enhancement was present in 11 cases (26.19 %) (Table 15 and Figure 37)

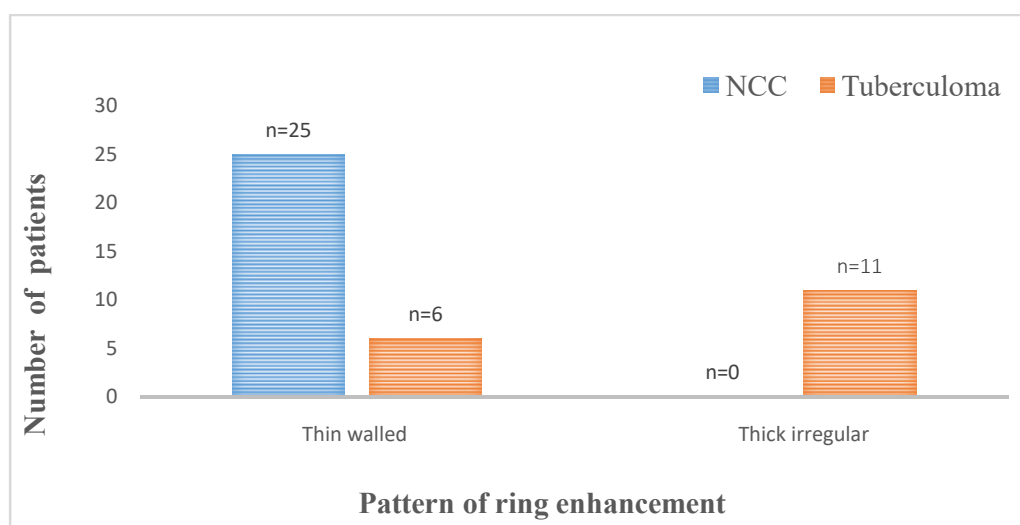


Figure 37 : Bar diagram showing pattern of ring enhancement of lesions in the study population (n=42)

Out of 25 cases of Neurocysticercosis, thin ring enhancement was seen in all 25 cases of Neurocysticercosis (100 %). Out of the 17 cases of Tuberculoma, thin ring enhancement was seen in 6 cases (35.29 %) and thick irregular ring enhancement was seen in 11 cases (64.70 %). (Figure 37)

Table 16: Descriptive analysis of diffusion-weighted imaging findings of lesions in the study population (n=42)

DIFFUSION-WEIGHTED IMAGING FINDINGS		
DWI	Restricting	Not restricting
Neurocysticercosis (n =25)	3 (12 %)	22 (88.0 %)
Tuberculoma (n =17)	12 (70.58 %)	5 (29.41 %)
Total (n=42)	15	27

Among 42 cases, Restriction of diffusion was seen in 15 cases (35.71 %) and restriction of diffusion was absent in 27 cases (64.28 %).

Out of 25 Neurocysticercosis cases, Restriction of diffusion was present in 3 cases which had scolex (12 %) and restriction of diffusion was absent in 22 cases (88 %).

Out of 17 Tuberculoma cases, Restriction of diffusion (hyperintense on T2WI, indicative of caseating granulomas with central liquefaction) was present in 12 cases (70.58 %) and restriction of diffusion (hypointense on T2WI, indicative of caseating granulomas without central liquefaction) was absent in 5 cases. (29.41 %). (Table 16 and Figure 38)

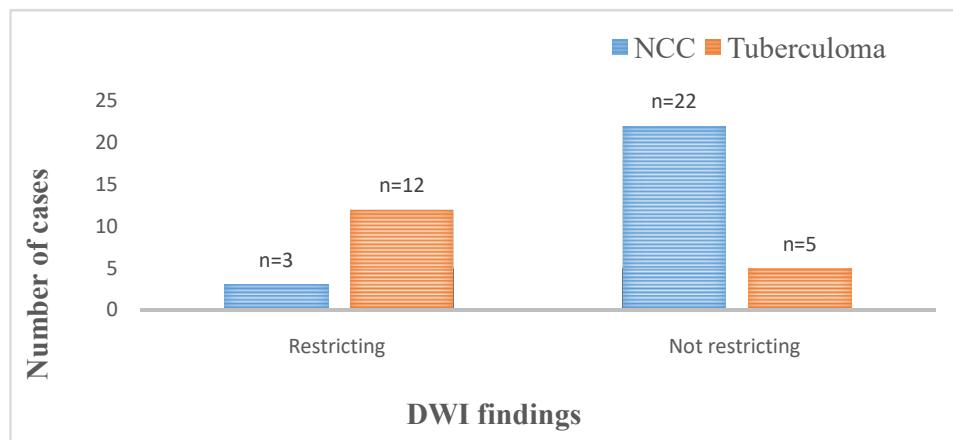


Figure 38: Bar diagram showing of diffusion-weighted imaging findings of lesions in the study population (n=42)

Table 17: Comparative analysis of ADC value of Neurocysticercosis and Tuberculoma in study population (n= 42)

Parameter	Group	Mean	Standard deviation	P value
ADC Values	NCC (n=25)	1.303	0.137	0.001
	TUBERCULOMA (n=17)	0.847	0.191	

The mean ADC value of Neurocysticercosis (n=25) obtained in our study is as $1.30 \pm 0.13 \times 10^{-3} \text{ mm}^2/\text{s}$, ranging between 0.92 to $1.51 \times 10^{-3} \text{ mm}^2/\text{s}$.

The mean ADC value of Tuberculoma (n=17) obtained in our study is as $0.84 \pm 0.191 \times 10^{-3} \text{ mm}^2/\text{s}$, ranging between 0.60 to $1.21 \times 10^{-3} \text{ mm}^2/\text{s}$.

The difference in the ADC values of between NCC and Tuberculoma was statistically significant(P-value<0.001) (Table 17)

Table 18: Comparative analysis of ADC value of T2 hyperintense tuberculoma (suggestive of caseating tuberculoma with central liquefaction) and T2 hypointense Tuberculoma (suggestive of caseating tuberculoma without central liquefaction) in study population(n= 17)

Parameter	Group	Mean	Standard deviation	P value
ADC Values	Hyperintense (n=12)	0.742	0.090	0.001
	Hypointense (n= 5)	1.100	0.102	

The mean ADC value of T2 hyperintense Tuberculoma lesions is obtained as $0.74 \pm 0.09 \times 10^{-3} \text{ mm}^2/\text{s}$, rangingbetween0.62 to $0.91 \times 10^{-3} \text{ mm}^2/\text{s}$.

The mean ADC value of T2 hypointense Tuberculoma lesions is obtained as $1.10 \pm 0.102 \times 10^{-3} \text{ mm}^2/\text{s}$, rangingbetween0.97 to $1.27 \times 10^{-3} \text{ mm}^2/\text{s}$.

The difference in the ADC values between T2 hypointense and T2 hyperintense Tuberculoma was statistically significant (P-value<0.001) (Table 18)

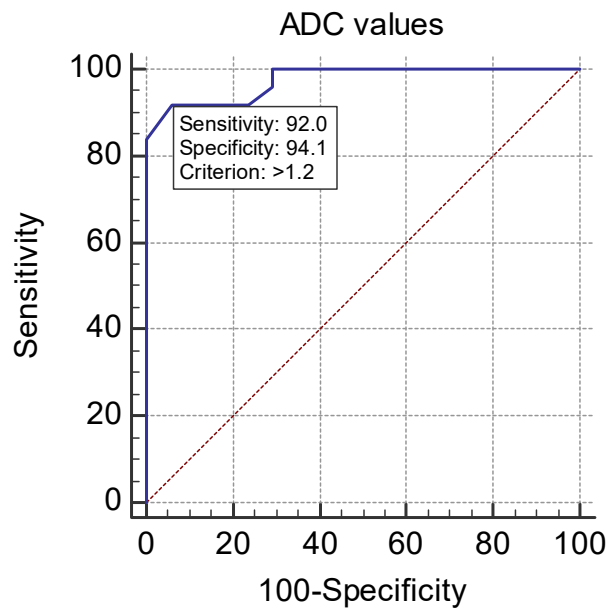


Figure39: ROC analysis of predictive Validity of ADC to differentiate Neurocysticercosis from Tuberculoma

The ADC value derived was 1.2×10^{-3} . This ADC value had excellent predictive validity in differentiating Neurocysticercosis and Tuberculomas as indicated by the area under the curve of 0.975. The derived ADC value had sensitivity of sensitivity of 92 % and Specificity of 94.12% in differentiating Neurocysticercosis from Tuberculoma.

Table 19: Descriptive analysis of ADC cut off value in study population (n= 42)

ADC CUT-OFF VALUE		
ADC Values	< 1.2 x 10⁻³	> 1.2 x 10⁻³.
Neurocysticercosis	2 (8.0 %)	23 (92.0 %)
Tuberculoma	16 (94.11 %)	1 (5.88 %)
Total	18	24

Out of 25 cases of Neurocysticercosis, 23 cases (92.0 %) showed ADC value

> 1.2 x 10⁻³, however 2 cases (8.0 %) showed ADC value < 1.2 x 10⁻³.

Out of 17 cases of Tuberculoma, 16 cases (94.11 %) showed value < 1.1 x 10⁻³

however one case (5.88 %) showed ADC value of > 1.2 x 10⁻³ (value of 1.27 x 10⁻³)

(Table 19)

Table 20: Predictive validity of ADC cut off value of 1.2×10^{-3} in differentiating NCC from Tuberculoma (n=42)

Parameter	Value	95%CI	
		Lower limit	Upper limit
Sensitivity	92.0 %	74.0 %	99.0 %
Specificity	94.12 %	71.3 %	99.9 %
Positive predictive value	95.8 %	78.9 %	99.9 %
Negative predictive value	88.9 %	65.3 %	98.6 %
False positive rate	15.64 %	2.3 %	99.1 %
False negative rate	0.085 %	0.02 %	0.3 %

The ADC cut off value of $1.2 \times 10^{-3} \text{ mm}^2/\text{s}$ had sensitivity of 92 % (95% CI 74.0% to 99.0%), Specificity of 94.12% (95% CI 71.3 % to 99.9 %), positive predictive value was 95.8 % (95% CI 78.9 % to 99.9 %), negative predictive value was 88.9 % (95% CI 65.3 % to 98.6 %), false positive rate was 15.64 % (95% CI 2.3 % to 99.1 %) and false negative rate was 0.085 % (95% CI 0.02 % to 0.3 %). (Table 20)

Table 21: Descriptive analysis of MR Spectroscopy imaging findings of lesions in the study population (n=42)

MR SPECTROSCOPY PEAKS		
	Amino acid peak	Lipid lactate peak
Neurocysticercosis (n =25)	25 (100 %)	0
Tuberculoma (n =17)	0	17 (100 %)
Total (n=42)	25	17

Among 42 cases, 25 cases (59.52 %) showed amino acid peaks and 17 cases (40.47 %) showed lipid lactate peak.

In our study, all 25 cases (100 %) of NCC showed amino acid peak. Out of 25 cases, 14 (56 %) had raised acetate peak (1.9 ppm), 7 (28 %) had raised succinate peaks (2.4 ppm), 1 (4 %) had raised lactate peak (1.3 ppm) and 3 (9.3 %) had both acetate and succinate peaks. All cases had normal choline and creatinine levels, as well as normal choline/creatinine ratios. There was no lipid peak in NCC noted in our study.

In our study, all 17 cases (100 %) of Tuberculoma showed lipid lactate peak at 1.3 ppm. Out of 17 cases, 8 cases (47 %) showed increased Cho/creatinine ratio (Table 21)

**Table 22 : Descriptive analysis of final MRI diagnosis and final clinical diagnosis
(n=42)**

Frequency	Final radiological diagnosis based on multiparametric MRI findings	Final clinical diagnosis based on symptoms/ Sputum analysis / Serological tests/ Chest X Ray Findings/ Response to therapy/ changes on follow up scans
Neurocysticercosis (n=25)	25	25
Tuberculoma (n=17)	17	17

Out of 25 cases where radiological diagnosis was given as Neurocysticercosis, all 25 cases were finally given the clinical diagnosis of Neurocysticercosis based on clinical symptoms and response to therapy (Albendazole). In few of the patients, on follow up scans, decrease in the number and size of lesions as well as degree of peri-lesional edema was noted. However, in few of the patients, the lesions completely disappeared and in the rest, the lesions were found to be calcified on follow up scans.

Out of 17 cases where radiological diagnosis was given as Tuberculoma, all 17 cases were finally given the clinical diagnosis of Tuberculoma based on clinical symptoms, sputum analysis, chest X ray findings and response to treatment. In few of the patients, decrease in the number and size of lesions as well as peri-lesional edema was noted whereas in the other patients, lesions were found to be calcified on follow up scans. (Table 22)

IMAGES



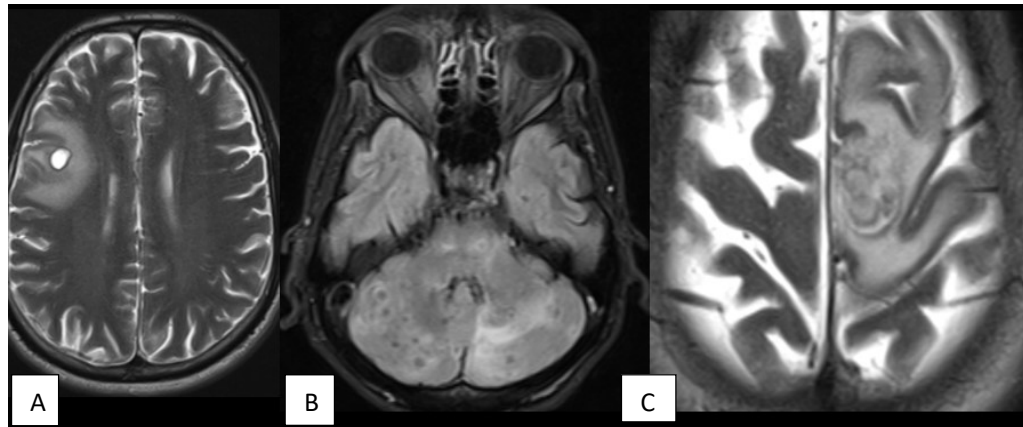


Figure 40 : MRI images demonstrating number of lesions in our study cases

- A) MRI Axial T2WI- A single lesion noted in right frontal lobe- Case of Neurocysticercosis
- B) MRI Axial FLAIR-Multiple lesions in bilateral cerebellar hemispheres- Case of Tuberculoma
- C) MRI Axial T2WI- Conglomerate lesion in left parietal lobe - Case of Tuberculoma

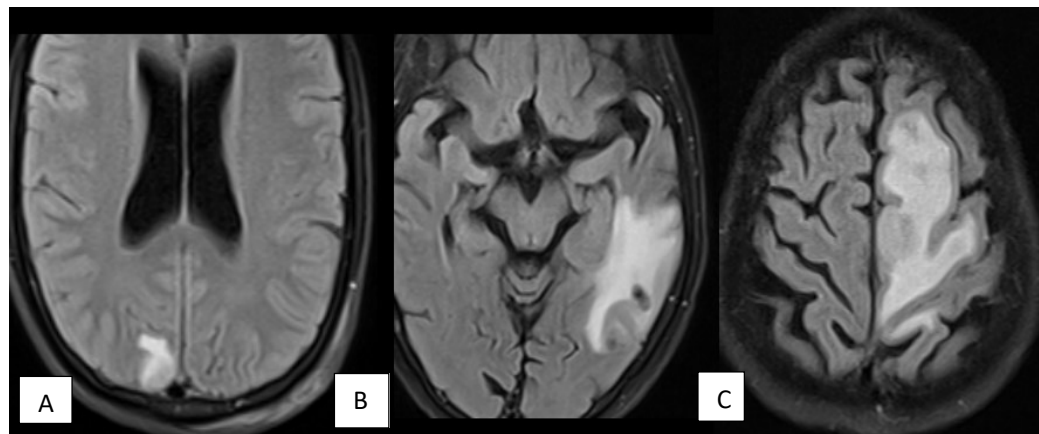


Figure 41 : MRI FLAIR images showing Degrees of edema surrounding lesions

- A) MRI FLAIR images : Case of Neurocysticercosis- Lesion in right occipital lobe with mild perilesional edema
- B) MRI FLAIR images: Case of Tuberculoma- Lesion in left temporal lobe with moderate perilesional edema
- C) MRI FLAIR images: Case of Tuberculoma - Lesion in left high frontal lobe with severe perilesional edema

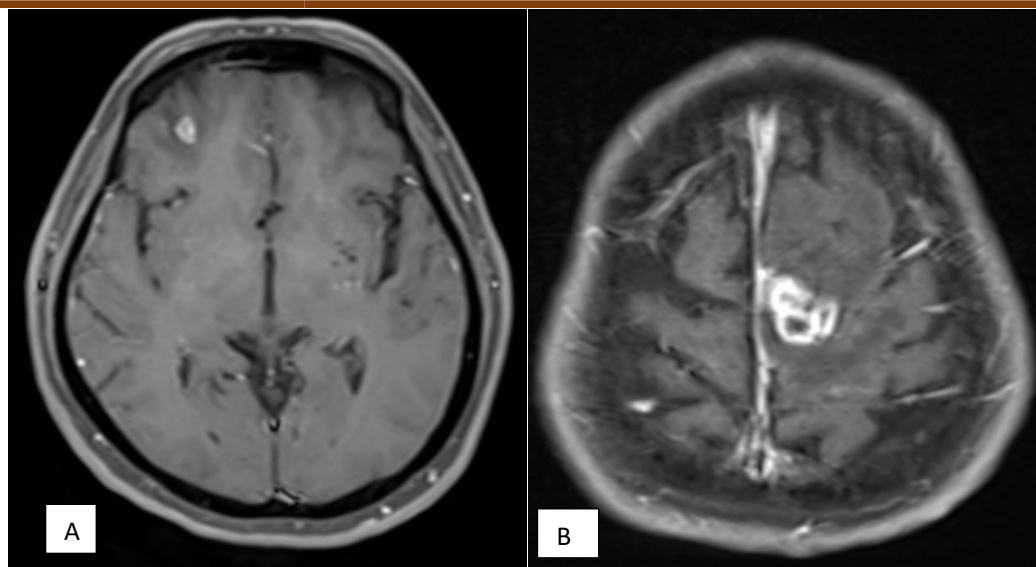


Figure 42 : MRI images demonstrating size of lesions in our study cases

- A) MRI T1W Post contrast image shows a lesion measuring ~ 4.7 mm in left frontal lobe in a case of Neurocysticercosis.
- B) MRI T1W Post contrast image shows a conglomerate lesion measuring ~ 17.3 mm in left parietal lobe in a case of Tuberculoma.

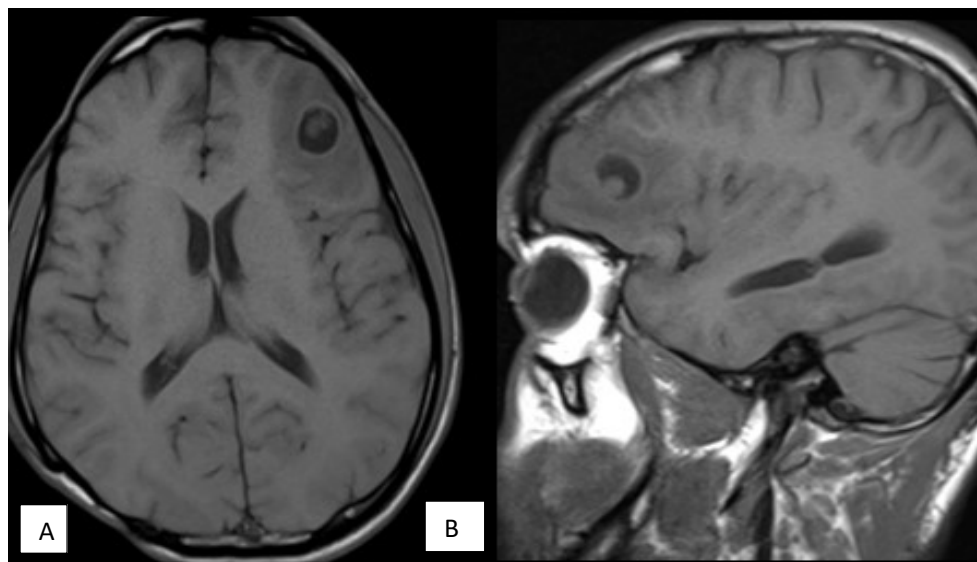


Figure 43 : MRI T1W Axial and Saggital images showing Scolex in a case of Neurocysticercosis

MRI Brain (Plain) A) Axial T1WI B) Sagittal T1WI shows an oval T1 hypointense lesion in left frontal lobe with central T1 hyper intensity suggestive of scolex.

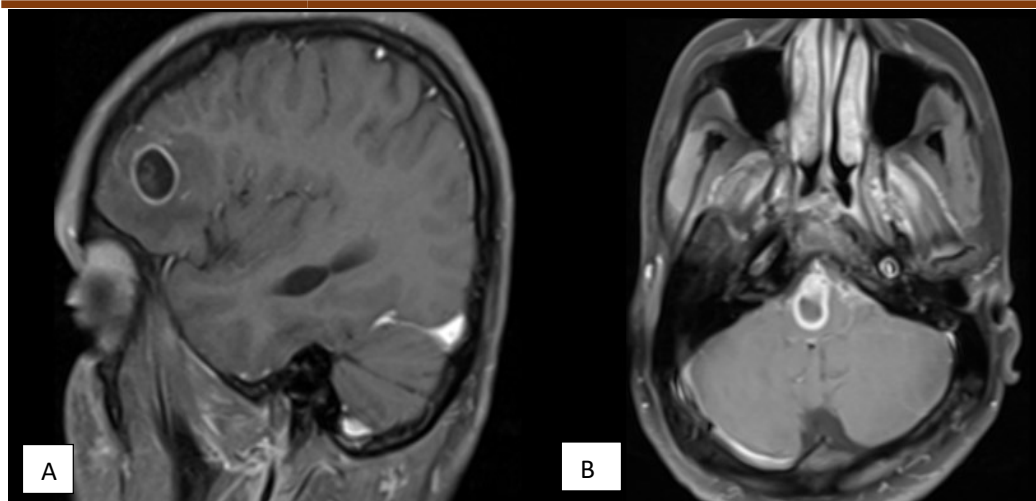


Figure 44: MR Post Contrast images in Neurocysticercosis and Tuberculoma

- A) Case of Neurocysticercosis- MRI T1W Post contrast image shows thin ring enhancement of lesion in left frontal lobe.
- B) Case of Tuberculoma- MRI T1W Post contrast image shows thick irregular enhancement of lesion.

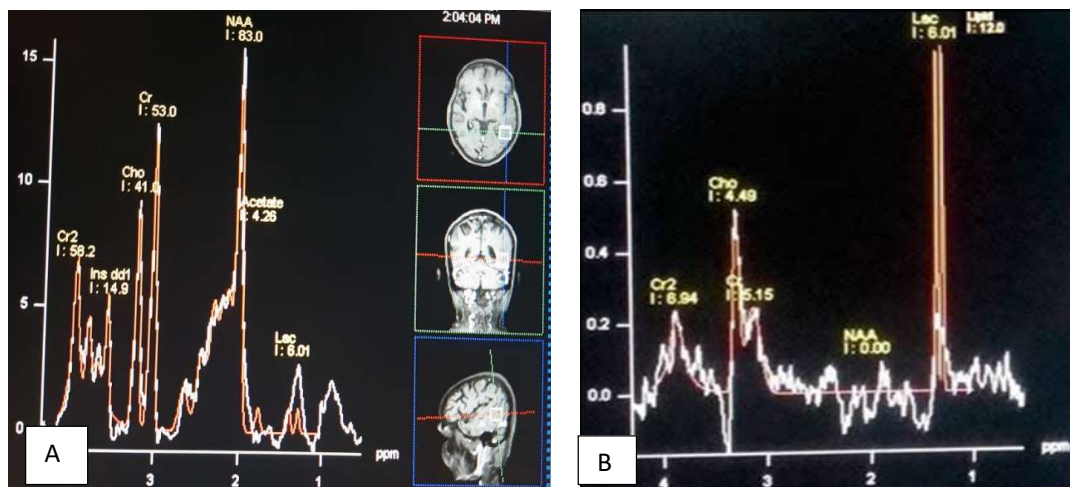


Figure 45: MR Spectroscopy peaks in NCC and Tuberculoma.

- A) Case of Neurocysticercosis: Single Voxel MR Spectroscopy shows acetate peak at 1.9 ppm.
- B) Case of Tuberculoma: Single Voxel MR Spectroscopy shows lipid lactate peak at 1.3 ppm.

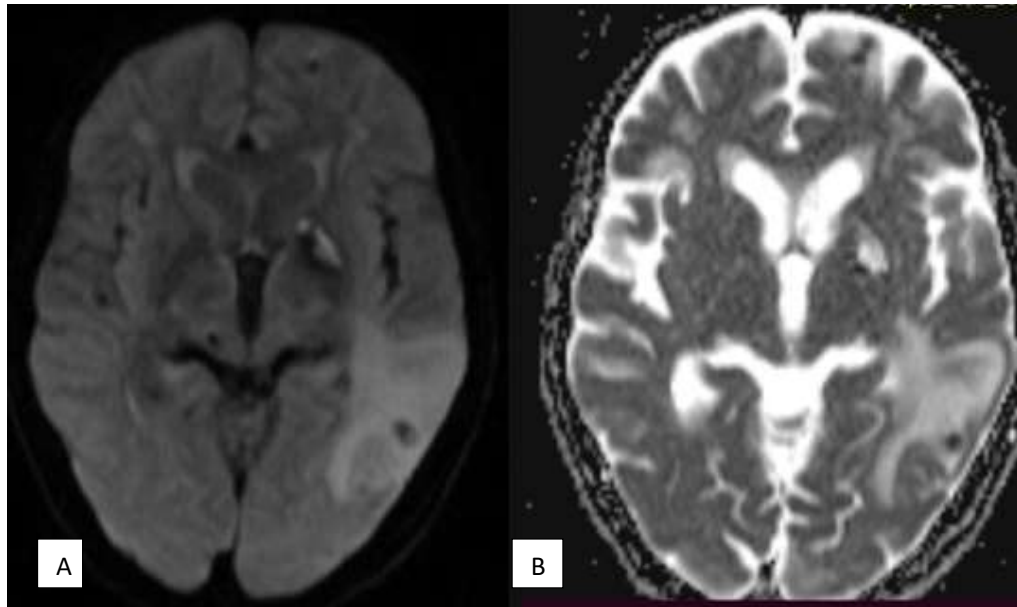


Figure 46: Diffusion weighted imaging features in a case of Neurocysticercosis
MRI Brain Axial sections A) Axial DWI (B) Axial ADC map – No restriction of diffusion.

ADC value obtained was $1.3 \times 10^{-3} \text{ mm}^2/\text{s}$

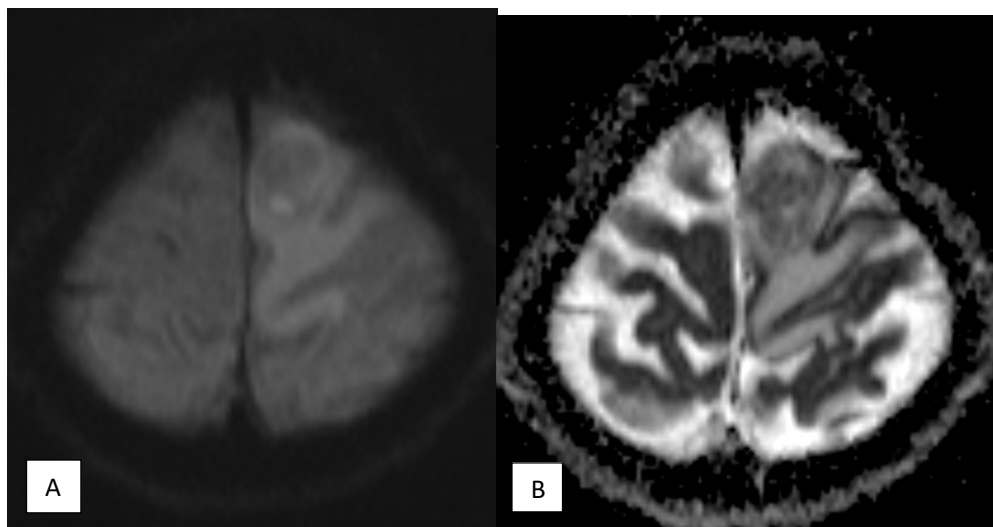


Figure 47: Diffusion weighted imaging features in a case of Tuberculoma

MRI Brain Axial sections A) Axial DWI (B) Axial ADC map – Patchy areas of restriction of diffusion. ADC value obtained was $0.73 \times 10^{-3} \text{ mm}^2/\text{s}$

STAGES OF NEUROCYSTICERCOSIS

VESICULAR STAGE OF NEUROCYSTICERCOSIS

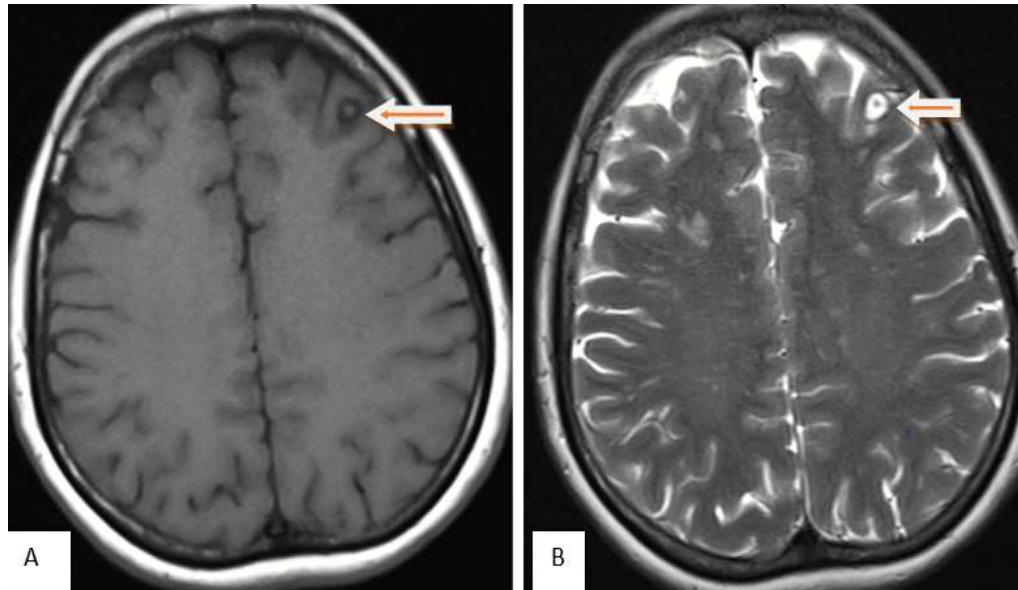


Figure 48: Vesicular Stage of Neurocysticercosis

(A–B) MRI images (A) Axial T1WI B) Axial T2 W images. These images show a well-defined, subcentimetric CSF intensity lesion (orange arrow) demonstrating central T1 hyperintense dot sign in left frontal lobe–Neurocysticercosis (Vesicular stage).

COLLOIDAL VESICULAR STAGE OF NEUROCYSTICERCOSIS

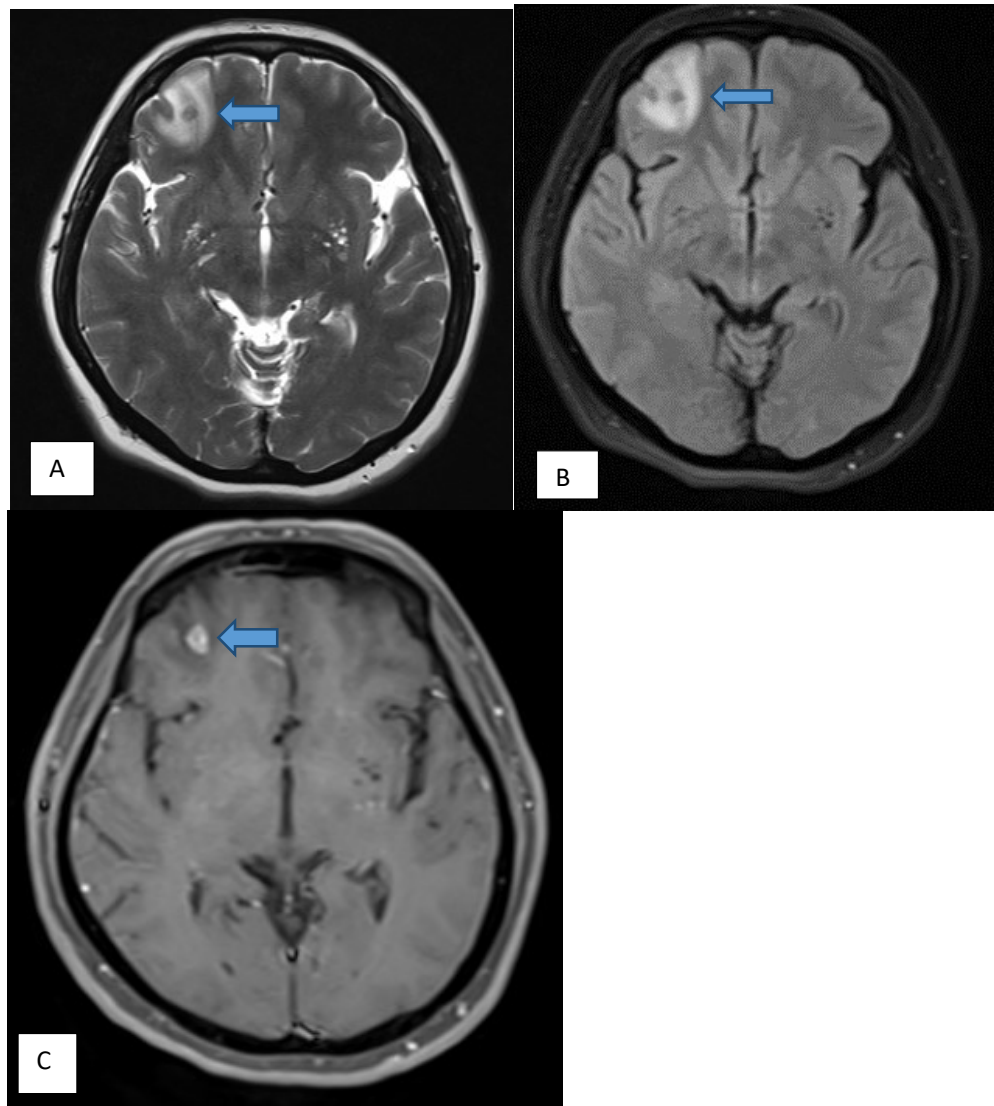


Figure 49 : Colloidal vesicular stage of neurocysticercosis

(A-C) MRI images (A) Axial T2 WI B) Axial FLAIR images C) Axial T1 W post contrast images : These images show a well-defined T2/ FLAIR hypointense focus (measuring ~ 6 mm) (blue arrows) in right frontal lobe with mild perilesional edema. The lesion shows ring enhancement on post contrast study – Neurocysticercosis (Colloid Vesicular stage).

GRANULAR NODULAR STAGE OF NEUROCYSTICERCOSIS

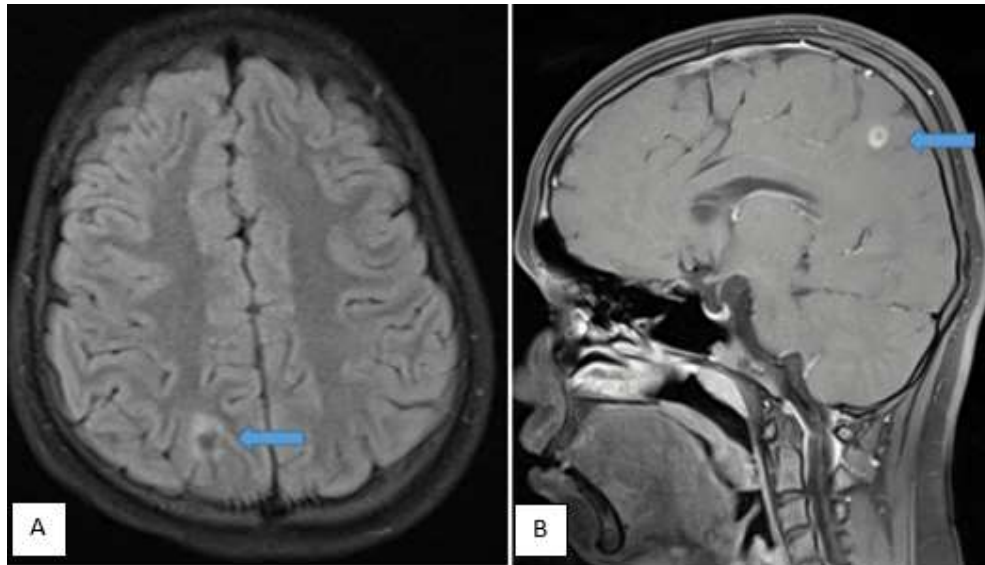


Figure 50 : Granular nodular stage of Neurocysticercosis

(A-B) MRI images (A) Axial FLAIR B) Sagittal Post Contrast images. These images show a FLAIR hypointense lesions with hyperintense rim and minimal perilesional edema(blue arrows) noted in right parietal lobe demonstrating peripheral rim enhancement on post contrast study.

CALCIFIED STAGE OF NEUROCYSTICERCOSIS

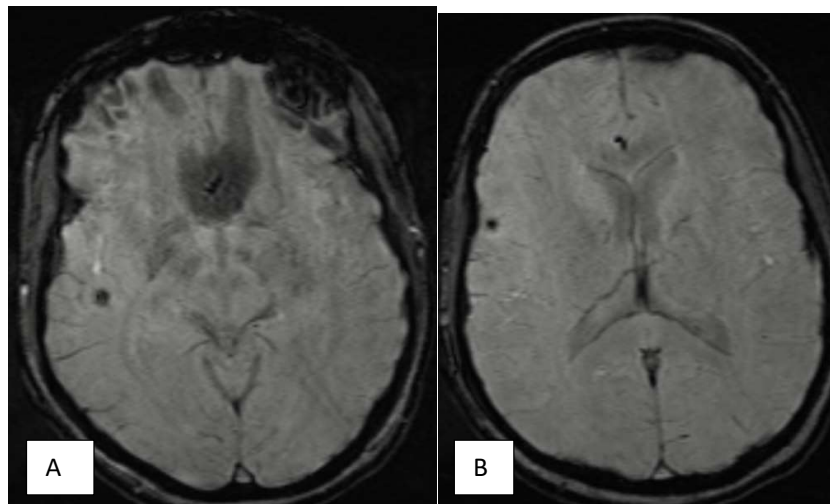


Figure 51: Calcified stage of Neurocysticercosis (A-B) MRI Axial SWI images. These images show two subcentimetric blooming foci in right temporal lobe with no perilesional edema –*healed calcified granuloma stage of neurocysticercosis.*

INTRAVENTRICULAR NEUROCYSTICERCOSIS

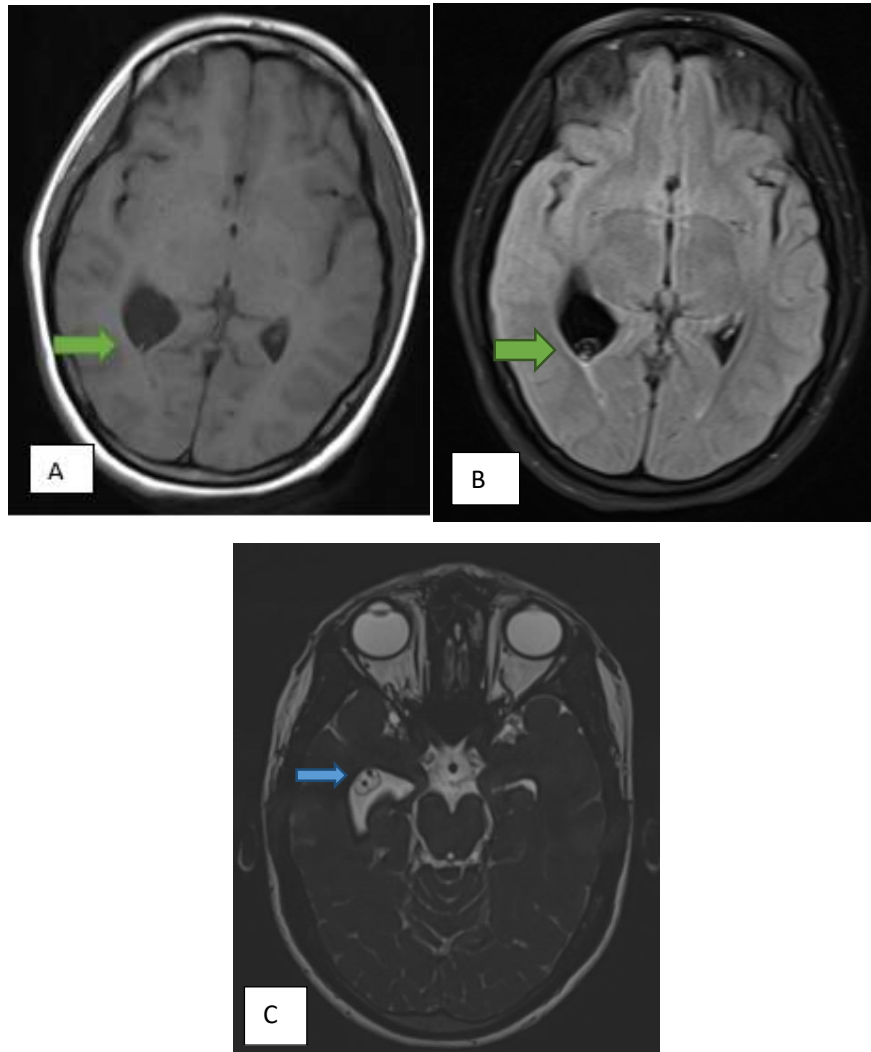


Figure 52: Intraventricular Neurocysticercosis

(A–C) MRI images. Axial FLAIR (A) & Axial T1W1 images (B) in prone position C) CISS sequence in supine position. (A & B) These images show a thin walled ovoid lesion (green arrow) demonstrating T1 hypointensity with central hyperintense dot (A) and FLAIR heterogenous hyperintensity (B) in dependent portion of right lateral ventricle, likely intraventricular neurocysticercosis. (C) On change in position of patient from prone to supine, we can see the change in position of lesion from atria of right lateral ventricle to temporal horn of right lateral ventricle (blue arrow).

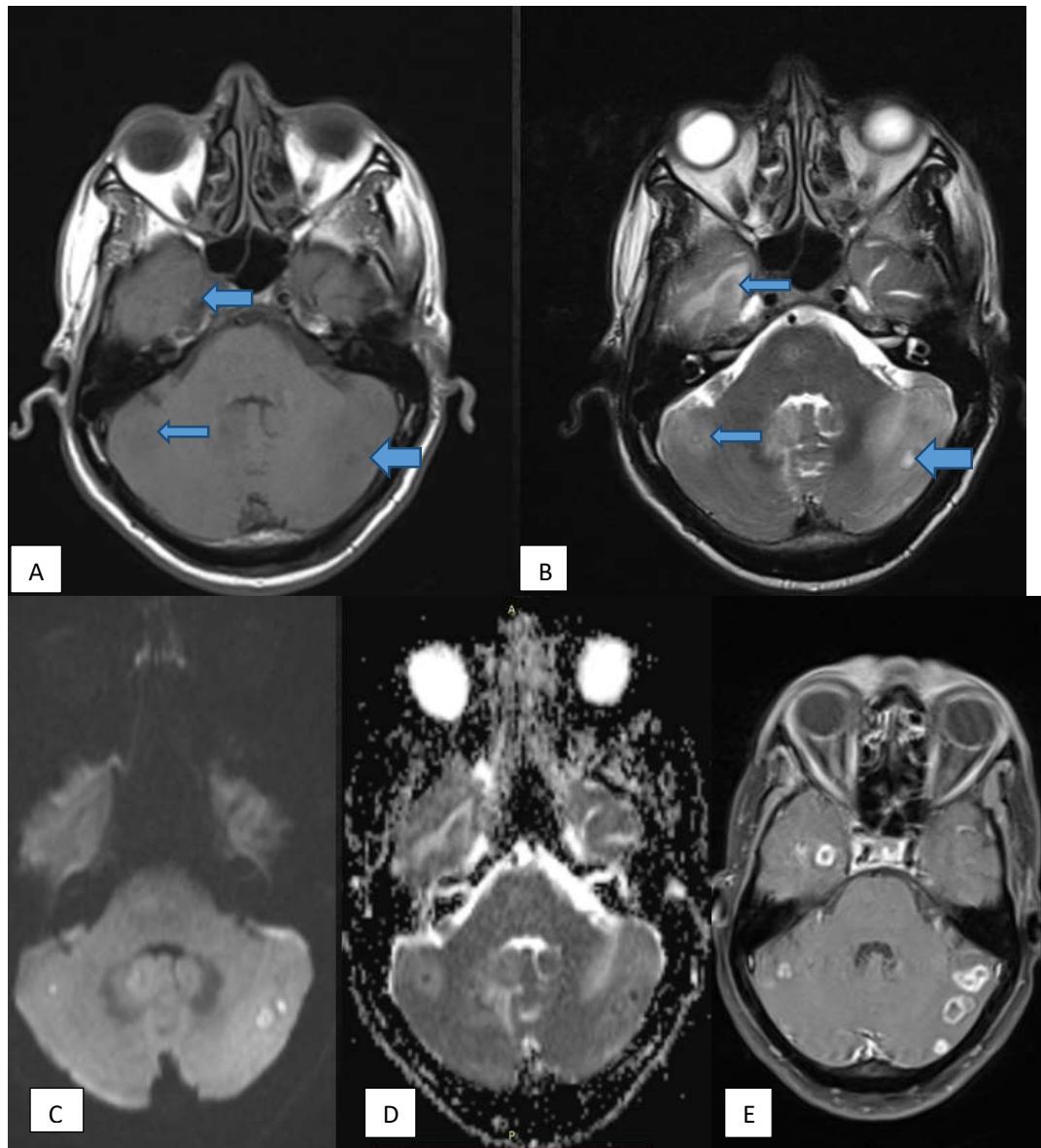


Figure 53: Tuberculoma- Caseating Granulomas with central liquefaction

(A–E) MRI images (A) Axial T1WI (B) Axial T2 WI (C) Axial DWI (D) Axial ADC map (E) Axial T1W post contrast. These images show few, variable sized, T1 iso and T2 hyperintense lesions with T2 hypointense rim (blue arrows) and moderate perilesional edema in bilateral cerebellar hemispheres and right temporal lobe with restricted diffusion on DWI. ADC value obtained was $0.9 \times 10^{-3} \text{ cm}^2/\text{s}$. On post contrast, the lesions show thick irregular ring enhancement – *likely caseating granulomas with central liquefaction*.

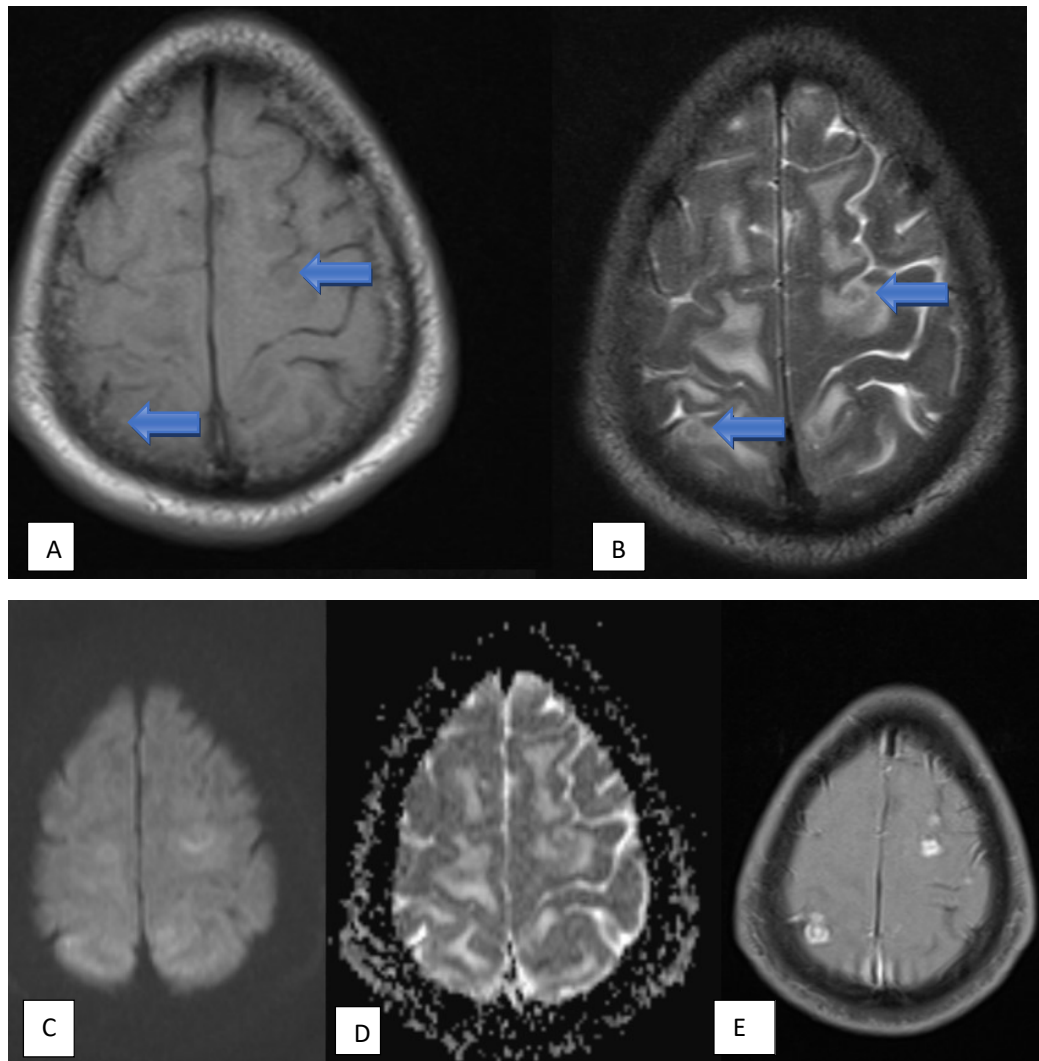


Figure 54 : Tuberculoma- Caseating Granulomas without central liquefaction
 (A–E) MRI images (A) Axial T1WI (B) Axial T2 WI (C) Axial DWI (D) Axial ADC map (E) Axial T1W post contrast. These images show few, variable sized , T1 iso and T2 hypointense lesions with T2 hypointense rim (blue arrows) and moderate perilesional edema in bilateral high parietal lobes with no restricted diffusion on DWI. ADC value obtained was 1.1×10^{-3} cm/s On post contrast, the lesions show thick ring enhancement – *likely caseating granulomas without central liquefaction*.

FOLLOW UP

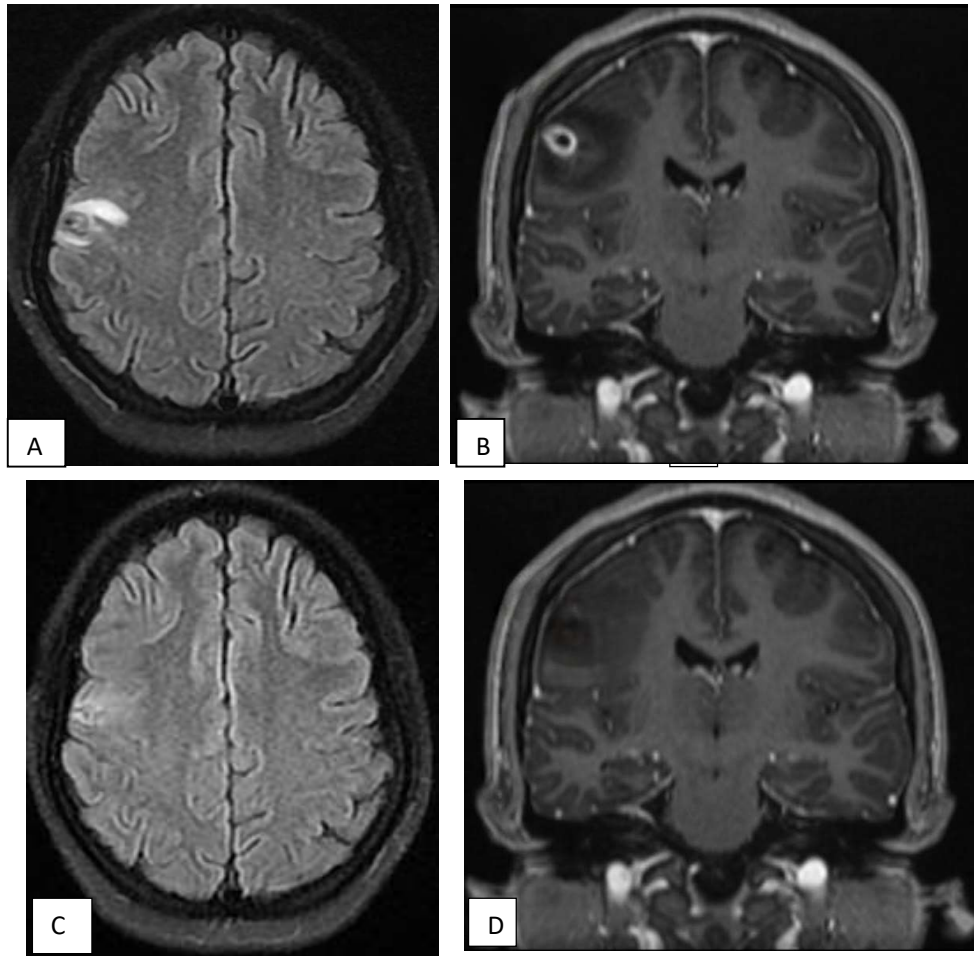


Figure 55 : Follow up of a case of Neurocysticercosis

(A–B) MRI images before treatment (A) Axial FLAIR images (B) Coronal T1W post contrast. A) A T2 heterogeneously hyperintense lesion is noted in right parietal lobe associated with mild perilesional edema. On post contrast study (B) thin rim enhancement is noted-*likely tuberculoma*.

(C-D) Follow up MRI images taken four months after initiation of treatment. (C) Axial FLAIR images D) Coronal T1W post contrast. These images show decrease in size of cystic lesion with decrease in peri-lesional edema.

FOLLOW UP

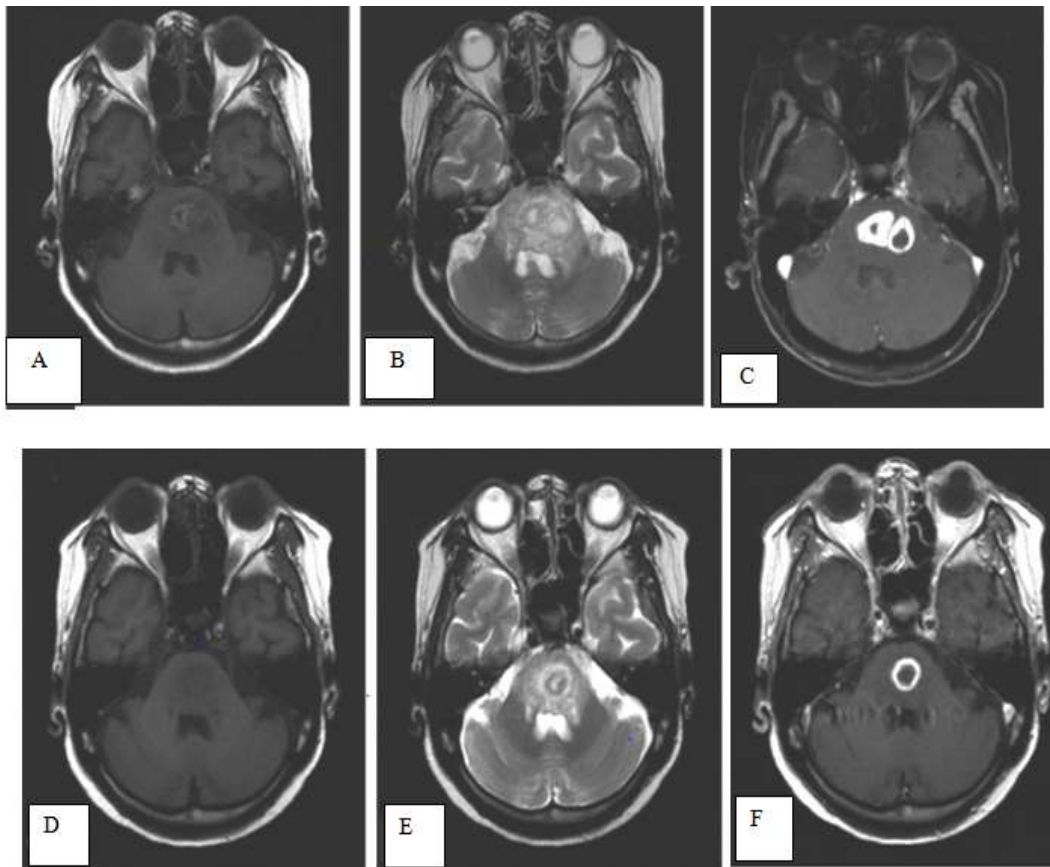


Figure 56: Follow up of a case of Tuberculoma

(A–C) MRI images before treatment (A) Axial T1WI (B) Axial T2 WI (C) Axial T1W fat saturated post contrast. These images show T1 hypointense, T2 iso-hyperintense signal intensity lesions in pons associated with moderate perilesional edema (A & B). On post contrast study (C) thick irregular nodular rim-enhancement is noted-*likely tuberculoma*.

(D-E) Follow up MRI images taken seven months after initiation of treatment. (D) Axial T1WI (E) Axial T2 WI (F) Axial T1W fat post contrast. These images show T1 hypointense, T2 iso- hyperintense signal intensity lesions in pons associated with moderate perilesional edema (D & E) with thick rim-enhancement on post contrast study (F). There is a decrease in size and number of lesions noted as compared to pre-treatment study.

DISCUSSION



DISCUSSION

The two most prevalent infectious causes of ring-enhancing lesions in developing nations are neurocysticercosis (NCC) and tuberculoma. Differentiating these lesions is a diagnostic challenge in neuroimaging. The differentials of ring enhancing lesions include both neoplastic and non-neoplastic origins. A diagnostic issue is telling NCC and tuberculoma apart.

NCC and tuberculomas exhibit similar imaging findings on computed tomography, making it difficult to distinguish them on CT. Therefore, a further advanced method is needed to accurately characterize the lesions. Conventional MRI combined with additional advanced imaging techniques like apparent diffusion coefficient (ADC), magnetic resonance spectroscopy (MRS), and post contrast T1 weighted imaging helps characterise the lesion and makes it easier to distinguish between NCC from tuberculomas for the purpose of appropriate patient management.

Our study included a total number of 42 patients. Out of 42 patients, total number of Neurocysticercosis cases were 25 (59.25%) and Tuberculoma was 17 (40.47%). This was in contrast to a study done by Jitendra Singh et al¹⁰⁶ where tuberculoma was found to be more common as compared to Neurocysticercosis.

In our study, mean age of patients included was 42.85 ± 14.76 years, ranging between 21 to 78 years in the study population. Out of the 42 patients included, 25 were male (59.52%) and 17 (40.47%) female. A similar study by Jitendra Singh et al¹⁰⁶ involving 100 patients showed majority of subjects being males than females (M -62.7%, F-37.3%).

Seizures were the most symptom. Headache came in second place in terms of frequency. Less common symptoms were included focal neurological deficit and altered sensorium. In our study, Supratentorial lesions (80%) were significantly greater than

infratentorial (19.04 %) lesions. This was in concordance with a study done by Maheshwarappa et al ¹⁶ where 96.6 % of cases were supratentorial and the rest were infratentorial.

Overall, Out of 42 cases, Single lesion was seen in 28 cases (66.66 %) , multiple lesions were seen in 12 cases (28.57 %) cases and conglomerate lesions were seen in (0.28 %) of cases. Out of 25 cases of Neurocysticercosis, single lesion was seen in 18 cases (72 %) and multiple lesions were seen in 7 cases (28 %).There were no conglomerate lesions in cases of Neurocysticercosis. Out of 17 cases of Tuberculoma, single lesion was seen in 10 cases (58.82 %), Multiple lesions were seen in 5 cases (29.41 %) cases and conglomerate lesion were seen in 2 cases (0.22 %).This was in concordance with a study done by Sharma B et al¹⁰⁴ which showed that single or multiple lesions were seen in neurocysticercosis whereas single, multiple and conglomerate lesions were seen in tuberculoma.

In our study, Out of 25 cases of Neurocysticercosis, mild perilesional was seen in 18 cases (72.0 %), moderate in 7 cases (28.0 %). Severe perilesional edema was not seen in any case of NCC. Out of 17 cases of Tuberculoma, mild perilesional was seen in 1 case (5.88 %), moderate in 7 cases (41.17 %) and severe perilesional edema in 6 cases (35.29 %). This was in concordance with a study done by Jayendra et.al ¹⁰⁷ which showed extensive perilesional edema in Tuberculomas.

Scolex was seen in 10 (40.0 %) cases of Neurocysticercosis and was absent in all cases of tuberculoma. The results obtained were in concordance with a study conducted by Nash et al. ⁹⁰ where scolex was seen in vesicular stage of Neurocysticercosis and absent in calcified stages.

Basal meningeal enhancement, indicating meningitis, was observed in 3 our study cases, all of which were cases of tuberculoma. No associated meningitis was seen in any case of NCC. Similar observation was also made in a study conducted by Chang et al³⁷

In our study, out of the 17 cases of Tuberculoma, thin ring enhancement was seen in 6 cases (35.29 %) and thick irregular ring enhancement was seen in 11 cases (64.70 %), This was in concordance with a study done by Triveni et al ³⁸ which showed that tubercular lesions more than > 1 cm showed thick nodular enhancement. Out of 25 cases of Neurocysticercosis, thin ring enhancement was seen in all 25 cases of Neurocysticercosis (100 %).

Out of 25 Neurocysticercosis cases, restriction of diffusion was absent in 22 cases (88 %) and was present in 3 cases which had scolex (12 %). In our study, scolex was present in 9 cases and out of these 9 cases with scolex, restricted diffusion was present in 3 cases. A study by Shetty B et al.¹⁰⁸, showed similar results with presence of restriction of diffusion in scolex in vesicular stage of NCC.

A study done by Raffin LS et al¹⁰⁹, also showed similar results in their study and concluded NCC lesions had hypointense signal on DWI.

Out of 17 Tuberculoma cases, 12 cases (70.58 %) which were hyperintense on T2, indicative of caseating tuberculoma with central liquefaction showed restriction of diffusion whereas 5 cases (29.41 %) which were hypointense on T2, indicative of caseating tuberculomas without central liquefaction showed no restriction of diffusion. In T2 hyperintense tuberculoma, the presence of inflammatory cells is responsible for the restriction of diffusion that is absent in Neurocysticercosis and T2 hypointense Tuberculomas. This was in concordance with a study done by Batra A et al¹¹⁰ which showed similar kind of results in the study by concluding that those Tuberculoma lesions which had hyperintense center on T2 were hyperintense on DWI and those

lesions which had hypointense center on T2 was hypointense on DWI. A study done by Shetty B et al.¹⁰⁸ showed peripheral diffusion restriction in tuberculoma and another study done reported the same results by concluding restricted diffusion with reduced ADC value in tuberculoma. However, our results were contradictory to the results of a study by Vasudev MK et al.¹¹¹, wherein there was no restriction of diffusion seen in Tuberculoma.

In our study, ADC of $1.2 \times 10^{-3} \text{ mm}^2/\text{sec}$ was taken as a cut off value. Out of 25 cases of Neurocysticercosis, 23 cases showed ADC value $> 1.2 \times 10^{-3}$ and two cases showed ADC value $< 1.2 \times 10^{-3}$. Out of 17 cases of Tuberculoma, 16 cases showed value $< 1.2 \times 10^{-3}$ however one case showed ADC value $> 1.2 \times 10^{-3}$. Similar observation was also made in a study conducted by Kanminigo et al.⁵⁴

In our study, Mean ADC value for Tuberculoma (n=17) is $0.84 \pm 0.191 \times 10^{-3}$ and Mean ADC value for Neurocysticercosis (n=25) is $1.30 \pm 0.137 \times 10^{-3}$. Mean ADC value of T2 hypointense tuberculomas (n=5), indicative of caseating granulomas without central liquefaction was $1.10 \pm 0.102 \times 10^{-3}$ and mean ADC value of T2 hyperintense tuberculomas (n=12), indicative of caseating granulomas with central liquefaction was $0.74 \pm 0.09 \times 10^{-3} \text{ mm}^2/\text{s}$. ADC values from the core of NCC were significantly higher compared to the ADC values from the core of Tuberculoma. It was also noted that the mean ADC value from the core of T2 hypointense lesions was significantly higher compared to mean ADC value from the core of T2 hyperintense tuberculoma lesions. A study by Gupta RK et al¹⁰³ showed similar results where the mean ADC value for Vesicular stages of cysticercus was $1.66 \pm 0.29 \times 10^{-3}$, mean ADC value from the core of mildly T2 hyperintense tuberculoma lesions was $0.80 \pm 0.08 \times 10^{-3}$ and mean ADC value from the core of T2 hypointense tuberculoma lesions was $1.24 \pm 0.32 \times 10^{-3}$. However, a study done by Basoglu et al⁵⁵ showed tubercular

lesions as isointense and having normal ADC values. Hence, it is possible to distinguish similar appearing cysticercus granulomas from tuberculomas with high ADC in the former compared to restricted diffusion in the later. In our study, derived ADC cut off value of $1.2 \times 10^{-3} \text{ mm}^2/\text{s}$ had a sensitivity of 92 % Specificity of 94.1 %, and the total diagnostic accuracy of 93.02% in differentiating Neurocysticercosis from Tuberculoma. The ADC value of lesions had excellent predictive validity in differentiating Neurocysticercosis and Tuberculoma, as indicated by the area under the curve of 0.975 (P-value <0.001).

From our study, we found a specific peak for Tuberculoma on Magnetic Resonance Spectroscopy. All 7 cases showed lipid lactate peak at 1.3 ppm. Out of 17 cases, 8 cases (47%) showed increased Cho/creatinine ratio. In our study, there was no correlation between presences of lipid peak on MRS with core signal intensity of lesion. A lipid peak in MR spectra was seen in lesions, caseating tuberculomas with central liquefaction as well as caseating tuberculomas without central liquefaction. In solid caseation necrosis, infiltration with lipid-laden macrophage contributes to lipid peak whereas presence of lipid in tubercular bacilli as well as breakdown products of gray-white matter is responsible for lipid peak in liquefied necrosis¹⁶. Gupta RK et al.⁵⁶ reported the same result in their study by showing raised lipid lactate peak in tuberculoma. Another study showed raised lipid lactate peak in all patients except two cases which showed raised choline peaks.

In our study, Out of 25 cases of NCC, all 25 cases (100%) showed amino acid peak. Out of 25 cases, 14 (56%) had raised acetate peak at 1.9 ppm , 7 (28%) had raised succinate peaks at 2.4 ppm , 1 (4%) had raised lactate peak and 3 (9.3%) had both acetate and succinate peaks. All cases had normal choline and creatinine levels, as well as normal choline/creatinine ratios. There was no lipid peak in NCC. Pretell et al⁹⁶,

reported the same result in their study by concluding raised acetate, lactate and succinate in NCC. This was also in concordance with a study done by Maheshwarappa et al.¹⁶ which showed similar results. Another study by Agrawal M et al.¹⁰⁷ also found similar results in MRS when he evaluated three large intraparenchymal isolated degenerating cysticerci. Hence, it can be concluded that MR Spectroscopy is useful in differentiating Neurocysticercosis from Tuberculoma. Incooperating MRS into routine imaging helps by increasing the diagnostic yield, and aiding the clinicians in immediate management.

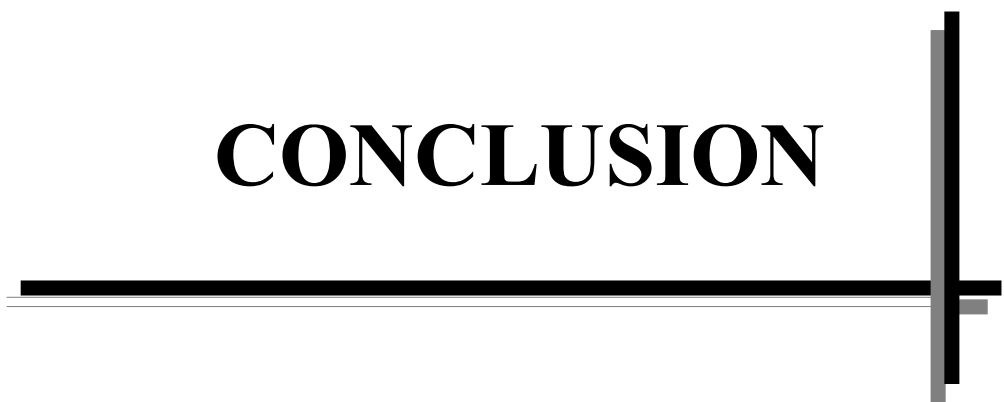
These constellation of findings help in differentiating Neurocysticercosis and Tuberculoma. Size of lesions, presence of scolex, degree of perilesional edema, Post contrast features, MRS & DWI findings as well as ADC cut off values are important for diagnosis ad differentiation of NCC and tuberculoma .

LIMITATIONS

There was no available histopathological correlation for the diagnosis.

Presumptive diagnosis of the lesions, followed by the appropriate clinical trial and follow up is preferred over biopsy for these lesions (ATT for tuberculoma and albendazole for NCC).

CONCLUSION



CONCLUSION

Neurocysticercosis and Tuberculoma are the most common granulomatous infections in India. It is a challenge to differentiate NCC and tuberculomas radiologically since they show the same imaging findings on computed tomography. This study was done to assess the role of MRI as an additional advanced modality to aptly characterize the lesion.

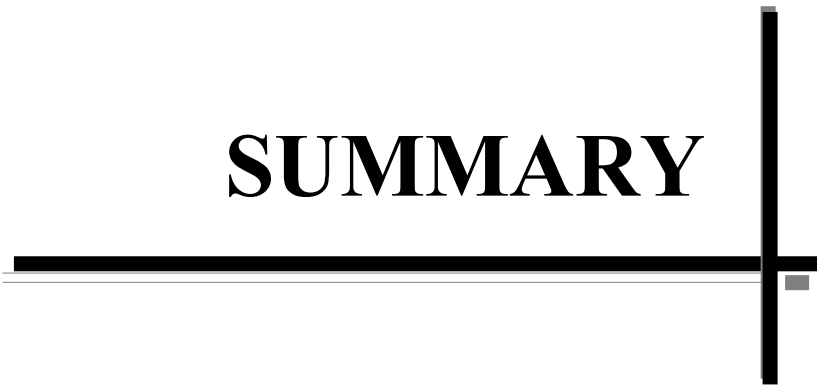
In our study, it was seen that after post contrast, thin ring enhancement was seen in Neurocysticercosis lesions whereas most cases of Tuberculoma showed thick, irregular, nodular pattern of enhancement. Hence, pattern of ring enhancement was helpful in differentiating Neurocysticercosis from Tuberculoma.

In our study, we have found specific peaks on MR Spectroscopy, namely acetate and succinate for Neurocysticercosis and lipid lactate peak for Tuberculoma. This further helped in differentiating these two granulomatous lesions.

On diffusion weighted imaging, restriction of diffusion was absent in almost all cases of Neurocysticercosis however, it was present in most cases of Tuberculoma. The mean ADC value of core of Neurocysticercosis was found to be higher than that of Tuberculoma lesions. The derived ADC cut off of 1.2×10^{-3} had a sensitivity of 92 % and Specificity of 94.1 %, in differentiating Neurocysticercosis from Tuberculoma. Hence, based on features of restriction of diffusion and derived ADC values of lesions, we could differentiate Neurocysticercosis and Tuberculoma.

Hence, rather than using these sequences alone, the combination of DWI, ADC MRS and post contrast T1 weighted imaging will boost the diagnostic yield, eliminate the need for unnecessary biopsy and aid the clinician in managing patients right away. Hence, Multiparametric MRI assessment helps to aptly characterize the lesions which plays a major role in patient management.

SUMMARY



SUMMARY

This study was a hospital based observational study involving 42 subjects, with male subjects in the majority. Out of 42 cases, total number of Neurocysticercosis cases included – 25 (59.25 %) and number of Tuberculoma cases included – 17 (40.47 %). Overall, Out of 42 cases, Single lesion was seen in 28 cases (66.66 %) and multiple lesions were seen in 12 cases (28.57 %) and conglomerate lesions were seen in 2 cases (4.76 %). In our study, supratentorial lesions were significantly greater than infratentorial.

In our study, out of 25 cases of Neurocysticercosis, mild perilesional was seen in 18 cases (72.0 %) and moderate in 7 cases (28.0 %). Out of 17 cases of Tuberculoma, mild perilesional was seen in 1 case (5.88 %), moderate in 7 cases (41.17 %) and severe perilesional edema in 6 cases (35.29 %).

Scolex was present in 10 cases (40.0 %) of Neurocysticercosis and was absent in all cases of Tuberculoma. Hence, presence of scolex within a lesion was indicative of Neurocysticercosis.

Thin ring enhancement was seen in all 25 cases of Neurocysticercosis (100 %). Out of the 17 cases of Tuberculoma, thick irregular ring enhancement was seen in 11 cases (64.70 %) and thin ring enhancement was seen in 6 cases (35.29 %). Among 17 cases of Tuberculoma, features of meningitis were present in 3 cases (17.64 %) and absent in 14 cases (82.35 %). Features of meningitis were absent in all 25 cases of Neurocysticercosis (100 %).

Out of 25 Neurocysticercosis cases, Restriction of diffusion was present in 3 cases which had scolex (7.14 %) and was absent in rest of the cases. Out of 17 cases of Tuberculoma, Restriction of diffusion was present in 12 cases (70.5 %) and was absent in 5 cases (29.40 %).

In our study, ADC cut-off value obtained was 1.2×10^{-3} . Out of 25 cases of Neurocysticercosis, 23 cases showed ADC value $> 1.2 \times 10^{-3}$; however two cases showed ADC value $< 1.2 \times 10^{-3}$. Out of 17 cases of Tuberculoma, 15 cases showed ADC value $< 1.2 \times 10^{-3}$, however one case showed ADC value $> 1.2 \times 10^{-3}$.

In our study, Mean ADC value for Tuberculoma is $0.84 \pm 0.191 \times 10^{-3}$ and mean ADC value for Neurocysticercosis is $1.30 \pm 0.137 \times 10^{-3}$. Hence, it was concluded that ADC value of core of NCC lesions was higher than that of Tuberculoma. Among Tuberculoma lesions, Mean ADC value of T2 hyperintense Tuberculoma lesions, indicative of caseating granulomas with central liquefaction is $0.74 \pm 0.090 \times 10^{-3}$ and mean ADC value of T2 hypointense Tuberculoma lesions, indicative of caseating granulomas without central liquefaction is $1.10 \pm 0.102 \times 10^{-3}$. It was concluded that the ADC value of T2 hyperintense tuberculoma was higher than that of T2 hypointense tuberculoma

The ADC cut off value of $1.2 \times 10^{-3} \text{ mm}^2/\text{s}$ had a sensitivity of 92 % and Specificity of 94.1 %, in differentiating Neurocysticercosis from Tuberculoma. This ADC cut off value had excellent predictive validity in differentiating Neurocysticercosis and Tuberculoma, as indicated by the area under the curve of 0.975 (P-value < 0.001).

On MR Spectroscopy, all 25 cases (100 %) cases of NCC showed amino acid peak, namely acetate at 1.9 ppm and succinate peak at 2.4 ppm. All 17 cases of Tuberculoma (100 %) showed lipid lactate peak at 1.3 ppm.

These constellation of findings helped in differentiating Neurocysticercosis from Tuberculoma with high confidence. Size and number of lesions, presence of scolex, degree of perilesional edema, features of associated meningitis, Post contrast features, MRS and DWI findings as well as ADC values are important for diagnosis and differentiation of NCC from tuberculoma.

BIBLIOGRAPHY



REFERENCES:

1. Maltezou HC, Spyridis P, Kafetzis DA. Extra-pulmonary tuberculosis in children. Archives of disease in childhood 2000;83:342-6.
2. Ogawa SK, Smith MA, Brennessel DJ, Lowy FD. Tuberculous Meningitis in an Urban Medical Center. Medicine 1987;66:317-26.
3. Gupta RK. Tuberculosis and other non Tuberculous Bacterial Granulomatous Infections. MR imaging and spectroscopy of central nervous system infection: Springer. 2001; 24 : 95-145.
4. DeLance AR, Safae M, Oh MC, Clark AJ, Kaur G, Sun MZ, et al. Tuberculoma of the central nervous system. J Neurosci 2013;20:1333-41.
5. Garcia HH, Del Brutto OH. Neurocysticercosis: updated concepts about an old disease. Lancet Neurol 2005;4:653-61.
6. Garg RK. Neurocysticercosis. Postgrad Med J 1998;74:321-6.
7. White Jr AC, Coyle CM, Rajshekhar V, Singh G, Hauser WA, Mohanty A, et al. Diagnosis and treatment of neurocysticercosis: 2017 clinical practice guidelines by the Infectious Diseases Society of America (IDSA) and the American Society of Tropical Medicine and Hygiene (ASTMH). Clin Infect Dis 2018;66:49-75.
8. Lerner A, Shiroishi MS, Zee C-S, Law M, Go JL. Imaging of neurocysticercosis. Neuroimaging Clin 2012;22:659-76.
9. Amaral LLF, Ferreira RM, da Rocha AJ, Ferreira NP. Neurocysticercosis: evaluation with advanced magnetic resonance techniques and atypical forms. Topics in Magnetic Resonance Imaging 2005;16:127-44.

-
10. Mezo RC, García JL, Arroyo M, Fleury A. Relevance of 3D magnetic resonance imaging sequences in diagnosing basal subarachnoid neurocysticercosis. *Acta tropica*. 2015;152:60-5.
 11. Callacondo D, Garcia HH, Gonzales I, Escalante D, Nash TE. High frequency of spinal involvement in patients with basal subarachnoid neurocysticercosis. *Neurology* 2012;78:1394-400.
 12. Bustos JA, Garcia HH, Dorregaray R, Naranjo M, Pretell EJ, Gonzalez AE, et al. Detection of muscle calcifications by thigh CT scan in neurocysticercosis patients. *Trans R Soc Trop Med Hyg* 2005;99:775-9.
 13. Shetty G, Avabratha KS, Rai BS. Ring-enhancing lesions in the brain: a diagnostic dilemma *Iran J Child Neurol* 2014;8:61.
 14. Ghosh RN, Vyas S, Singh P, Khandelwal N, Sankhyan N, Singhi P. Perfusion magnetic resonance imaging in differentiation of neurocysticercosis and tuberculoma. *Neuroradiol* 2019;61:257-63.
 15. Del Brutto OH, Nash TE, White AC, Jr., Rajshekhar V, Wilkins PP, Singh G, et al. Revised diagnostic criteria for neurocysticercosis. *J Neurol Sci* 2017;372:202-10.
 16. Maheshwarappa RP, Agrawal C, Bansal J. Tuberculoma Versus Neurocysticercosis: Can Magnetic Resonance Spectroscopy and Diffusion Weighted Imaging Solve the Diagnostic Conundrum? *Journ of Clinic & Diagnost Research* 2019;13.
 17. Peng J, Ouyang Y, Fang WD, Luo TY, Li YM, Lv FJ, et al. Differentiation of intracranial tuberculomas and high grade gliomas using proton MR spectroscopy and diffusion MR imaging. *Eur J Radiol* 2012;81:4057-63.
-

-
18. Cunliffe CH, Fischer I, Monoky D, Law M, Revercomb C, Elrich S, et al. Intracranial lesions mimicking neoplasms. *Arch Pathol Lab Med* 2009;133:101-23.
 19. Smirniotopoulos JG, Murphy FM, Rushing EJ, Rees JH, Schroeder JW. Patterns of contrast enhancement in the brain and meninges. *Radiographics* 2007;27:525-51.
 20. Omuro AM, Leite CC, Mokhtari K, Delattre JY. Pitfalls in the diagnosis of brain tumours. *Lancet Neurol* 2006;5:937-48.
 21. Garg RK, Desai P, Kar M, Kar AM. Multiple ring enhancing brain lesions on computed tomography: an Indian perspective. *J Neurol Sci* 2008;266:92-6.
 22. Kastrup O, Wanke I, Maschke M. Neuroimaging of infections of the central nervous system. *Semin Neurol* 2008;28:511-22.
 23. Sawlani V, Patel MD, Davies N, Flinham R, Wesolowski R, Ughratdar I, et al. Multiparametric MRI: practical approach and pictorial review of a useful tool in the evaluation of brain tumours and tumour-like lesions 2020;11:1-19.
 24. Malhotra HS, Jain KK, Agarwal A, Singh MK, Yadav SK, Husain M, et al. Characterization of tumefactive demyelinating lesions using MR imaging and in-vivo proton MR spectroscopy. *Mult Scler* 2009;15:193-203.
 25. Sawlani V, Davies N, Patel M, Flinham R, Fong C, Heyes G, et al. Evaluation of Response to Stereotactic Radiosurgery in Brain Metastases Using Multiparametric Magnetic Resonance Imaging and a Review of the Literature. *Clin Oncol* 2019;31:41-9.
 26. Sloot R, Schim van der Loeff MF, Kouw PM, Borgdorff MW. Risk of tuberculosis after recent exposure. A 10-year follow-up study of contacts in Amsterdam. *Am J Respir Crit Care Med* 2014;190:1044-52.
-

-
27. Horsburgh Jr CR, Rubin EJ. Latent tuberculosis infection in the United States. *New England Journal of Medicine* 2011;364:1441-8.
 28. Houben RMGJ, Dodd PJ. The global burden of latent tuberculosis infection: a re-estimation using mathematical modelling. *PLoS medicine* 2016;13:e1002152.
 29. Mazumdar S, Satyanarayana S, Pai M. Self-reported tuberculosis in India: evidence from NFHS-4. *BMJ Glob Health* 2019;4:217-9
 30. Leung AN. Pulmonary tuberculosis: the essentials. *Radiology*. 1999;210:307-22.
 31. Barnes HL, Barnes LRP. The duration of life in pulmonary tuberculosis with cavity. *Am Rev Tuberc* 1928;18:412-24.
 32. Bourgi K, Fiske C, Sterling TR. Tuberculosis Meningitis. *Curr Infect Dis Rep*. 2017;19:39.
 33. Kingkaew N, Sangtong B, Amnuaiphon W, Jongpaibulpatana J, Mankatittham W, Akksilp S, et al. HIV-associated extrapulmonary tuberculosis in Thailand: epidemiology and risk factors for death. *Int J Infect Dis* 2009;13:722-9.
 34. Leonard JM. Central Nervous System Tuberculosis. *Microbiol Spectr* 2017;5.
 35. Nahid P, Dorman SE, Alipanah N, Barry PM, Brozek JL, Cattamanchi A, et al. Official American Thoracic Society/Centers for Disease Control and Prevention/Infectious Diseases Society of America Clinical Practice Guidelines: Treatment of Drug-Susceptible Tuberculosis. *Clin Infect Dis* 2016;63:e147-e95.
 36. Dastur DK, Manghani DK, Udani PM. Pathology and pathogenetic mechanisms in neurotuberculosis. *Radiol Clin North Am* 1995;33:733-52.
 37. Chan KH, Cheung RTF, Lee R, Mak W, Ho SL. Cerebral infarcts complicating tuberculous meningitis. *Cerebrovascular Diseases* 2005;19:391-5.
 38. Trivedi R, Saksena S, Gupta RK. Magnetic resonance imaging in central nervous system tuberculosis. *Indian J Radiol Imaging* 2009;19:256-65.
-

-
39. Cherian A, Thomas SJAhs. Central nervous system tuberculosis. 2011;11.
 40. Stevens DL. Sequential Computerized Axial Tomography in Tuberculous Meningitis. JAMA: The Journ of the American Med Association 1978;239:642.
 41. Weisberg LA. Granulomatous diseases of the CNS as demonstrated by computerized tomography. Computerized Radiology 1984;8:309-17.
 42. Harder E, Al-Kawi MZ, Carney P. Intracranial tuberculoma: Conservative management. Am J Med 1983;74:570-6.
 43. Rock RB, Olin M, Baker CA, Molitor TW, Peterson PK. Central nervous system tuberculosis: pathogenesis and clinical aspects. Clin Microbiol Rev 2008;21: 243-61.
 44. Dastur DK, Manghani DK, Udani PM. Pathology and pathogenetic mechanisms in neurotuberculosis. Radiol Clin North Am 1995;33:733-52.
 45. Rohlwink UK, Kilborn T, Wieselthaler N, Banderker E, Zwane E, Figaji AA. Imaging Features of the Brain, Cerebral Vessels and Spine in Pediatric Tuberculous Meningitis With Associated Hydrocephalus. Pediatr Infect Dis J 2016;35:301-10.
 46. Whelan MA, Stern J. Intracranial tuberculoma. Radiology 1981;138:75-81.
 47. Vengsarkar US, Pisipaty RP, Parekh B, Panchal VG, Shetty MN. Intracranial tuberculoma and the CT scan. Journ of neurosurgery 1986;64:568-74.
 48. Salgado P, Del Brutto OH, Talamas O, Zenteno MA, Rodriguez-Carbajal J. Intracranial tuberculoma: MR imaging. Neuroradiol 1989;31:299-302.
 49. Lee WY, Pang KY, Wong CK. Brain tuberculoma in Hong Kong. Hong Kong Medical Journal= Xianggang yi xue za zhi 2002;8:52-6.
-

-
50. Wasay M, Kheleani BA, Moolani MK, Zaheer J, Pui M, Hasan S, et al. Brain CT and MRI findings in 100 consecutive patients with intracranial tuberculoma. *JNeuroimaging* 2003;13:240-7.
 51. Shanmuganathan R, Kumaresan R, Giri P. Prevalence of angiotensin converting enzyme (ACE) gene insertion/deletion polymorphism in South Indian population with hypertension and chronic kidney disease. *J Postgrad Med* 2015;61:230.
 52. Pinto DS, Joseph T, George A, Hoisala RV. A case report of racemose pattern of intracranial tuberculoma with brain stem and hypophyseal involvement developing paradoxically during treatment. *BJR Case Rep.* 2016;2:20160034.
 53. Ma H, Liu Y, Zhuang C, Shen Y, Wu R. Clinical features and MRI findings of intracranial tuberculomas. *Radiol Infect Dis* 2018;5:154-9.
 54. Kaminogo M, Ishimaru H, Morikawa M, Suzuki Y, Shibata S. Proton MR spectroscopy and diffusion-weighted MR imaging for the diagnosis of intracranial tuberculomas. Report of two cases. *Neurol Res* 2002;24:537-43.
 55. Basoglu OK, Savas R, Kitis O. Conventional and diffusion-weighted MR imaging of intracranial tuberculomas A case report. *Acta Radiologica* 2002;43:560-2.
 56. Gupta RK, Roy R, Dev R, Husain M, Poptani H, Pandey R, et al. Finger printing of *Mycobacterium tuberculosis* in patients with intracranial tuberculomas by using in vivo, ex vivo, and in vitro magnetic resonance spectroscopy. *Magn Reson Med* 1996;36:829-33.
 57. Gupta RK, Poptani H, Kohli A, Chhabra DK, Sharma B, Gujral RB. In vivo localized proton magnetic resonance spectroscopy of intracranial tuberculomas. *Indian J Med Res* 1995;101:19-24.
 58. Gupta RK, Vatsal DK, Husain N, Chawla S, Prasad KN, Roy R, et al. Differentiation of tuberculous from pyogenic brain abscesses with in vivo proton
-

-
- MR spectroscopy and magnetization transfer MR imaging. *AJNR Am J Neuroradiol* 2001;22:1503-9.
- 59.** Krouwer HG, Kim TA, Rand SD, Prost RW, Haughton VM, Ho KC, et al. Single-voxel proton MR spectroscopy of nonneoplastic brain lesions suggestive of a neoplasm. *Am J Neuroradiol* 1998;19:1695-703.
- 60.** Valdés-García J, Espinoza-Díaz DM, Paredes-Díaz E. Stereotactic Biopsy of Brain Stem and Posterior Fossa Lesions in Children. *Acta Neurochirurgica* 1998;140:899-903.
- 61.** Awada A, Daif AK, Pirani M, Khan MY, Memish Z, Al Rajeh S. Evolution of brain tuberculomas under standard antituberculous treatment. *J Neurol Sci* 1998;156:47-
- 62.** Selvapandian S, Rajshekhar V, Chandy MJ, Idikula J. Predictive value of computed tomography-based diagnosis of intracranial tuberculomas. *Neurosurgery* 1994;35:845-50.
- 63.** DeAngelis LM. Intracranial tuberculoma: case report and review of the literature. *Neurology* 1981;31:1133-7.
- 64.** Wasay M, Farooq S, Khowaja ZA, Bawa ZA, Ali SM, Awan S, et al. Cerebral infarction and tuberculoma in central nervous system tuberculosis: frequency and prognostic implications. *J Neurol Neurosurg Psychiatry* 2014;85:1260-4.
- 65.** Raut T, Garg RK, Jain A, Verma R, Singh MK, Malhotra HS, et al. Hydrocephalus in tuberculous meningitis: Incidence, its predictive factors and impact on the prognosis. *J Infect* 2013;66:330-7.
- 66.** Van Toorn R, Solomons R, editors. Update on the diagnosis and management of tuberculous meningitis in children 2014: Elsevier. 2014;31:1110-8
-

-
67. Lewinsohn DM, Leonard MK, LoBue PA, Cohn DL, Daley CL, Desmond E, et al. Official American Thoracic Society/Infectious Diseases Society of America/Centers for Disease Control and Prevention Clinical Practice Guidelines: Diagnosis of Tuberculosis in Adults and Children. *Clin Infect Dis* 2017;64:111-5.
68. White Jr AC, Coyle CM, Rajshekhar V, Singh G, Hauser WA, Mohanty A, et al. Diagnosis and treatment of neurocysticercosis: 2017 clinical practice guidelines by the Infectious Diseases Society of America (IDSA) and the American Society of Tropical Medicine and Hygiene (ASTMH). *Clin Infect Dis* 2018;66:49-75.
69. Winkler AS. Neurocysticercosis in sub-Saharan Africa: a review of prevalence, clinical characteristics, diagnosis, and management. *Pathogens and global health* 2012;106:261-74.
70. Rajshekhar V, Raghava MV, Prabhakaran V, Oommen A, Muliylil J. Active epilepsy as an index of burden of neurocysticercosis in Vellore district, India. *Neurology* 2006;67:2135-9.
71. Prasad KN, Verma A, Srivastava S, Gupta RK, Pandey CM, Paliwal VK. An epidemiological study of asymptomatic neurocysticercosis in a pig farming community in northern India. *Trans R Soc Trop Med Hyg* 2011;105:531-6.
72. Dixon MA, Winskill P, Harrison WE, Basáñez MG. *Taenia solium* taeniasis/cysticercosis: From parasite biology and immunology to diagnosis and control. *Adv Parasitol* 2021;112:133-217.
73. Sorvillo F, Wilkins P, Shafir S, Eberhard M. Public health implications of cysticercosis acquired in the United States. *Emerging infectious diseases* 2011;17:1-7
-

-
74. Lescano AG, Garcia HH, Gilman RH, Gavidia CM, Tsang VC, Rodriguez S, et al. *Taenia solium* cysticercosis hotspots surrounding tapeworm carriers: clustering on human seroprevalence but not on seizures. 2009;3:371.
75. Fabiani S, Bruschi F. Neurocysticercosis in Europe: Still a public health concern not only for imported cases. *Acta Trop* 2013;128:18-26.
76. Nikolić S, Stevanović G. [Neurocysticercosis--pathogenesis and clinical aspects]. *Srp Arh Celok Lek* 2006;134:246-50.
77. Alarcón F. [Neurocysticercosis: its aetiopathogenesis, clinical manifestations, diagnosis and treatment]. *Rev Neurol* 2006;43 Suppl 1:S93-100.
78. Chimelli L, Lovalho AF, Takayanagui OM. [Neurocysticercosis: contribution of autopsies in the consolidation of mandatory notification in Ribeirão Preto-SP,Brazil]. *Arq Neuropsiquiatr* 1998;56:577-84.
79. Pittella JE. Neurocysticercosis. *Brain Pathol* 1997;7:681-93.
80. Fleury A, Carrillo-Mezo R, Flisser A, Sciutto E, Corona T. Subarachnoid basal neurocysticercosis: a focus on the most severe form of the disease. *Expert Rev Anti Infect Ther.* 2011;9:123-33.
81. Sotelo J, Marin C. Hydrocephalus secondary to cysticercotic arachnoiditis. A long-term follow-up review of 92 cases. *J Neurosurg* 1987;66:686-9.
82. Estañol B, Corona T, Abad P. A prognostic classification of cerebral cysticercosis: therapeutic implications. *J Neurol Neurosurg Psychiatry* 1986;49:1131-4.
83. Escobar A, Aruffo C, Cruz-Sánchez F, Cervos-Navarro J. [Neuropathologic findings in neurocysticercosis]. *Archivos de neurobiologia* 1985;48:151-6.
84. Singhi P, Ray M, Singhi S, Khandelwal N. Clinical spectrum of 500 children with neurocysticercosis and response to albendazole therapy. *J Child Neurol* 2000;15:207-13.
-

-
85. Serpa JA, Graviss EA, Kass JS, White AC, Jr. Neurocysticercosis in Houston, Texas: an update. *Medicine* 011;90:81-6.
 86. Garcia HH, Gonzalez AE, Gilman RH. *Taenia solium* Cysticercosis and Its Impact in Neurological Disease. *Clin Microbiol Rev* 2020;33.
 87. Coyle CM. Neurocysticercosis: An Individualized Approach. *Infect Dis Clin North Am.* 2019;33:153-68.
 88. Nash TE, O'Connell EM. Subarachnoid neurocysticercosis: emerging concepts and treatment. *Curr Opin Infect Dis.* 2020;33:339-46.
 89. Sevdâ Diker, Derlen Özgeç Ruso, Nesil Bayraktar, and Uğurcan Balyemez. Intracranial tuberculomas or neurocysticercosis: differentiated by cervical lymph node pathology. *Egypt J Neurol Psychiatr Neurosurg.* 2022; 58: 117-8.
 90. Nash TE, Pretell EJ, Lescano AG, Bustos JA, Gilman RH, Gonzalez AE, et al. Perilesional brain oedema and seizure activity in patients with calcified neurocysticercosis: a prospective cohort and nested case-control study. *Lancet Neurol* 2008;7:1099-105.
 91. Rangel R, Torres B, Del Bruto O, Sotelo J. Cysticercotic encephalitis: a severe form in young females. *Am J Trop Med Hyg.* 1987;36:387-92.
 92. Singh G, Burneo JG, Sander JW. From seizures to epilepsy and its substrates: neurocysticercosis. *Epilepsia.* 2013;54:783-92.
 93. Zee CS, Go JL, Kim PE, DiGiorgio CM. Imaging of neurocysticercosis. *Neuroimaging Clin N Am.* 2000;10:391-407.
 94. Zhao J-L, Lerner A, Shu Z, Gao X-J, Zee C-S. Imaging spectrum of neurocysticercosis. *Radiol Infect Dis* 2015;1:94-102.
-

-
95. Zee CS, Segall HD, Miller C, Tsai FY, Teal JS, Hieshima G, et al. Unusual neuroradiological features of intracranial cysticercosis. *Radiology*. 1980;137:397-407.
 96. Santos GT, Leite CC, Machado LR, McKinney AM, Lucato LT. Reduced diffusion in neurocysticercosis: circumstances of appearance and possible natural history implications. *Am J Neuroradiol* 2013;34:310-6.
 97. Pretell EJ, Martinot C, Jr., Garcia HH, Alvarado M, Bustos JA, Martinot C. Differential diagnosis between cerebral tuberculosis and neurocysticercosis by magnetic resonance spectroscopy. *J Comput Assist Tomogr* 2005;29:112-4.
 98. Sako Y, Nakao M, Ikejima T, Piao XZ, Nakaya K, Ito A. Molecular characterization and diagnostic value of *Taenia solium* low-molecular-weight antigen genes. *J Clin Microbiol* 2000;38:4439-44.
 99. Harrison LJ, Joshua GW, Wright SH, Parkhouse RM. Specific detection of circulating surface/secreted glycoproteins of viable cysticerci in *Taenia saginata* cysticercosis. *Parasite Immunol*. 1989;11:351-70.
 100. Rosas N, Sotelo J, Nieto D. ELISA in the diagnosis of neurocysticercosis. *Arch Neurol* 1986;43:353-6.
 101. White AC, Jr., Coyle CM, Rajshekhar V, Singh G, Hauser WA, Mohanty A, et al. Diagnosis and Treatment of Neurocysticercosis: 2017 Clinical Practice Guidelines by the Infectious Diseases Society of America (IDSA) and the American Society of Tropical Medicine and Hygiene (ASTMH). *Clin Infect Dis* 2018;66:e49-e75.
 102. Garcia HH, Lescano AG, Lanchote VL, Pretell EJ, Gonzales I, Bustos JA, et al. Pharmacokinetics of combined treatment with praziquantel and albendazole in neurocysticercosis. *Br J Clin Pharmacol* 2011;72:77-84.
-

-
- 103.** Sachin L. JMU, Gurumurthy B and Fahid Rahman CH Role of MRI in evaluation of ring enhancing lesions in brain in correlation with MR spectroscopy. Int Journ of Recent Scientific Research 2018;9:26840-5.
- 104.** Sharma B-B, Sharma S. Neurocysticercosis (NCC) vs Central Nervous System (CNS) Tuberculoma in Children—Dilemma over Clinico-Radiological Diagnosis? Open J Pediatr 2016;6:245-51.
- 105.** Gupta RK, Prakash M, Mishra AM, Husain M, Prasad KN, Husain N. Role of diffusion weighted imaging in differentiation of intracranial tuberculoma and tuberculous abscess from cysticercus granulomas-a report of more than 100 lesions. Eur J Radiol 2005;55:384-92.
- 106.** Singh S, Munikrishna M. Diagnostic Dilemma: Neurocysticercosis—A Differential Diagnosis for Seizures in Pregnancy and Early Postpartum Period. Journ of South Asian Federation of Obstet and Gynaecol 2021 9;13:84-6.
- 107.** Agarwal M, Chawla S. Higher succinate than acetate levels differentiate cerebral degenerating cysticercosis from anaerobic abscess on in vivo HMRS. J Neuroradiol 2004;46:211.
- 108.** Shetty B, Ballal S, Reddy S. Diffusion weighted images to differentiate neurocysticercosis and tuberculomas. Neuroradiol Head and Neck 2005;13:82-7.
- 109.** Raffin LS, Bacheschi LA, Machado LR, Nóbrega JPS, Coelho C, Leite CC. DW MR imaging cystic lesion of NCC. Arq Neuropsiquiatr 2001;59:839-42.
- 110.** Batra A, Tripathi RP. Diffusion weighted MRI and MRS. In evaluation of focal cerebral tubercular lesions. Acta Radiologica 2004;45:679-88.
- 111.** Vasudev MK, Jayakumar PN, Srikanth SG, Nagarajan K, Mohanty A. Quantitative magnetic resonance technique in evaluation of intracranial tuberculosis. Acta Radiologica 2007;48:200-06.
-

ANNEXURES



**SRI DEVARAJ URS ACADEMY OF HIGHER EDUCATION
ANDRESEARCH, TAMAKA, KOLAR, KARNATAKA**

ANNEXURE I - PATIENTPROFORMA

**“ROLE OF MULTIPARAMETRIC MAGNETIC RESONANCE IMAGING OF
BRAIN IN DIFFERENTIATING NEUROCYSTICERCOSIS FROM
TUBERCULOMA”**

DEMOGRAPHIC DETAILS:

Name :

Age :

Sex :

UHID :

CLINICAL HISTORY :

MRI PARAMETERS ASSESSED	
Number of lesions	
Size	
Margin	
Scolex	
Perilesional edema	
Features of meningitis	
Post contrast features	
Diffusion weighted imaging ADC values	
Mr spectroscopy peaks	

**SRI DEVARAJ URS ACADEMY OF HIGHER EDUCATION AND
RESEARCH, TAMAKA, KOLAR, KARNATAKA**

ANNEXURE II - INFORMED CONSENT FORM

STUDY TITLE: **ROLE OF MULTIPARAMETRIC MAGNETIC RESONANCE
IMAGING OF BRAIN IN DIFFERENTIATING NEUROCYSTICERCOSIS FROM
TUBERCULOMA**

CHIEF RESEARCHER/ PG GUIDE'S NAME: Dr. ANIL KUMAR SAKALECHA

PRINCIPAL INVESTIGATOR: Dr. LYNN JOY

NAME OF THE SUBJECT :

AGE :

GENDER :

- a. I have been informed in my own language that this study involves MRI Brain with contrast as part of procedure. I have been explained thoroughly and understand the procedure.
- b. I understand that the medical information produced by this study will become part of institutional record and will be kept confidential by the said institute.
- c. I understand that my participation is voluntary and may refuse to participate or may withdraw my consent and discontinue participation at any time without prejudice to my present or future care at this institution.
- d. I agree not to restrict the use of any data or results that arise from this study provided such a use is only for scientific purpose(s).
- e. I confirm that Dr. ANIL KUMAR SAKALECHA / Dr. LYNN JOY (chief researcher/ name of PG guide/name of the principal investigator) has explained to me the purpose of research and the study procedure that I will undergo and the possible risks and discomforts that I may experience, in my own language. I hereby agree to give valid consent to participate as a subject in this research project.

Participant's signature /thumb impression

Signature of the witness:

Date:

1)

2)

I have explained to (subject) the purpose of the research, the possible risk and benefits to the best of my ability.

Chief Researcher/ Guide signature

Date:

**SRI DEVARAJ URS ACADEMY OF HIGHER EDUCATION AND
RESEARCH, TAMAKA, KOLAR, KARNATAKA**

ANNEXURE III – PATIENT INFORMATION SHEET

Principal Investigator : Dr. Lynn Joy / Dr. Anil Kumar Sakalecha

I, Dr. Lynn Joy, post-graduate student in Department of Radio-Diagnosis at Sri Devaraj Urs Medical College, will be conducting a study titled “ROLE OF MULTIPARAMETRIC MAGNETIC RESONANCE IMAGING OF BRAIN IN DIFFERENTIATING NEUROCYSTICERCOSIS FROM TUBERCULOMA” form dissertation under the guidance of Dr. Anil Kumar Sakalecha, Professor, Department of Radio-Diagnosis. In this study, we will assess the Brain magnetic resonance imaging features in differentiating Neurocysticercosis from Tuberculoma. You will undergo MRI Brain with contrast to enter the study. You will not be paid any financial compensation for participating in this research project.

All of your personal data will be kept confidential and will be used only for research purpose by this institution. You are free to participate in the study. You can also withdraw from the study at any point of time without giving any reasons whatsoever. Your refusal to participate will not prejudice you to any present or future care at this institution

Name and Signature of the Principal Investigator

Phone number- 9741971175

Email id: lynnjoy26@gmail.com

Date:

MASTER CHART



LIST OF ABBREVIATIONS

GLOSSARY	EXPANSION
A	Absent
ADC	Apparent diffusion coefficient
AA	Amino Acid
AFB	Acid Fast bacilli
F	Female
F/U	Follow Up
LL	Lipid Lactate
M	Male
MRS	MR Spectroscopy
P	Present
Tx	Treatment
TB	Tuberculosis

S.No	uHID no	SEX	age	Size (mm)	number	location	edema	Scolex	margins	Post contrast Ring Enhancement	meningitis	MRS peaks	DWI features	ADC values (x 10-3)	Follow up
1	155320	M	52	8 x 11	Single	right frontal	moderate	A	smooth	Thick irregular	A	LL	Patchy areas of restriction	0.62	F / U scan showed decrease in size and number of lesions, K/c/ o tuberculosis
2	164419	F	30	10 x 11	Single	left frontal	Severe	A	smooth	Thick irregular	A	LL	Patchy areas of restriction	0.65	F / U scan showed decrease in size and number of lesions , Sputum AFB positive.
3	166787	M	21	16 x 6	Conglomerate	diffuse	Moderate	A	irregular	Thick irregular	P	LL	Patchy areas of restriction	0.69	F / U scan showed decrease in size, Sputum AFB Positive
4	166238	F	24	10 x 8	Multiple	diffuse	Severe	A	irregular	Thick irregular	A	LL	Patchy areas of restriction	0.69	K/c/o tuberculosis ,Follow up scan done showed decrease in size of lesion,
5	164528	M	45	14 x 10	Single	Bilateral Cerebellar hemisphere	Moderate	A	irregular	Thick irregular	A	LL	Patchy areas of restriction	0.71	F / U scan showed decrease, Sputum AFB positive. Started on anti TB therapy
6	160451	M	57	10 x 8	Single	Left Cerebellar hemisphere	Moderate	A	Irregular	Thick irregular	A	LL	Patchy areas of restriction	0.72	F / U scan showed decrease, K/c/ o tuberculosis
7	155595	F	28	11 x 7	Multiple	Diffuse	Mild	A	Smooth	Thin	A	LL	Patchy areas of restriction	0.70	F / U scan showed decrease in size and number of lesions ,Already K/C/O tuberculosis. Already taking anti TB medications.
8	163438	M	52	8 x 7	Multiple	Left frontal	Severe	A	irregular	Thick irregular	A	LL	Patchy areas of restriction	0.75	F / U scan showed decrease in size and number, k/c/o TB
9	155907	F	45	8 x 7	Single	Right Cerebellar hemisphere	Severe	A	Irregular	Thick irregular	A	LL	Patchy areas of restriction	0.76	F / U scan showed decrease K/c/o tuberculosis, Chest X ray done
10	162805	M	56	8 x 7	Single	left frontal	Moderate	A	Smooth	Thin	A	LL	Patchy areas of restriction	0.81	F / U scan showed decrease in size and number
11	164087	M	34	17 x 11	Conglomerate	Right frontal	Severe	A	Irregular	Thick irregular	A	LL	Patchy areas of restriction	0.9	F / U scan showed decrease in size and number, Sputum AFB positive,

12	159351	M	32	9 x 8	Multiple	Right frontal	Severe	A	Irregular	Thick irregular	A	LL	Patchy areas of restriction	0.91	F / U scan showed decrease in size and number, K/c/o tuberculosis,
13	158702	M	47	10 x 9	Multiple	Right parietal	Moderate	A	Irregular	Thick irregular	A	LL	No restriction	0.97	F / U scan showed decrease in size and number, Sputum AFB positive. Started on anti TB therapy
14	164326	M	64	8 x 11	Single	Left occipital	Moderate	A	Smooth	Thin	P	LL	No restriction	1.05	F / U scan showed decrease in size and number, Sputum AFB positive. Started on anti TB therapy
15	157735	F	52	16 x 9	Multiple	Right frontal	Moderate	A	Smooth	Thin	A	LL	No restriction	1.07	F / U scan showed decrease in size and number Already K/C/O tuberculosis. Already taking anti TB medications.
16	161244	F	57	11 x 10	Single	Left occipital	Severe	A	Smooth	Thin	A	LL	No restriction	1.2	F / U scan showed decrease in size and number
17	167248	F	32	7 x 7	Multiple	Right frontal	Moderate	A	Smooth	Thin	P	LL	no restriction	1.21	F / U scan showed decrease in size of lesions, Already K/C/O tuberculosis.
18	173252	F	47	12 x 10	Single	Left occipital	Severe	A	Smooth	Thin	A	LL	No restriction	1.2	F / U scan showed decrease in size and number
19	165726	M	78	9 x 7	Multiple	Multiple	mild	A	smooth	thin walled	A	AA - acetate	no restriction	1.25	F / U scan showed decrease in size and number Remission of symptoms following albendazole therapy
20	165727	M	54	10 x 7	Multiple	Multiple	mild	A	smooth	thin walled	A	AA - acetate	no restriction	1.25	F / U scan showed decrease in size and number Remission of symptoms following albendazole therapy
21	167107	M	24	5 x 4	Single	left frontal	moderate	A	smooth	thin walled	A	AA - acetate -	no restriction	1.32	F / U scan showed decrease in size and number
22	161188	M	23	4 x 3	Single	right frontal	Moderate	A	smooth	thin walled	A	AA - acetate	no restriction	1.41	F / U scan done. Decrease in size of lesion following tx
23	160652	F	45	2 x 2	Single	left parietal	Mild	A	smooth	thin walled	A	AA - acetate	no restriction	1.51	F / U scan done. Decrease in size of lesion following tx

24	155112	F	26	5 x 4	Single	right frontal	Mild	A	smooth	thin walled	A	AA - acetate	no restriction	1.23	F / U scan done. Decrease in size of lesion following tx, Remission of symptoms following albendazole therapy
25	166575	F	43	9 x 7	Multiple	Diffuse	Mild	A	smooth	thin walled	A	AA - acetate	restriction in scolex	0.97	F / U scan showed decrease in size and number, Remission of symptoms following albendazole therapy
26	163249	F	16	9 x 7	Multiple	left frontal	Moderate	A	smooth	thin walled	A	AA - acetate	No restriction	1.31	F / U scan showed decrease in size and number, Remission of symptoms following albendazole therapy
27	163173	M	24	5 x 4	Single	right frontal	Mild	A	smooth	thin walled	A	AA - acetate	No restriction	1.22	F / U scan showed decrease in size and number, Remission of symptoms following albendazole therapy
28	158835	F	35	3 x 3	Single	left parieto-occipital	Mild	A	Smooth	thin walled	A	AA - acetate	No restriction	1.32	F / U scan showed decrease in size and number, Remission of symptoms following albendazole therapy
29	164925	M	40	4 x 3	Single	left parietal	mild	P	smooth	thin walled	A	AA - acetate	No restriction	1.34	F / U scan showed decrease in size and number, Remission of symptoms following albendazole therapy
30	166996	F	25	3 x 2	Single	left temporal	Moderate	P	Smooth	thin walled	A	AA - acetate	No restriction	1.42	F / U Scan done. Decrease in size of lesion following tx
31	157938	M	25	8 x 7	Single	left frontal	Mild	P	smooth	thin walled	A	AA - acetate	no restriction	1.32	F / U scan showed decrease in size and number, Remission of symptoms following albendazole therapy
32	166087	M	23	3 x 3	Single	right frontal	Mild	P	smooth	thin walled	A	AA - acetate	no restriction	1.37	F / U scan showed decrease in size and number, Remission of symptoms following albendazole therapy
33	167516	M	26	4 x 3	Single	left parietla	Mild	P	smooth	thin walled	A	AA - succinate	No restriction	1.34	F / U scan showed decrease in size and number, Remission of symptoms following albendazole

															therapy
34	164704	M	26	3x2	Single	left frontal	Moderate	P	smooth	thin walled	A	AA - succinate	Restriction in scolex	1.34	F / U scan showed calcified lesion, Remission of symptoms following albendazole therapy
35	164138	F	25	5 x 5	Single	left occipital	Mild	A	smooth	thin walled	A	AA - succinate	No restriction	1.31	F / U scan - calcified lesion, Remission of symptoms following albendazole therapy
36	166507	F	20	9 x 8	Single	Intraventricular, Right frontal	Mild	P	smooth	thin walled	A	AA - succinate	No restriction	1.51	F / U scan done, - calcified lesion .Remission of symptoms following albendazole therapy
37	156340	F	45	6 x 5	Multiple	Diffuse	Mild	P	Smooth	Thin walled	A	AA - succinate	No restriction	1.42	F / U scan-calcified lesion Remission of symptoms following albendazole therapy
38	155629	M	47	6 x 6	Multiple	Right frontal	Moderate	P	Smooth	Thin walled	A	AA - succinate	No restriction	1.22	F / U scan -decrease in size and number, Remission of symptoms following albendazole therapy
39	160813	M	51	7 x 4	Multiple	Right frontal	Mild	A	Smooth	Thin walled	A	AA - succinate	No restriction	1.32	F / U scan - decrease in size and number, Remission of symptoms following albendazole therapy
40	162920	M	58	6 x 5	Multiple	Left parietal	Moderate	A	Smooth	Thin walled	A	AA - lactate	No restriction	1.43	F / U scan -decrease in size and number, Remission of symptoms following albendazole therapy
41	161253	M	55	7 x 7	Single	Left parietal	Mild	A	Smooth	Thin walled	A	AA - acetate & succinate	No restriction	1.21	F / U scan -decrease in size and number, Remission of symptoms following albendazole therapy
42	165543	M	59	8 x 7	Single	Right frontal	Mild	A	Smooth	Thin walled	A	AA - acetate & succinate	No restriction	1.37	F / U scan -decrease in size, Remission of symptoms following albendazole therapy